Flanders
State of
the Art

14_024_6
FHR reports

Agenda for the future – Hydro- and sediment dynamics in the Schelde estuary

Sub report 6
Validation of the SCALDIS-model on intertidal areas

DEPARTMENT
**MOBILITY &
PUBLIC
WORKS**

www.flandershydraulicsresearch.be

Agenda for the future – Hydro- and sediment dynamics in the Schelde estuary

Sub report 6: Validation of the SCALDIS-model on intertidal areas

Hassan, W.; Meire, D.; Plancke, Y.; Mostaert, F.

Waterbouwkundig Laboratorium
Vlaanderen is wetenschap

Cover figuur © Vlaamse overheid, Departement Mobiliteit en Openbare Werken, Waterbouwkundig Laboratorium 2017

Juridische kennisgeving

Copyright en wijze van citeren

Deze publicatie dient als volgt geciteerd te worden:

Hassan, W.; Meire, D.; Plancke, Y.; Mostaert, F. (2017). Agenda for the future – Hydro- and sediment dynamics in the Schelde estuary: Sub report 6: Validation of the SCALDIS-model on intertidal areas. Versie 2.0. WL Rapporten, 14_024_6. Waterbouwkundig Laboratorium: Antwerpen.

Documentidentificatie

Opdrachtgever:	Waterbouwkundig Laboratorium	Ref.:	WL2017R14_024_6
Keywords (3-5):	Stroming, intergetijdegebied, Zeeschelde, SCALDIS		
Tekst (p.):	75	Bijlagen (p.):	20
Vertrouwelijk:	☒ Nee	☒ Online beschikbaar	

Auteur(s):	Hassan, W.

Controle

	Naam	Handtekening
Revisor(en):	Meire, D.	
Projectleider:	Plancke, Y.	

Goedkeuring

Afdelingshoofd:	Mostaert, F.	

Abstract

Within the framework of the “Integraal Plan Boven-Zeeschelde”, a new unstructured high-resolution model, the SCALDIS-model, is developed in TELEMAC-3D, for the entire Schelde estuary and with special attention to the upstream parts.

The present study describes the SCALDIS-model validation with new hydrodynamic data in the intertidal zones of the estuary. The new velocity data, measured at various locations between 2014 and 2016, are limited to the intertidal zones in the Flemish part of the Scheldt estuary, and in total 10 measuring locations along the estuary are selected. The model is calibrated for one spring-neap tidal-cycle in 2013, based on water level measurements and point and transect measurements of flow velocities (and discharge) in deep and shallow zones. These new velocity measurements in intertidal areas are important to test the model performance in shallow zones in the estuary, which are e.g. of interest in ecological studies.

Contents

List of tables

List of figures

1 Introduction

In the framework of the project 'Integraal Plan Boven-Zeeschelde', a new hydrodynamic model that covers the entire tidally influenced zone of the Scheldt estuary and the mouth area with a sufficient resolution in the upstream part was built. This model, the SCALDIS model, developed within TELEMAC-3D, was developed because existing models lack a high resolution in the upper sea Scheldt, Durme, Rupel and Nete. Special attention in this model was paid to the upstream parts. The use of an unstructured grid allows combining a large model extent with a high resolution upstream.

The present report describes the model validation with new hydrodynamic data at various locations in the intertidal zones of the estuary. The model was calibrated for one spring-neap tidal-cycle in 2013 against field data: water levels, velocities (in deep and shallow zones) and discharges. The new measured velocity data are limited to the intertidal zones in the Flemish part of the Scheldt estuary. 10 measuring locations were selected along the estuary.

2 Units and reference plane

Time is expressed in CET (Central European Time).

Depth, height and water levels are expressed in meter TAW (Tweede Algemene Waterpassing).

Bathymetry and water levels are positive above the reference plane.

The horizontal coordinate system is RD Parijs.

3 SCALDIS-model

Existing hydrodynamic models lack a high resolution in the Upper Sea Scheldt and its tributaries as the Durme, Rupel and Nete. For this reason, a new unstructured high resolution model of the (tidal) Schelde Estuary is developed in TELEMAC-3D for the entire estuary with special attention to the upstream parts (Smolders et al., (2016)). The use of an unstructured grid allows the combination of a large model extent together with a high resolution upstream.

Smolders et al. (2016) described in detail the model development, calibration and validation of the hydrodynamics. The model is calibrated for one spring-neap tidal-cycle in 2013 against different types of field data: water levels, velocities (in deep and shallow zones) and discharges. In this section a short description of the model is presented, more details can be found in Smolders et al. (2016).

3.1 Model grid and resolution

The SCALDIS-model is developed in the TELEMAC software (version: V6P3), which is based on the finite element method. The model domain is discretized into an unstructured grid of triangular elements. Therefore, the complex geometry of the study area can be taken into account in a more flexible way compared to a structured grid.

The model domain (Figure 1) covers the entire tidal Schelde estuary, including the mouth area and the Belgian Coastal Zone from Dunkerque (France), until Goeree (The Netherlands), including the Eastern Schelde. Upstream the model extends to the limits of the tidal intrusion. All tributaries of the Scheldt are included. The model grid consists of +460 000 nodes in the horizontal plane. The model is 3D with 5 sigma planes over the vertical, which gives a total of +2 300 000 of nodes. The resolution in the coastal area varies from 200 to 500 m depending on the water depth. The resolution in the Eastern Schelde is 200 m. In the Western Scheldt, the resolution is 120 m. In the Sea Scheldt, the resolution increases to 30 m near Antwerp and 10 m in the Upper Sea Scheldt. Upstream the tributaries the resolution can reach up to 4 m. More details about the model description and calibration can be found in Smolders et al. (2016).

3.2 Bathymetry

The model bathymetry is presented in Figure 1. For this large model domain, several different bathymetry datasets were used and pasted together from different sources and in different coordinate systems. All coordinate conversions were done with the Open Earth Toolbox in Matlab. All data were converted to the RD Paris coordinate system.

The Belgian Continental Shelf and the Belgian coastal zone were measured in 2007-2009 by MDK-aKust. The bathymetry of the Dutch coast (mostly 2010-2012) was measured by Rijkswaterstaat and downloaded from Open Earth. The bathymetry of the Western Scheldt (2013) and the Eastern Scheldt (2010) was measured by Rijkswaterstaat. For the lower Sea Scheldt, bathymetric data of 2011 was provided by Maritime Access division. Bathymetric data for the Upper Sea Scheldt and Rupel basin (2014) was completed with data for the Dijle and Lower Nete (2010-2013) and for the Zenne and Grote and Kleine Nete (2001) which was provided by W&Z, Sea Scheldt division. All details about the used bathymetry can be found in Smolders et al. (2016).

Figure 1 – SCALDIS: grid extent and model bathymetry (m TAW).

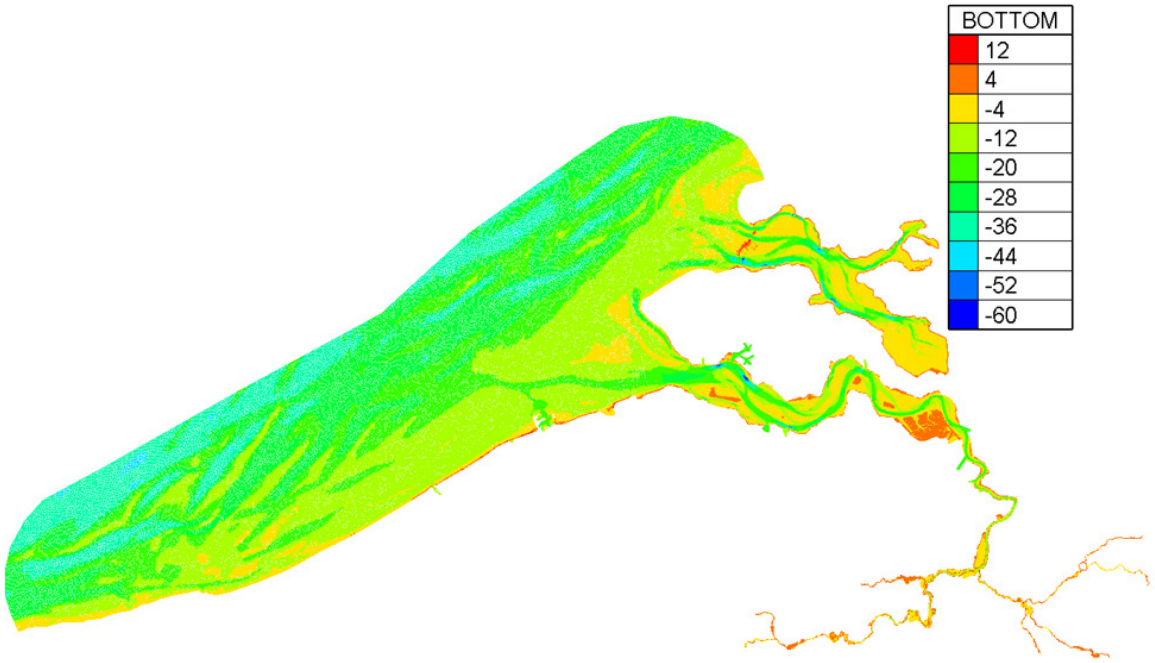

3.3 Boundary conditions

The downstream boundary of SCALDIS-model is located in the North Sea. The model is nested in the regional ZUNO model of the southern North Sea (Rijkswaterstaat, 2009) from which it gets the downstream boundary conditions for water level and salinity.

The time series of the boundary conditions of the SCALDIS-model are “harmonically corrected”. This means that the time series at the boundary locations of SCALDIS-model that are obtained out of ZUNO are decomposed in harmonic components and a residual term. The harmonic components are corrected, and the signal is re-synthesized. The correction of the harmonic components is calculated based on the comparison of the harmonic components of the ZUNO results and measurements for a period of 1 year (Maximova et al., 2015). Applying these corrected boundary conditions in SCALDIS-model eliminates the systematic bias in harmonic components that are present in ZUNO.

There are 8 upstream boundaries with prescribed discharge and free tracer. The measured daily average discharges are defined as upstream boundary conditions at the Upper Sea Scheldt for Merelbeke, Dender, Zenne, Dijle, Kleine Nete, Grote Nete and channel Ghent–Terneuzen. All these daily averaged discharge values are recalculated, by interpolation, to hourly values. For the channel of Bath hourly discharge measurements were available. So all discharge boundaries have hourly discharge values.

Wind is also applied on the coastal zone. All details about the used boundary conditions can be found in Smolders et al. (2016).

3.4 Simulation period and time step

The SCALDIS-model runs were performed from 17/09/2013 00:00 to 20/12/2013 00:00. Smolders et al., (2016) found that, the relationship between the time step and the grid size has an effect on the model accuracy and stability. The time step used for the model simulations is 4 s. This time step, based on the sensitivity analysis, showed an optimum for computational speed and a stable computation.

3.5 Model calibration

Smolders et al. (2016) performed a detailed analysis of SCALDIS-model. They investigated also the model sensitivity to different input parameters before the model calibration. The model is calibrated against water levels, discharges and velocity measurements (sailed ADCP and stationary velocity measurements in shallow and deep areas).

The model was calibrated with measured data in the year 2013, data was available from different sources:

- Water level measurements were retrieved from the Hydro Meteo Centrum Zeeland database (HMCZ, www.hmcz.nl) for the stations located in the Netherlands and some Belgian stations;
- Measured water levels for the coastal Belgian stations were available from the Meetnet Vlaamse banken (www.kustdata.be) for Zeebrugge, Oostende and Nieuwpoort;
- For other Belgian coastal stations the data were received from the Afdeling Kust;
- For the Belgian stations in the Sea Scheldt and Rupel the data were available from Hydrologisch Informatie Centrum (HIC).

The modeled horizontal and vertical tide is calibrated by adapting the bottom roughness, which is represented by Manning's equation for the dimensionless friction coefficient. The bed roughness was adapted in various model runs, from Scaldis_036_0 to Scaldis_040_0. From these runs **Scaldis_039_0** produced the best results. The quality of the calibrated model Scaldis_039_0 is described in Smolders et al. (2016). The comparison of the measured flow velocity profiles at several upstream locations showed a good agreement with the model results Scaldis_039_0.

The results of the calibrated model (**Scaldis_039_0**) are used in the present study to validate the model with the new measurements at the intertidal areas. The model validation focuses mainly on flow velocity magnitudes at certain point locations, on intertidal areas.

4 Validation data on intertidal areas

The available data of flow velocity measurements are rather scarce in the Scheldt estuary. In some places in the Flemish part of the Scheldt estuary there are continuous measuring posts, where flow speeds are measured at various locations, at the edge of the navigation channel (e.g. measurements at Oosterweel, Meetpaal Lillo, …). These data are measured in the context of the MONEOS monitoring program, and are e.g. reported in Vanlierde et al. (2016). Flow velocity measurements on the intertidal areas in the Sea Scheldt were lacking, however they are very important for ecology (e.g. habitat mapping).

The first measurement campaign (shallow zones) in the Sea Scheldt on intertidal areas was carried out in 2014 and is described in Plancke et al. (2014). More recent measurements were carried out in 2015 and 2016 at various locations in de Zeeschelde, as is presented by Meire et al. (2017). These measurements range spatially from the east side of Saeftinghe (most downstream location) to Appels (most upstream location). The locations of all measurements are shown in Figure 2.

Figure 2 – Overview of the measuring locations along Scheldt estuary, used for model validation.

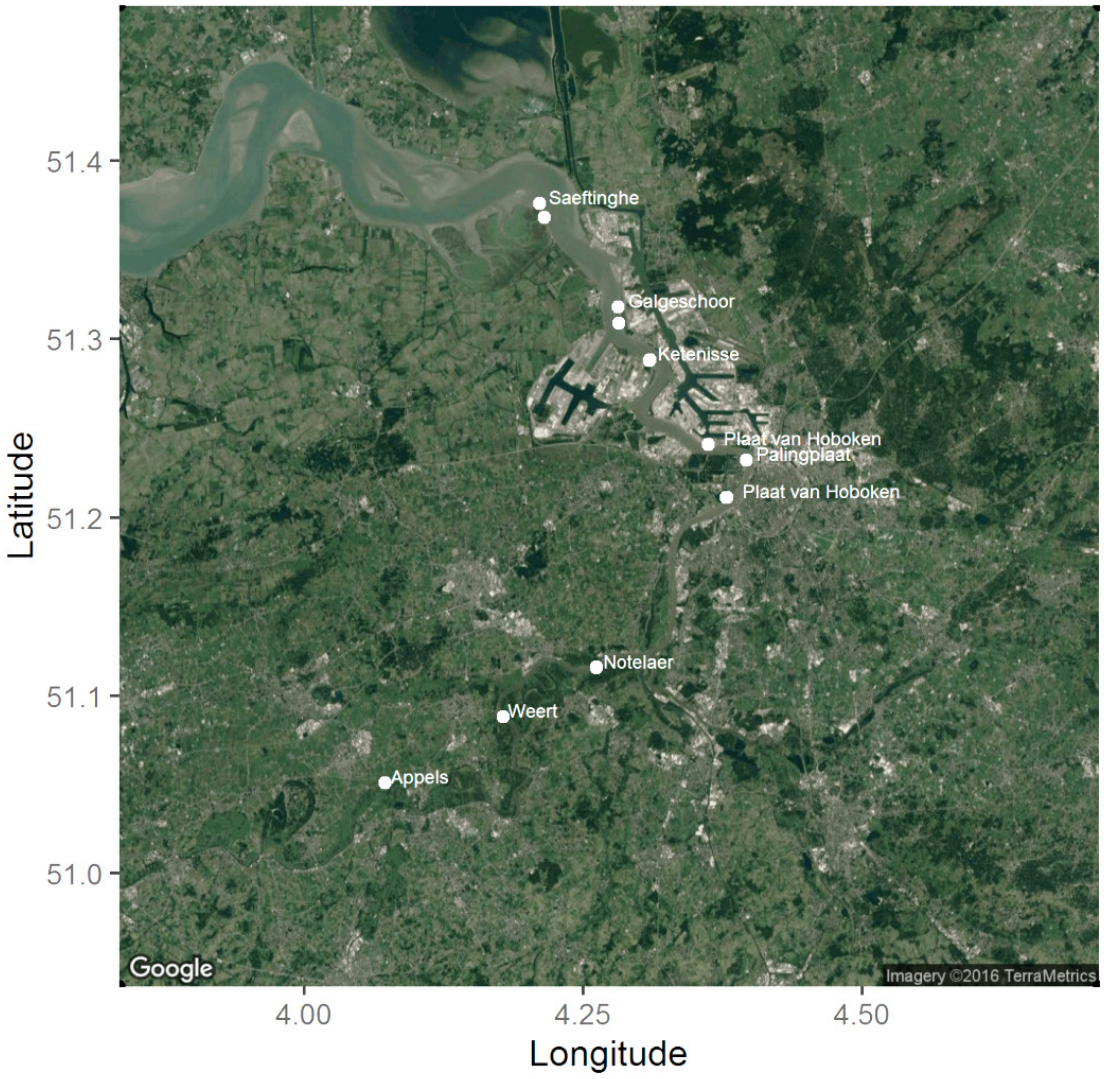

The new measurements on intertidal areas were conducted at 10 different locations in the Sea Scheldt. The geographical coordinates of the different monitoring locations are shown in Table 1 and Figure 1.

Flow velocity measurements were carried out with two Aquadopp® profilers (Nortek), 2.0 MHz. They are buried into the bottom soil, with the head of the instrument about 0.2 to 0.3 m above the bottom. The Aquadopp® measures flow velocities in maximal 70 cells, where the height of each cell equals 0.1 m. Two measuring devices were used at each location. At most locations one device was located close to the deep water ("laag slik"), and a second device located at shallow water ("hoog slik"). Table 2 gives general information about starting date and time of the measurements, the Aquadopp® level (m TAW) and number of tides at each location. More details about the used Aquadopp profiler and the measurements can be found in Meire et al. (2017).

The pressure sensor on the Aquadopp® was used to measure water levels at each location in combination with flow velocity magnitudes and directions. As the sensors are placed around the low water line (the exact position is practically determined during the installation of the instruments), the observed tidal range on the instruments is not the full tidal range. To avoid influence of the exact position of the instruments and to take into account the complete tidal range, measured water levels at the closest tidal gauges have been used in the analysis of the SCALDIS-model validation.

Ten minute interval time series of the water level measurements (m NAP, CET) were retrieved from the Belgian stations. For the Belgian stations in the Sea Scheldt and Rupel the data (m TAW, UTC) were available from Hydrologisch Informatie Centrum (HIC).

Table 1 – Geographical coordinates of velocity measurements at different locations in WGS 84.

Location	**Aquadopp low**		**Aquadopp high**	
	North [°]	East [°]	North [°]	East [°]
Saeftinghe North Saeftinghe South	51.37614 51.36805	4.21122 4.21545	- -	- -
Galgeschoor North Galgeschoor South	51.31816 51.30881	4.281020 4.281759	- -	- -
Plaat van Ketenisse	51.28843	4.30972	51.28806	4.30902
Plaat van Boomke	51.241028	4.362028	51.241111	4.362028
Palingplaat	51.23228	4.39662	51.23223	4.39642
Plaat van Hoboken	51.21115	4.37887	51.21147	4.37848
Notelaer	51.11575	4.26188	51.11579	4.26180
Weert	51.08797	4.178083	51.08809	4.178186
Appels – LO	51.050583	4.072517	51.050750	4.072383
Appels – RO	51.04848	4.068041	51.04866	4.068117

Table 2 – General overview of the measuring campaigns at each location, time in UTC.

Location	**Position**	**Date and Time**		**Height [m TAW]**	**Number of Tides**
		Start	**End**		
Saeftinghe	North South	20/07/2016 12:00	22/08/2016 13:00	+ 0.09 + 0.54	64
Galgeschoor	North South	30/10/2015 12:00	2/12/2015 12:00	+ 0.57 + 1.17	65
Plaat van Ketenisse	High Low	20/08/2015 12:00	22/09/2015 14:35	+ 0.18 + 3.34	50
Plaat van Boomke	High Low	09/07/2015 16:00	10/08/2015 14:40	+ 0.09 + 2.41	54
Palingplaat	High Low	12/01/2016 09:00	10/02/2016 13:20	+ 0.85 + 1.76	55 43
Plaat van Hoboken	High Low	28/09/2015 12:00	28/10/2015 11:05	+ 0.10 + 2.10	56 56
Notelaer	High Laag	23/02/2016 09:00	24/03/2016 17:05	+ 1.01 + 1.33	52 43
Weert	High Low	21/01/2014 23:00	18/02/2014 22:00	+ 2.27 + 0.05	53 40
Appels LO	High Low	13/06/2014 17:00	22/07/2014 21:00	not available	74 74
Appels RO	High Low	28/04/2014 23:00	29/05/2014 21:00	not available	60 60

(green = measurements in 2014, red = measurements in 2015 and white = measurements of 2016)

4.1 An example of the measured data

An example of the measured velocities and water depth variations at Palingplaat is presented in Figure 3 for the two measuring points during one week (from Meire et al., 2017). The upper panel shows the water depth variation measured by the pressure sensors of the two Aquadopp® (on low and middle-high tidal flat), the middle and lower panels show the magnitudes of the measured depth-averaged flow velocities.

Ensemble-averaged or phase averaging analysis was carried out to the depth-averaged velocities and for water depths. For this analysis the depth-averaged velocities are split into individual tidal-cycles and averaged out at various time steps during the full tidal-cycle. An example of the ensemble-averaged results at Palingplaat is presented in Figure 4. This figure shows the depth-averaged values at both Palingplaat-High (red-line) and Palingplaat-Low (blue-line) position. The top panel shows the water level variation, the middle panel the total velocity magnitude and the lower panel the velocity direction.

Figure 3 – Measured time series of water depth (top) and depth-averaged velocities (bottom) at Palingplaat (week 2).

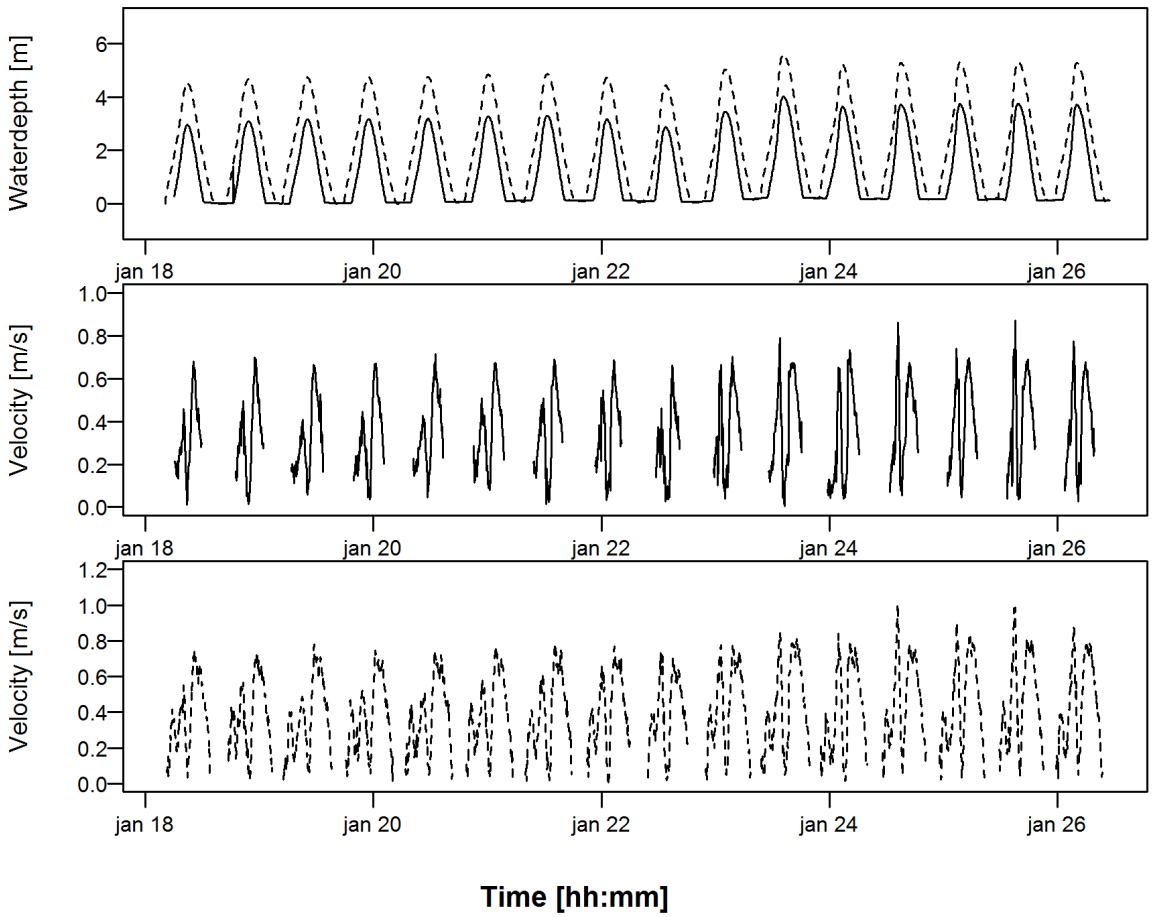

Figure 4 – Measured water depth, depth-averaged velocity and direction at Palingplaat-Low (blue) and Palingplaat_High (red).

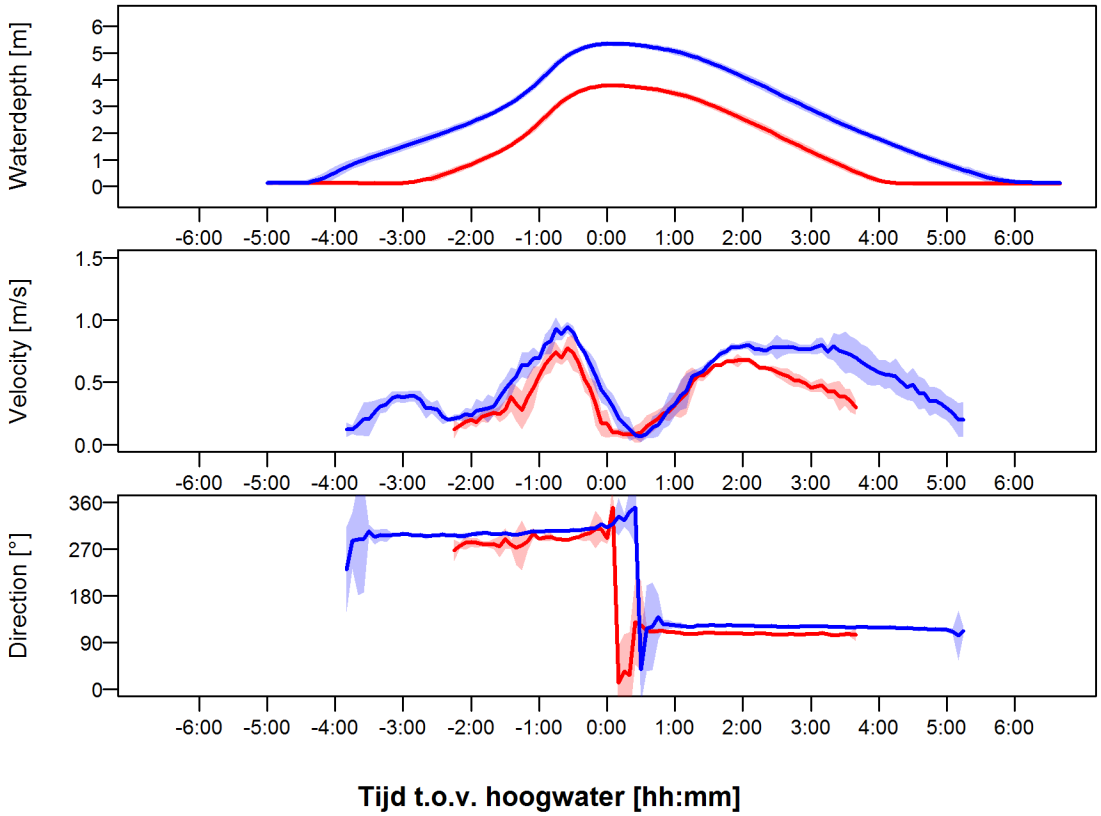

Similar results were obtained at all other locations along the Scheldt estuary as shown in Figure 2. These data form the basics for the SCALDIS-model validation at intertidal areas.

5 SCALDIS-model validation

The main objective of the present study is to validate the SCALDIS-model, presented in Smolders et al. (2016), on intertidal areas, using the newly available intertidal velocity data in the Sea Scheldt. No calibration parameters (bed roughness or other model parameters) are changed during the model validation compared to the model run **Scaldis_039_0.** As such, this version is used for the model validation in this report. The SCALDIS-model run were carried out from 17/09/2013 00:00 to 20/12/2013 00:00.

5.1 Validation protocol

In the present study the SCALDIS-model is validated with the measured data from 2014, 2015 and 2016 with different time intervals as shown in Table 2. Measured water levels during the same measuring period of flow velocities (Table 2) have been used for model validations in combination with the measured flow velocities using the Aquadopp®.

Model validation and comparison with measurements are carried out and presented in two different ways:

- A comparison between the measured and computed water depth variation and the correspondent maximum depth-averaged flow velocity, both during flood and ebb phases. These information are extracted from the measured time series of velocities, measured by the Aquadopp® and the measured water levels at one of the fixed measuring tidal gauges;
- Comparing the measured and computed ensemble-averaged velocities, for spring-, neap- and averaged-tides. The comparison between measured and computed velocities of spring-tide are discussed and presented in section 6. Results of neap- and averaged-tides are presented in Appendix 9.

The model results are compared with the stationary velocity measurements at 20 different locations as described in Table 2 and in Figure 2.

5.2 Sensitivity of results to depth location

For the analysis of flow velocities in shallow zones it is very important that the measurement point and the analyzed point (node) in the model have similar depths. It was not always possible to find a model node with a similar depth close to the measurement location. This may result in differences between the calculated and the measured velocities. Table 3 presents the information about the used model nodes that have been used for comparison with the measurements. The table includes also the bottom levels as measured in the field and computed at each node (m TAW).

At some locations the output in different points was tested to study the effect of using the real coordinates of a certain measuring point and using only the nearest node in the model on the results. Figure 5 presents two examples at two different locations (Notelaer-High and Galgeschoor-south) to compare model results with data. This comparison includes ensemble-averaged velocities during spring-tide, which have been measured (blue-lines) and the computed velocities using SCALDIS-model (red-line for the nearest node) and (green-line for interpolation of three nodes). The bottom levels are presented in Table 4. It is clear from Figure 5 that both methods give more or less the same velocity magnitudes with negligible differences. Therefore, in the present study all model results are presented using only the nearest node, close to the measured points as collected in the field.

Table 3 – Used node numbers at each location in the SCALDIS-model.

Location	**Position**	**Node Nr.**	**Bottom level at nearest node in SCALDIS-model [m TAW]**	**Height measured [m TAW]**
Saeftinghe	North	273846	+ 0.86	+ 0.09
	South	275307	+ 0.46	+ 0.54
Galgeschoor	North	294917	+ 0.48	+ 0.57
	South	295010	+ 0.29	+ 1.17
Plaat van Ketenisse	High	305434	+ 3.52	+ 3.34
	Low	305931	+ 0.38	+ 0.18
Plaat van Boomke	High	336870	+ 1.84	+ 2.41
	Low	336871	- 0.36	+ 0.09
Palingplaat	High	344122	+ 1.62	+ 1.76
	Low	344153	+ 0.35	+ 0.85
Plaat van Hoboken	High	340312	+ 1.69	+ 2.10
	Low	340384	+ 0.24	+ 0.10
Notelaer	High	287013	+ 1.41	+ 1.34
	Low	286960	+ 1.29	+ 1.00
Weert	High	235716	+ 1.44	+ 2.27
	Low	235654	+ 0.43	+ 0.05
Appels LO	High	170384	+ 3.17	not available
	Low	170420	+ 1.22	
Appels RO	High	168596	+ 2.25	not available
	Low	168641	+ 0.05	

Figure 5 – Measured and computed at nearest node and
computed flow velocities at Notelaer-High and Galgeschoor-south (spring tide).

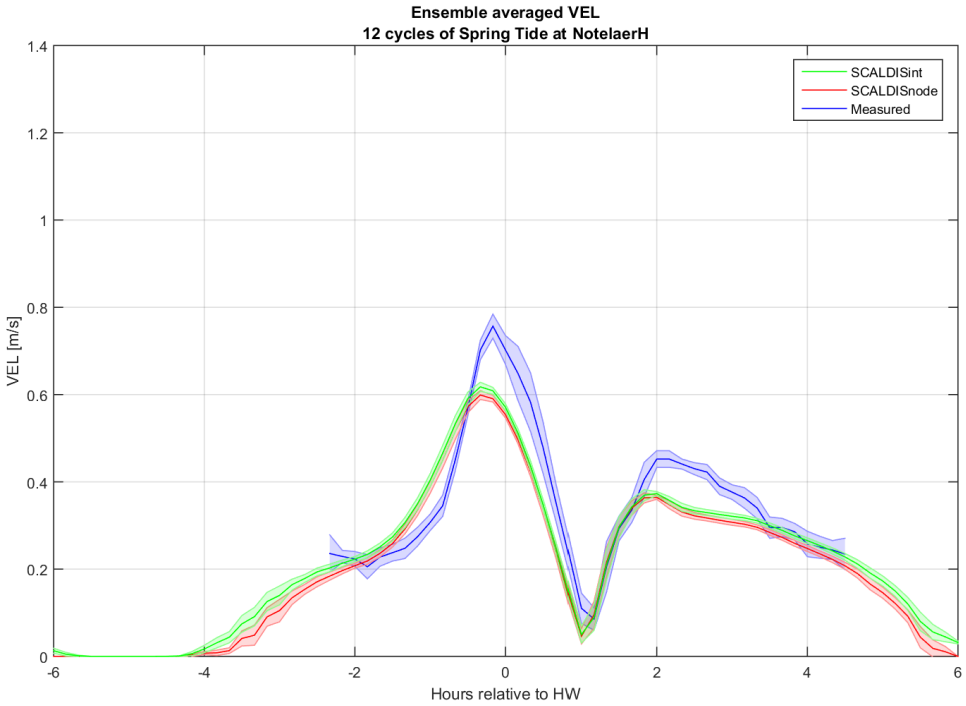

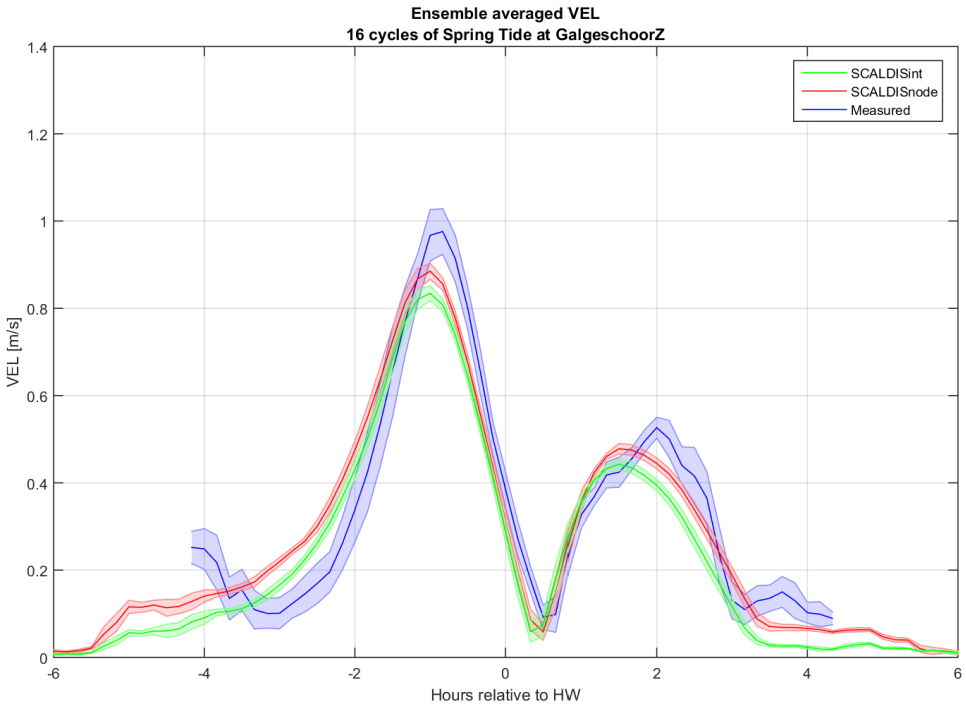

Measured (blue) – Computed at nearest node (red) – Computed (interpolation of nearest three nodes) (green)

Table 4 – Used node numbers at two selected locations in the SCALDIS-model.

Location	**Position**	**Node Nr.**		**Bottom level in SCALDIS-model [m TAW]**		**Height measured [m TAW]**
		nearest node	Interpolation nodes	nearest node	interpolation	
Galgeschoor South	South	295010	295010 295320 295204	+ 0.29	+ 0.923	+ 1.17
Notelaer	High	287013	287013 286981 286960	+ 1.41	+ 1.134	+ 1.34

6 Model validation results

This section describes the results of the SCALDIS-model with the new velocity measurements at each location separately. Results are presented beginning from the most downstream location “Saeftinghe” to the most upstream point “Appels”. For each location along the estuary, a short description of the layout of the measuring location and the cross-section profiles are presented.

SCALDIS-model results are compared with flow velocity measurements, using two different methods as described earlier in Section 5. The first one introduces the maximum water depth variation during flood phase and during ebb phase with the predicted, maximal depth-averaged velocities. This analysis starts from the hypothesis that high flow velocities are associated with high tidal ranges. Previous results of field measurements in the 'Westerschelde' showed a linear relationship between these two parameters (e.g. Jentink e.a. (2013)). Other results showed a rather logarithmic relationship (Plancke et al., 2014). In the second method the computed ensemble-averaged velocities are compared with the measured ensemble-averaged velocities, both averaged over depth. Ensemble-averaged velocities are computed for spring-, neap- and mean-tides.

6.1 Saeftinghe

On the east side of Saeftinghe, velocities were measured at two different locations. These two locations are shown in Figure 6 and are located about 930 meters apart. The velocity measurements were carried out between 20 July and 22 Augustus 2016 (see also Table 2). The measuring point at the north side was located at + 0.09 m TAW, the second point at the south is located at + 0.54 m TAW.

Figure 6 – Measuring locations at Saeftinghe (yellow dots).

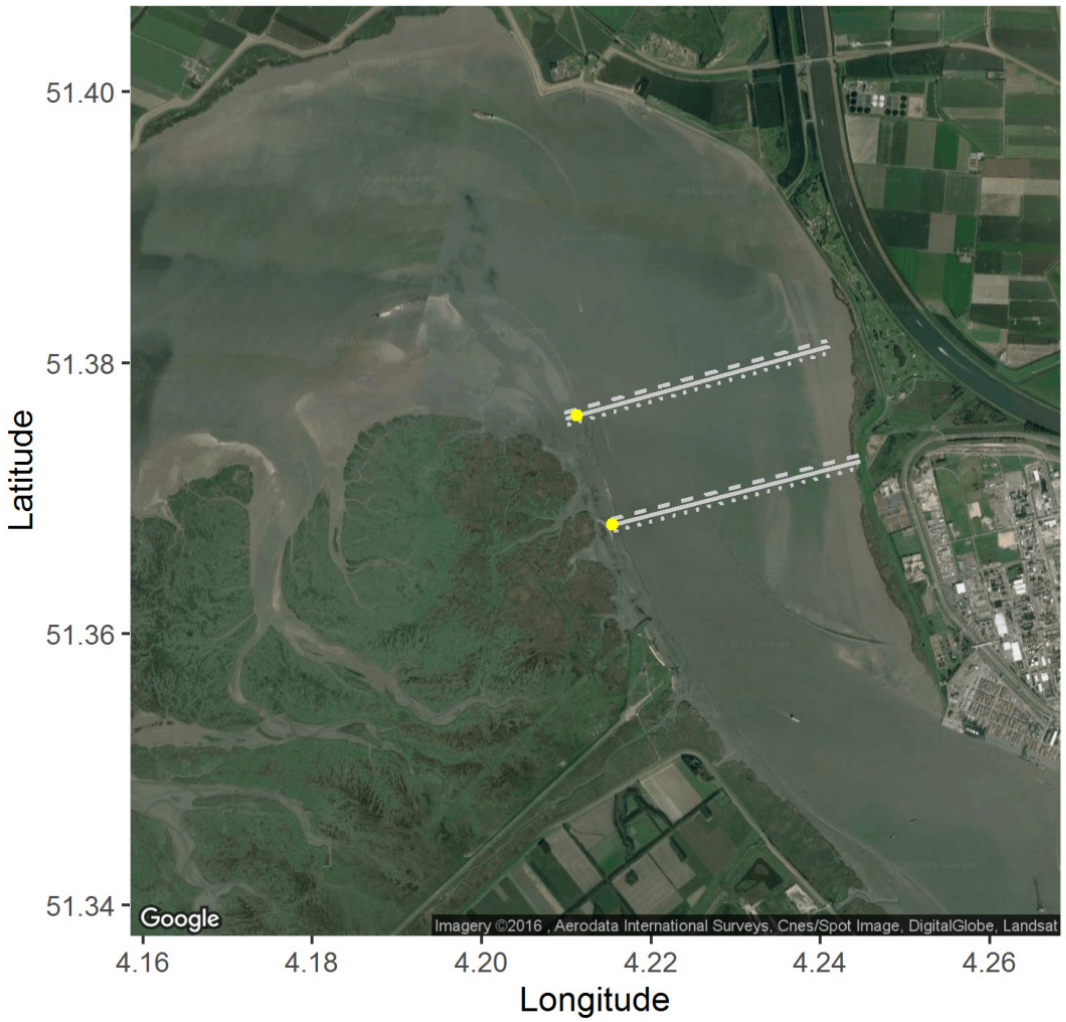

Figure 7 and Figure 8 present the measured cross-section profiles at Saeftinghe-North and Saeftinghe-South in the upper panels, respectively. The lower panels in the two figures introduce a comparison between the cross-section profiles as used in the SCALDIS-model and the measured profiles. In Figure 7 we can clearly observe a wall in the cross-section profile. In Figure 8 there is a clear increase in bottom height close to the fairway (around 750 m), due to the construction of the guiding wall. Two extra cross-section profiles at 50 m up- and down-stream of each location are presented as well in Figure 7 and Figure 8 (dashed lines in each figure) to check bottom variation around the measuring points.

Figure 7– Cross-section profiles at the measuring point, Saeftinghe-North, 50 m up- and down-stream (upper panel). The position of the measuring sensor is marked with a red circle. SCALDIS-model cross-section in the lower panel.

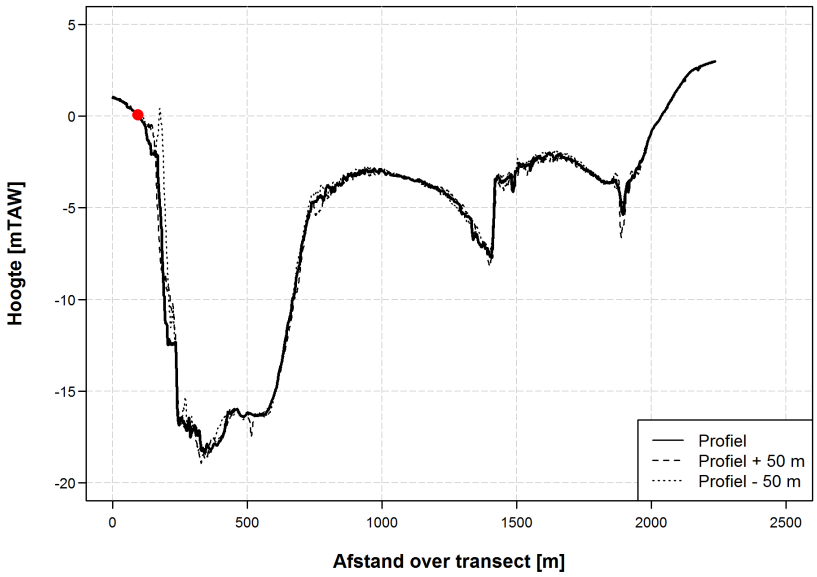

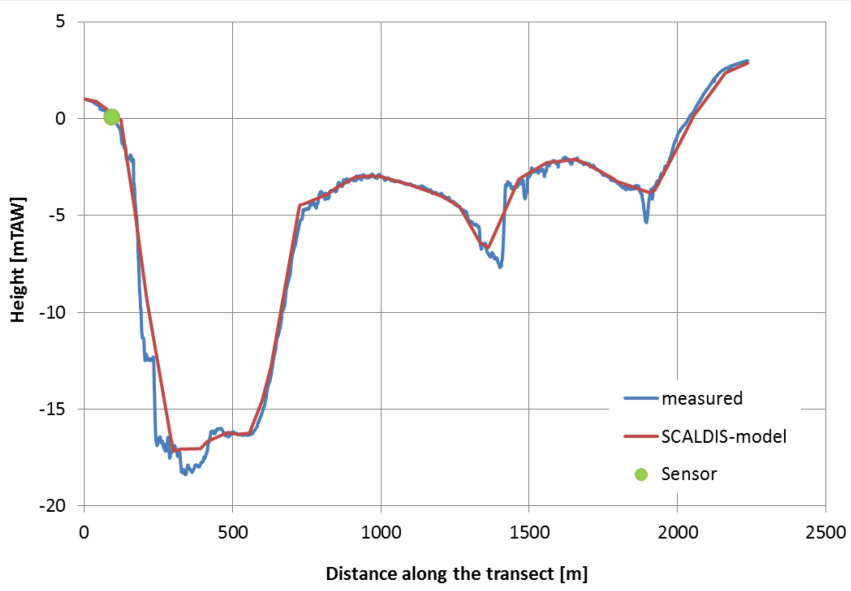

Figure 8 – Cross-section profiles at the measuring point, Saeftinghe-South, 50 m up- and down-stream.
The position of the measuring sensor is marked with a red circle. SCALDIS-model cross-section in the lower panel.

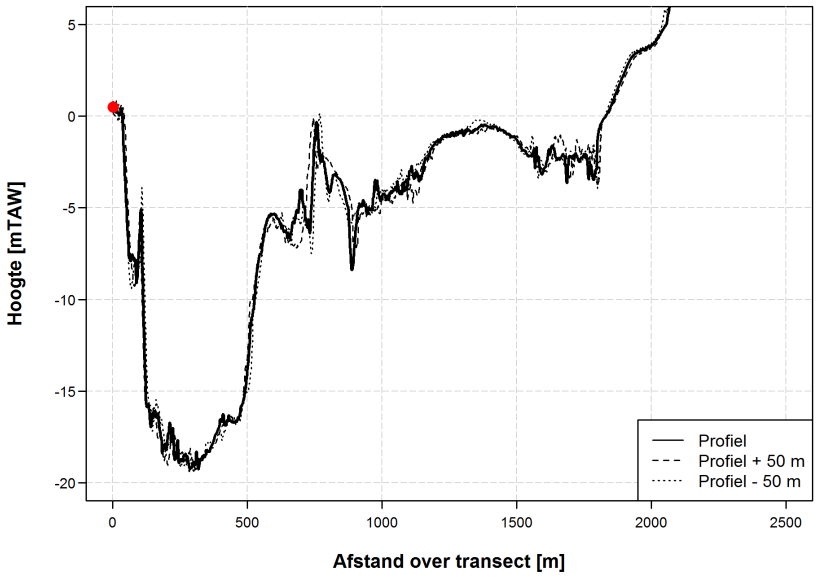

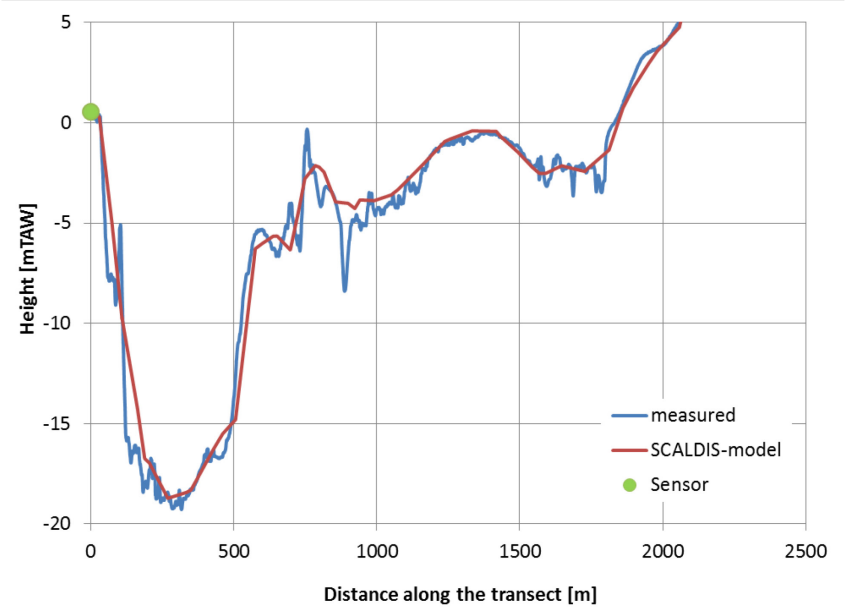

6.1.1 Ensemble-averaged velocities

The ensemble-averaged or phase-averaging analysis of model results is compared with the ensemble-averaged velocity measurements at Saeftinghe-North and Saeftinghe-south. In this analysis the measured and modeled depth-averaged velocities are split into individual tidal-cycles and averaged out over neap-, normal- and spring-tide. Figure 9 and Figure 10 show the results of this comparison of the spring-tide. Phase-averaging provides useful information on intertidal dynamics, and focuses the attention on flow system behavior by averaging out events that are more episodic. Results of averaged- and neap-tides are presented in Appendix 9.1.

Figure 9 and Figure 10 introduce the mean values of the ensemble-averaged velocities of the spring-tides as measured and computed at the two locations of Saeftinghe-North and Saeftinghe-South, respectively. Each mean value (solid-line) is surrounded by the STD (standard deviation) of the ensemble-averaged velocities. In general the model underpredicts the measured velocities at Saeftinghe-North during the full tidal-cycle (except around the moment of flow reversal). At Saeftinghe-South, the model shows a good performance during the flood phase. For the ebb phase, similar maximal velocities are found, but the peak in the measurements is shorter compared to the smooth peak in the model results.

Figure 9 – Measured (blue) and computed (red) flow velocities at Saeftinghe-North (spring tide).
The orange arrow shows the flood direction.

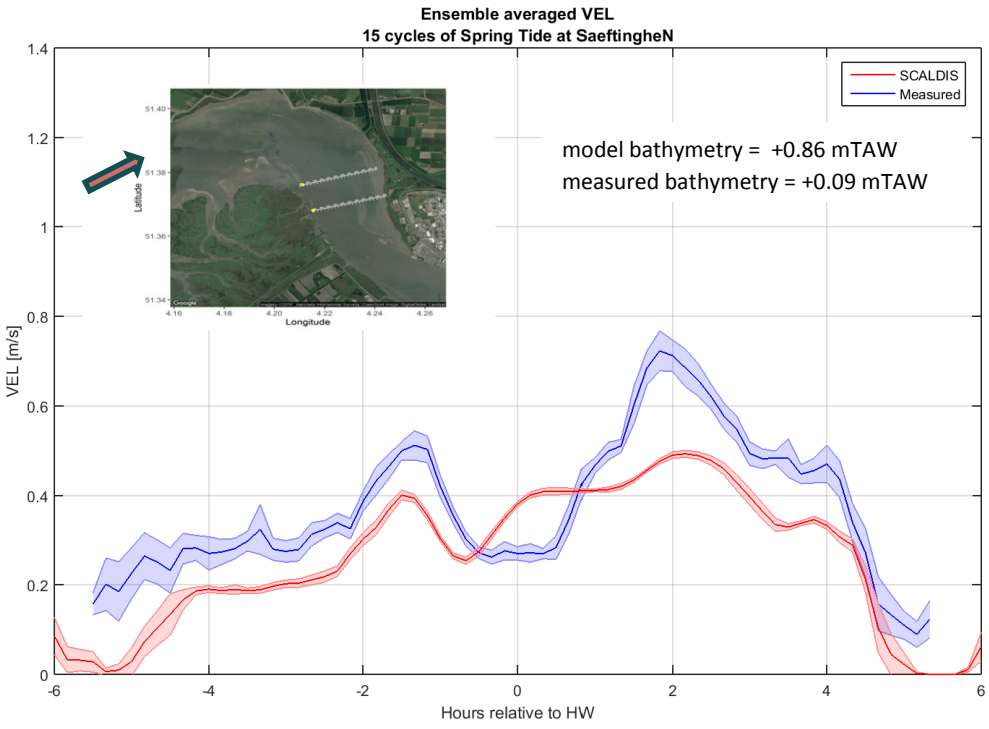

Figure 10 – Measured (blue) and computed (red) flow velocities at Saeftinghe-South (spring tide).
The orange arrow shows the flood direction.

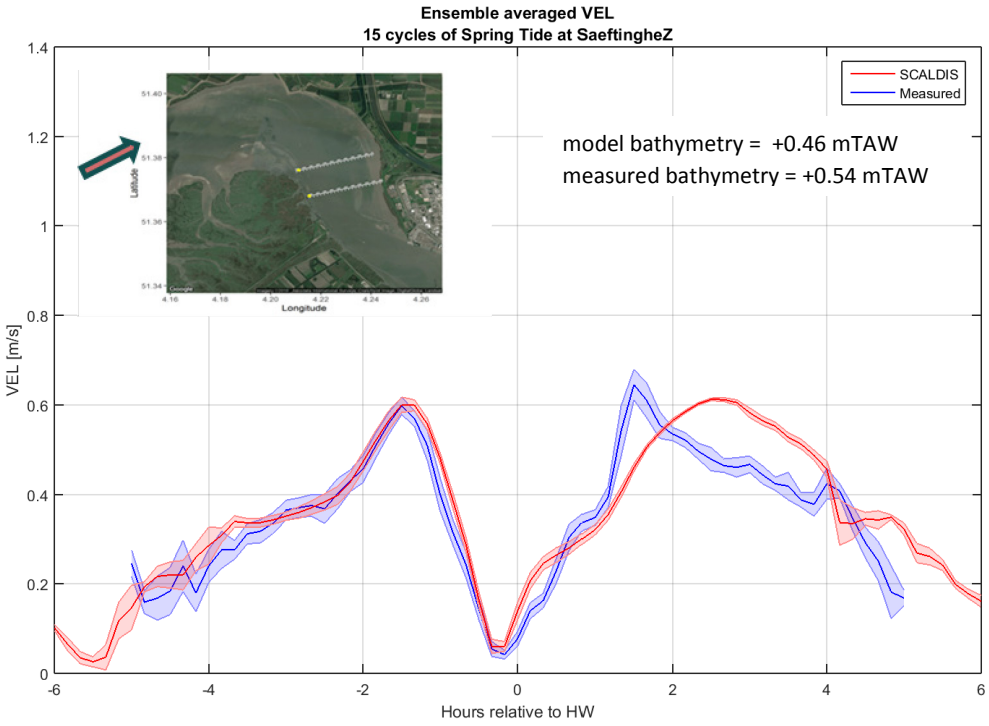

6.1.2 Water depth variation and flow velocities

Figure 11 shows the relationship between the increase in water levels and the depth-averaged maximum flood velocities (of each tidal-cycle) as measured and computed by SCALDIS-model. Figure 12 presents the same results with the maximum reduction of water levels and the depth-averaged maximum ebb velocities. In Figure 11 and Figure 12, closed symbols indicate the insitu measurements, and open symbols presents SCALDIS-model results. The two figures include also information about the layout of the location, cross-section profiles and the main flow direction, during flood and ebb phases (the orange arrows).

It is clear from the results that the measured flow velocities have more or less the same values during flood and ebb phases. Depth-averaged velocity magnitudes are increased with increasing water depth variation with almost a linear relation.

It is clear from the results that SCALDIS-model is in general underpredicting the measured velocities at Saeftinghe-North and Saeftinghe-South. However, the model shows a better agreement with the measurements at Saeftinghe-South during flood phase. Also for the ebb phase, the model and measurmeents agree better in the southern transect. In general, we can observe a linear relation between water depth variation and the depth-averaged velocities both in Figure 11 and Figure 12 for both the measured and computed values.

Figure 11 – Relation between water depth variation and depth-averaged maximum flow velocities as measured and computed by SCALDIS-model during flood at Saeftinghe, Saeftinghe-North (orange) and Saeftinghe-south (purple).

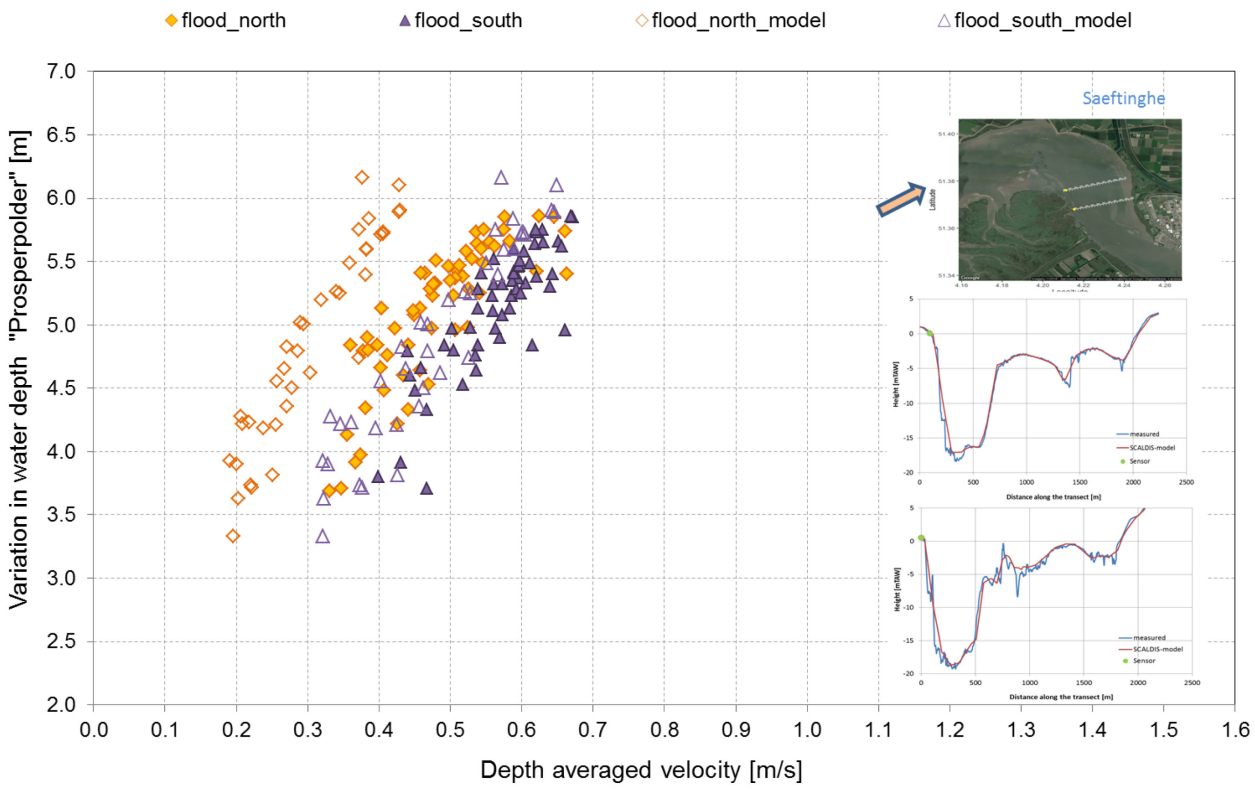

Figure 12 – Relation between water depth variation and depth-averaged maximum flow velocities as measured and computed by SCALDIS-model during ebb at Saeftinghe, Saeftinghe-North (orange) and Saeftinghe-south (purple).

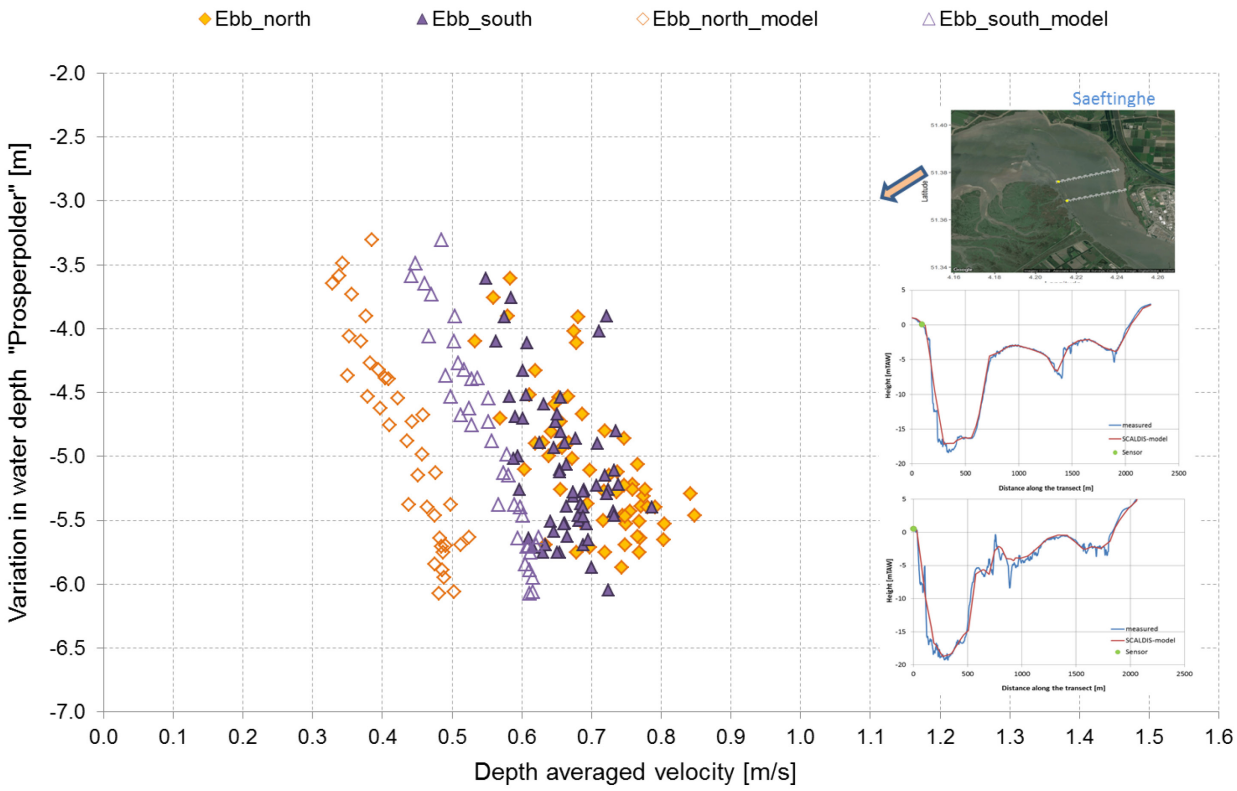

6.2 Galgeschoor

The measuring locations at Galgeschoor are shown in Figure 13. These measurements are just similar to Saeftinghe locations, at low locations close to the low water line. One measurement was performed at the north side (+ 0.59 m TAW) and the second measurement, at the south side of Galgeschoor (+ 1.17 m TAW). The distance between the two points is approximately 1040 m. The measurements were carried out from 28 October to 2 December 2016.

Figure 13 – Measuring locations at Galgeschoor (yellow dots).

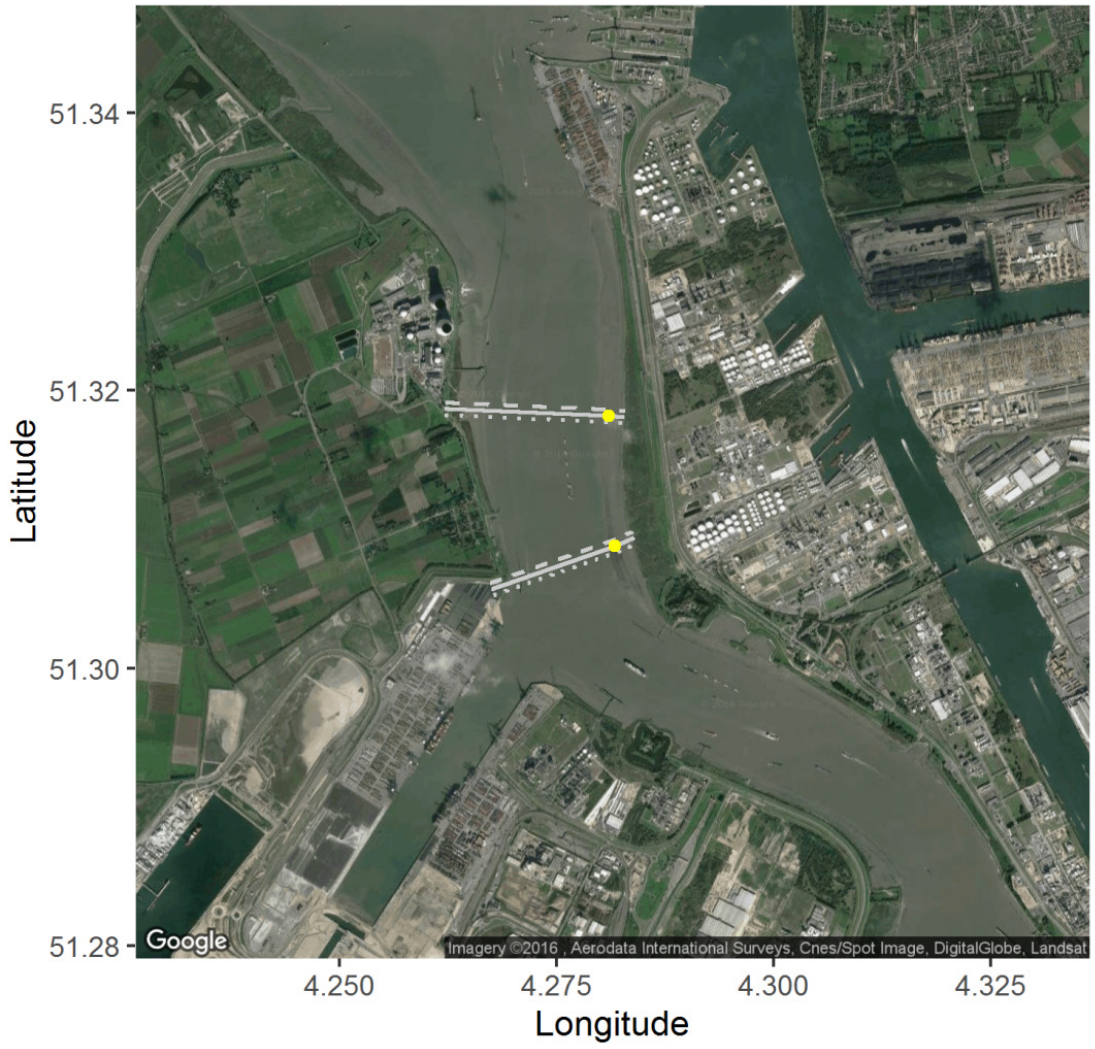

The cross-section profiles at the two measuring locations are shown in the upper panels of Figure 14 and Figure 15 for Galgeschoor-North and Galgeschoor-South, respectively. The transition from the fairway to the shallow area is more gradual in the northern transect (Figure 14) than in the southern transect (Figure 15). The lower panels in Figure 14 and Figure 15 introduce comparison between the cross-section profiles as used in the SCALDIS-model and the measured profiles.

Figure 14 – Cross-section profiles at the measuring point, Galgeschoor-North, 50 m up- and down-stream.
The position of the measuring sensor is marked with a red circle. SCALDIS-model cross-section in the lower panel.

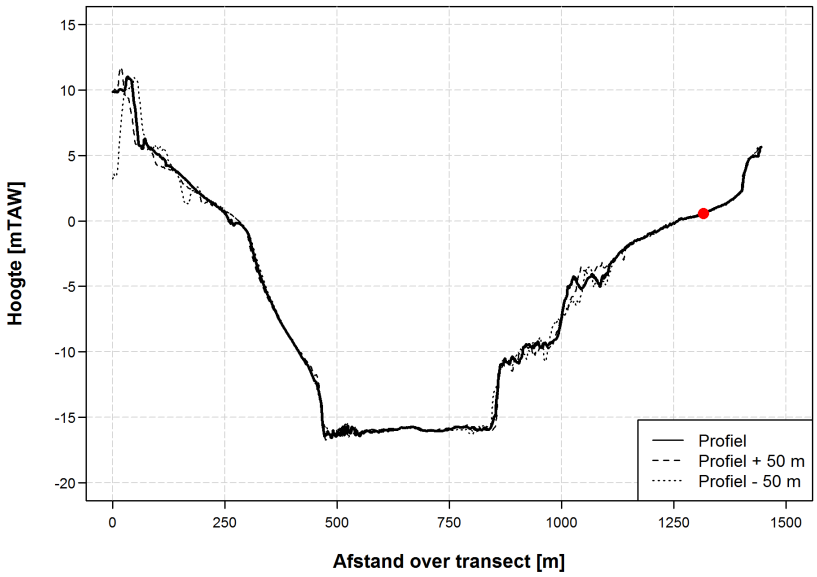

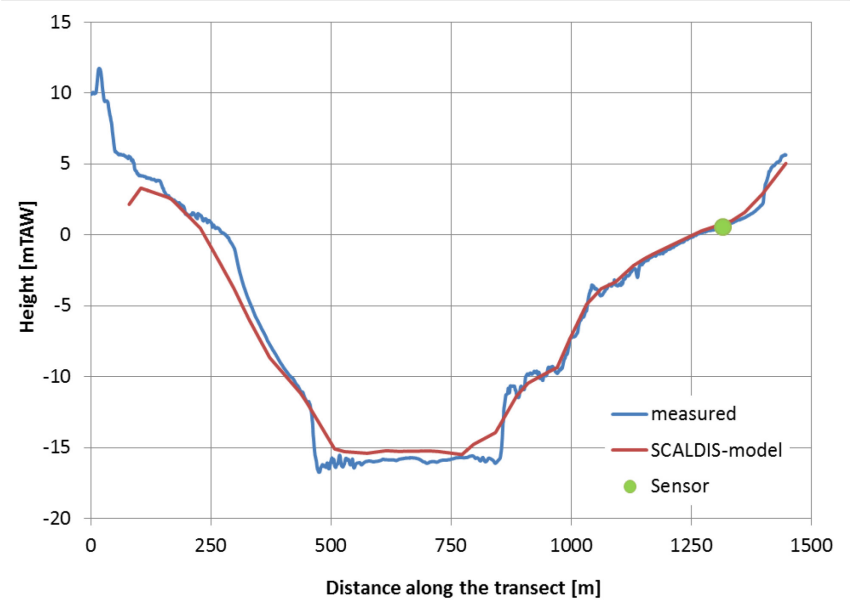

Figure 15 – Cross-section profiles at the measuring point, Galgeschoor-South, 50 m up- and down-stream.
The position of the measuring sensor is marked with a red circle. SCALDIS-model cross-section in the lower panel.

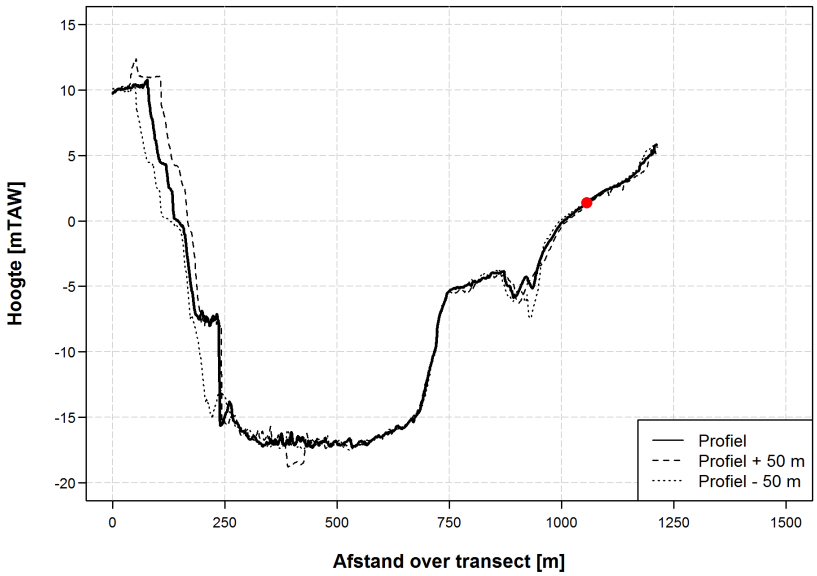

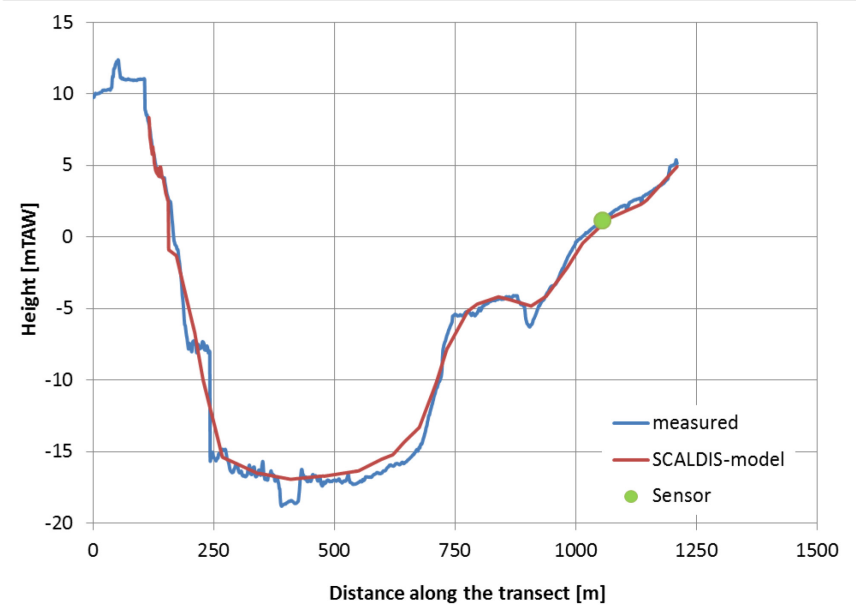

6.2.1 Ensemble-averaged velocities

Figure 16 and Figure 17 introduce the mean values of the ensemble-averaged velocities of the spring tides as measured and computed at the two locations of Galgeschoor-North and Galgeschoor-South, respectively. Each mean value (solid-line) is surrounded by the STD (standard deviation) of the ensemble-averaged velocities. Results of averaged and neap tides are presented in Appendix 9.2.

In general the model is able to show a good agreement with the measured data, with little underproductions of velocity magnitudes, during the maximum flood and maximum ebb flows. The order of magnitude difference between the maximum velocities (measured vs. computed) is approximately 0.1 m/s. The model is able to show the same form of velocity magnitudes at the two locations of Galgeschoor.

Figure 16 – Measured (blue) and computed (red) flow velocities at Galgeschoor-North (spring tide). The orange arrow shows the flood direction.

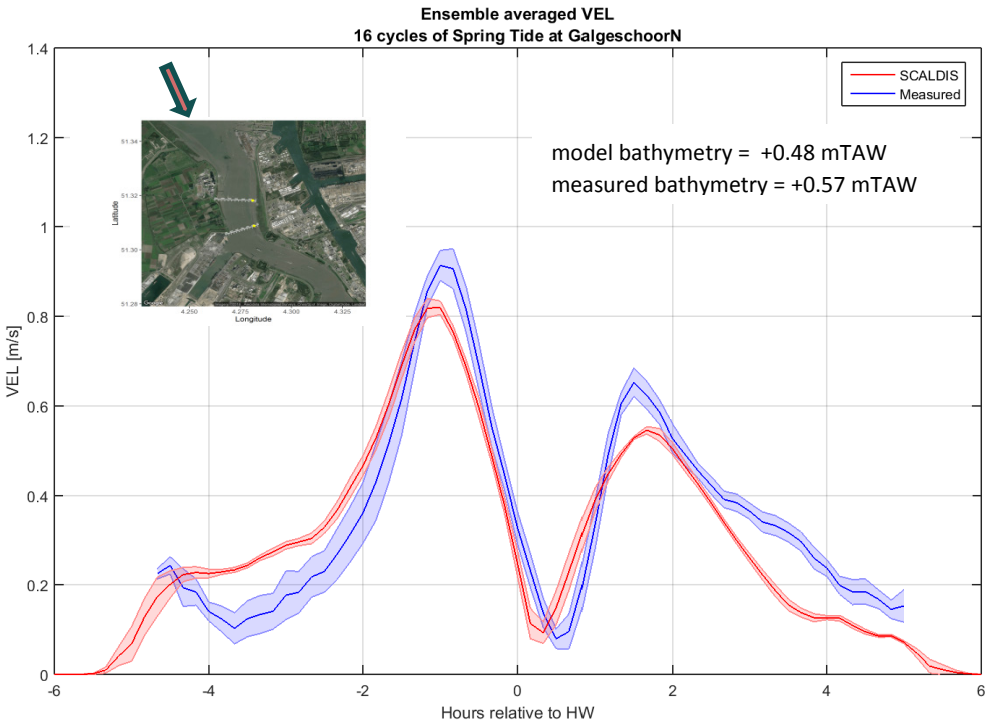

Figure 17 – Measured (blue) and computed (red) flow velocities at Galgeschoor-South (spring tide).
The orange arrow shows the flood direction.

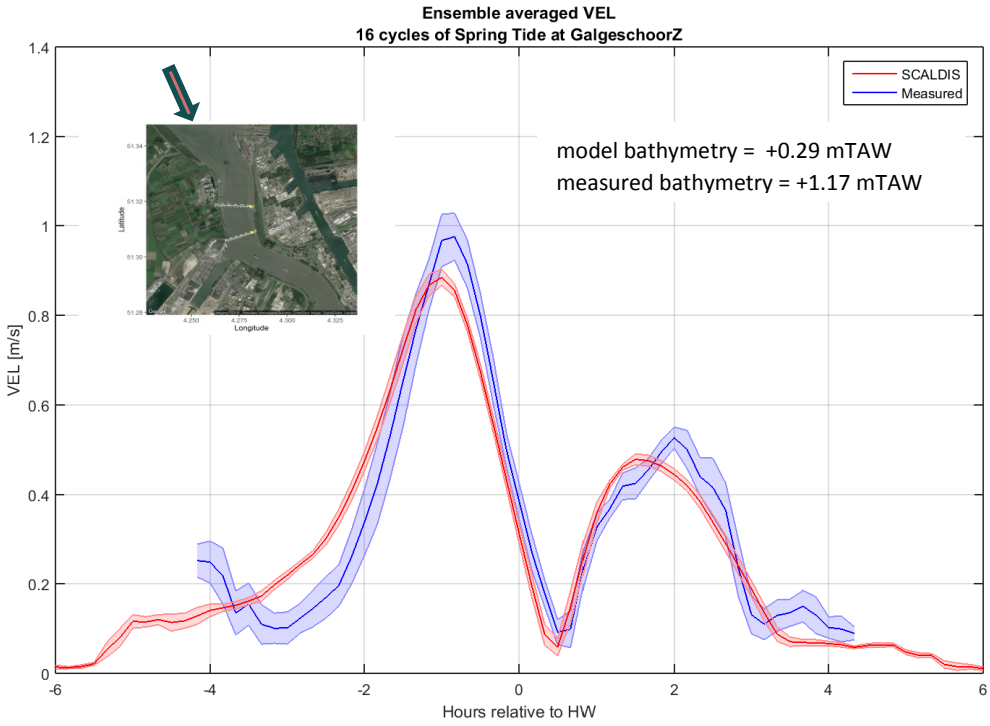

6.2.2 Water depth variation and flow velocities

Similar results as presented previously at Saeftinghe are introduced at the location of Galgeschoor, to show the relation between the increase/decrease in water levels and the depth-averaged maximum flood velocities. The measured and computed by SCALDIS-model results are presented in Figure 18 and Figure 19 for flood and ebb phases, respectively.

It is clear from the results that the model is able to predict quite well the measured velocities, except at high velocity range u > 0.8 m/s, during flood phase (Figure 18).

Measured flow velocities during the ebb phase (Figure 19) showed a large scatter at the two measuring locations. These velocities are slightly underestimated by the model. Again the depth-averaged-velocity magnitudes are increased with increasing water depth variation with a linear relation as shown at Saeftinghe.

Figure 18 – Relation between water depth variation and depth-averaged maximum flow velocities as measured and computed by SCALDIS-model during flood at Galgeschoor, Galgeschoor-North (orange) and Galgeschoor-south (purple).

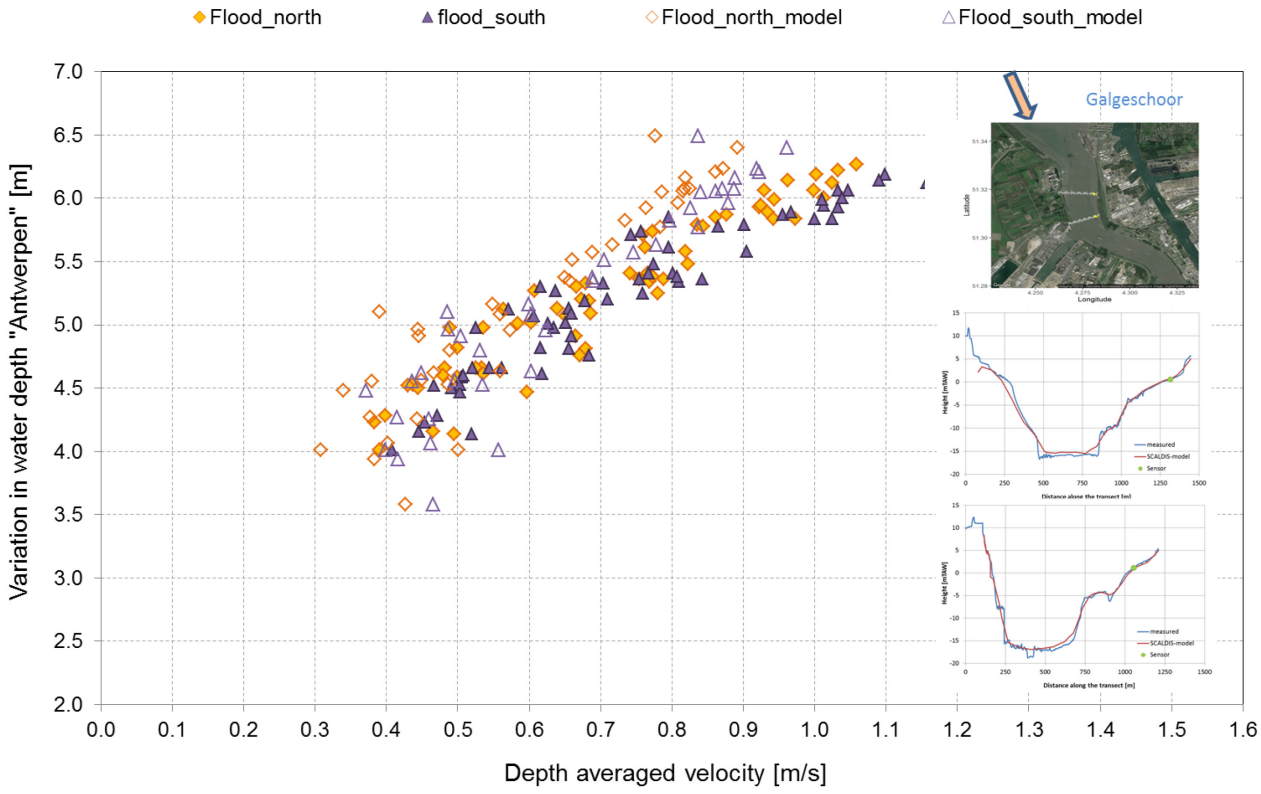

Figure 19 – Relation between water depth variation and depth-averaged maximum flow velocities as measured and computed by SCALDIS-model during ebb at Galgeschoor, Galgeschoor-North (orange) and Galgeschoor-south (purple).

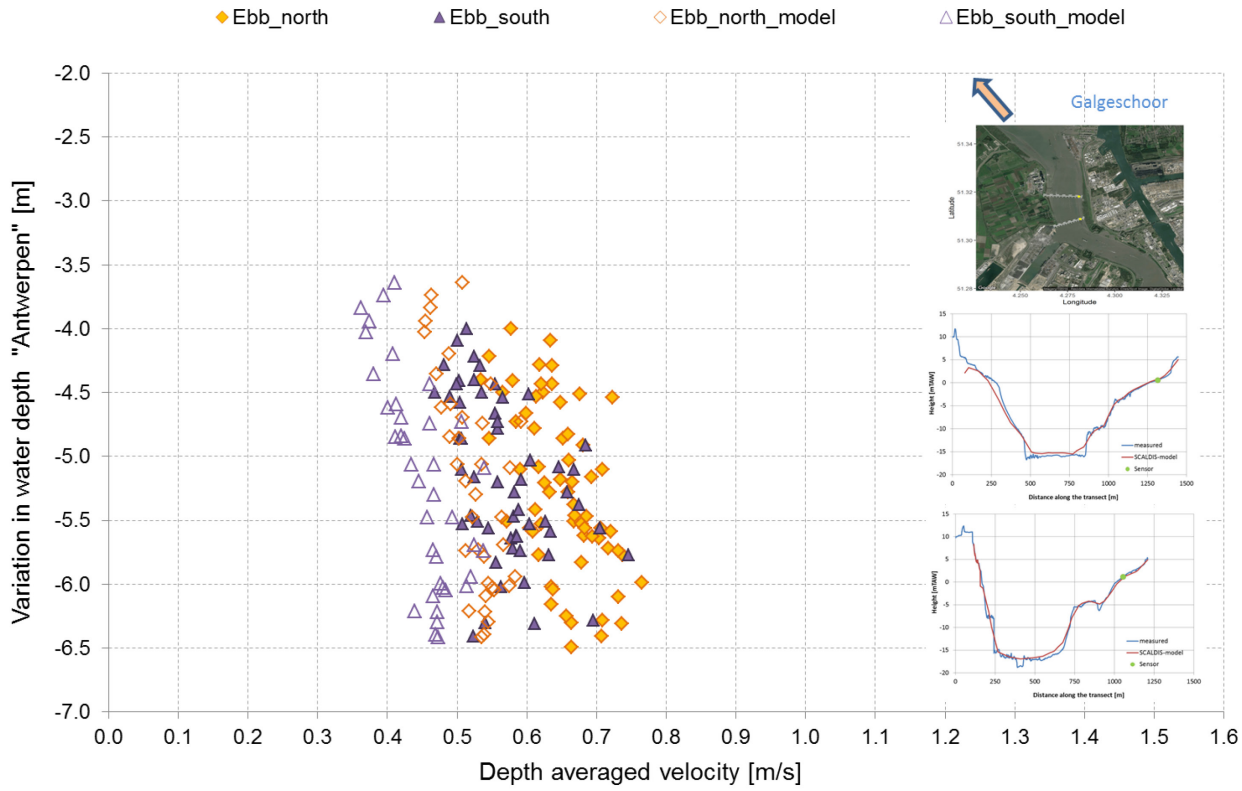

6.3 Ketenisse

The locations of the measuring points at Ketenisse are presented in Figure 20, which are located on the same cross-section. One location is located on low level 'laag slik' (+ 0.19 m TAW) and the second one on high level 'hoog slik' (+ 3.34 m TAW). The distance between the two points is about 60 m. The velocity measurements were carried out from 20 August to 22 September 2015. Figure 21 presents the cross-section profiles at Ketenisse as measured in the field (upper panel) and as used in the SCALDIS-model (lower panel).

Figure 20 – Measuring locations at Ketenisse (yellow dots).

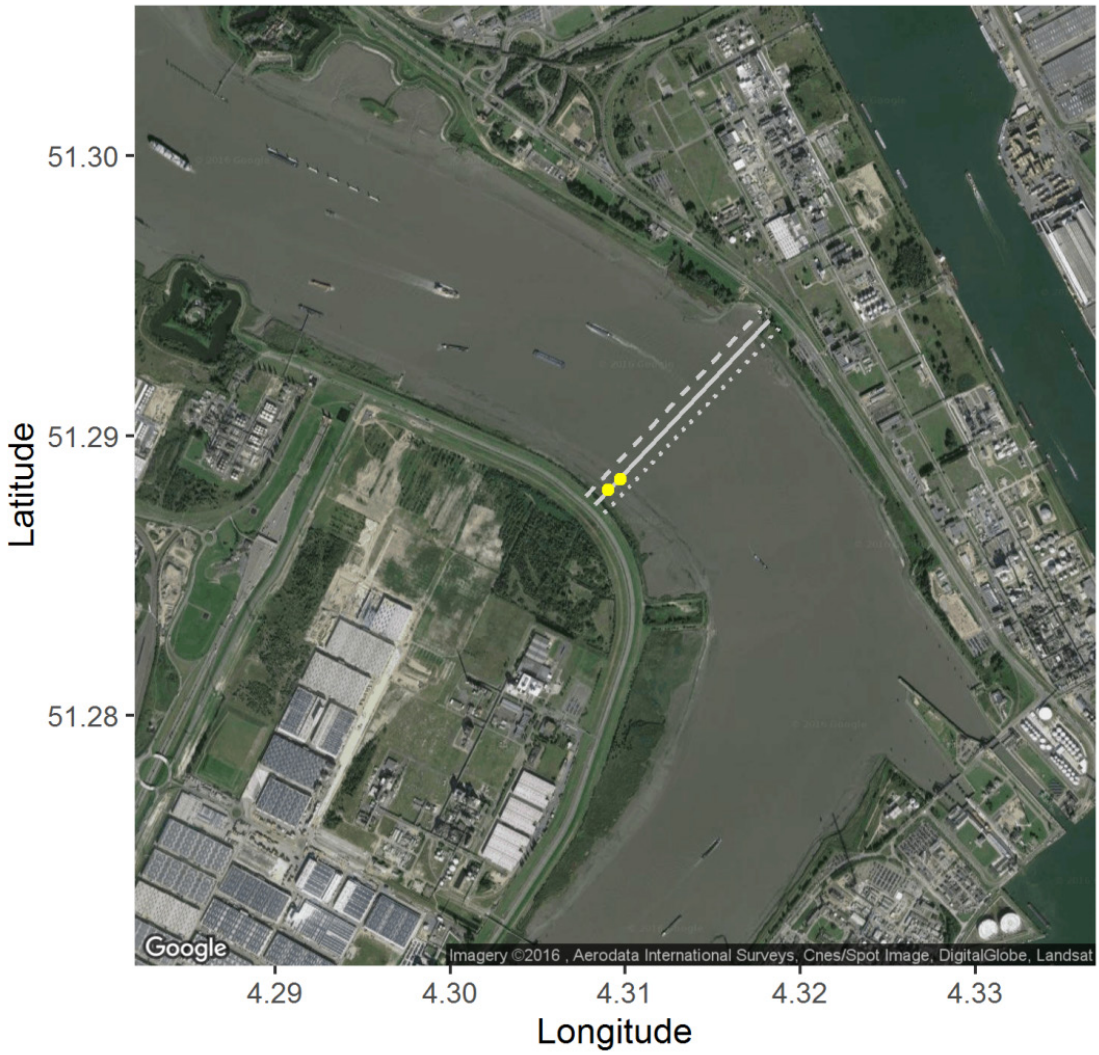

Figure 21 – Cross-section profiles at the measuring points, Ketenisse, 50 m up- and down-stream. The position of the measuring sensors is marked with a red circle. SCALDIS-model cross-section in the lower panel.

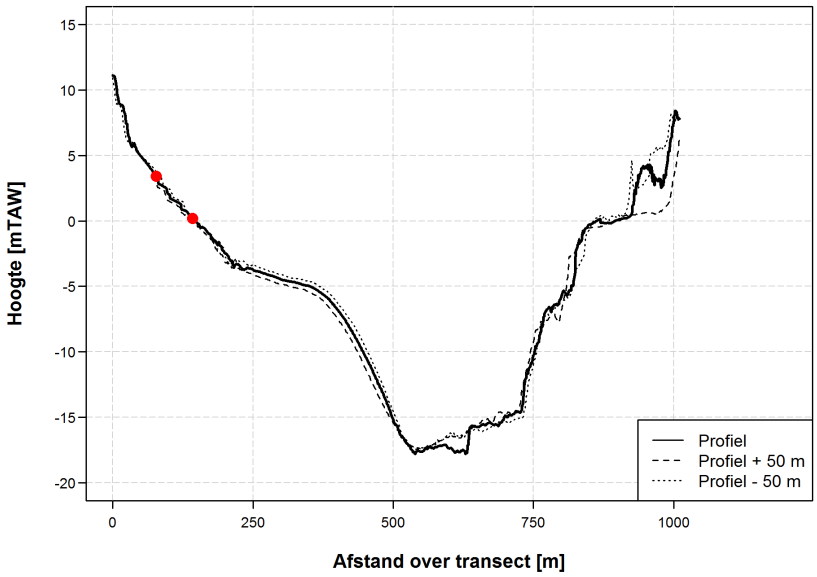

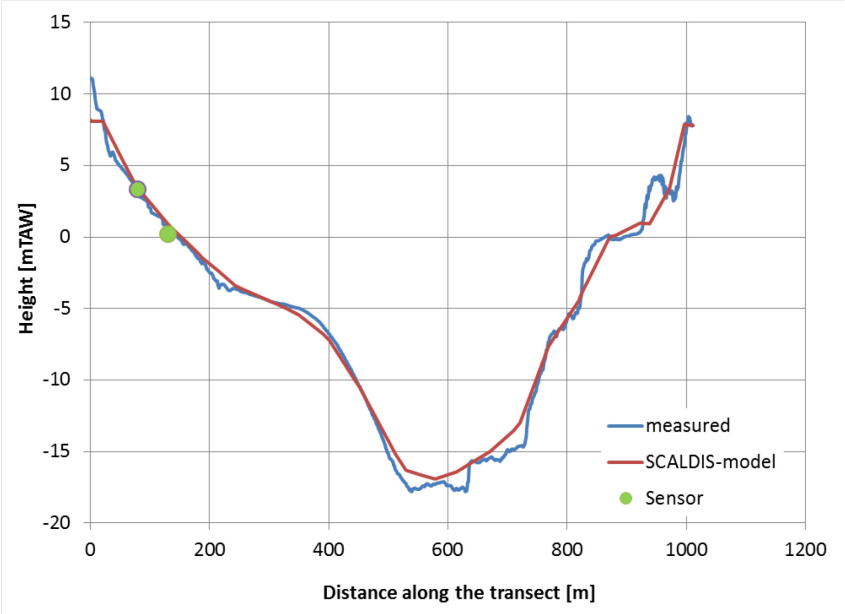

6.3.1 Ensemble-averaged velocities

Figure 22 and Figure 23 introduce the mean values of the ensemble-averaged velocities of the spring tides as measured and computed at the two locations of Ketenisse-high and Ketenisse-low, respectively. Each mean value (solid-line) is surrounded by the STD (standard deviation) of the ensemble-averaged velocities. Results of averaged- and neap-tides are presented in Appendix 9.3.

In general the model is able to produce the same velocity form at Ketenisse-high with a slight overestimation of the maximum flood velocity (Figure 22) of approximately 0.1 m/s. On the other hand the model underestimates maximum flood velocities at Ketenisse-low (Figure 23), with a difference of approx. 0.2 m/s. The velocity variation during ebb phase is not reproduced correctly, as the recirculation cell is not shown in model results.

Figure 22 – Measured (blue) and computed (red) flow velocities at Ketenisse-High (spring tide). The orange arrow shows the flood direction.

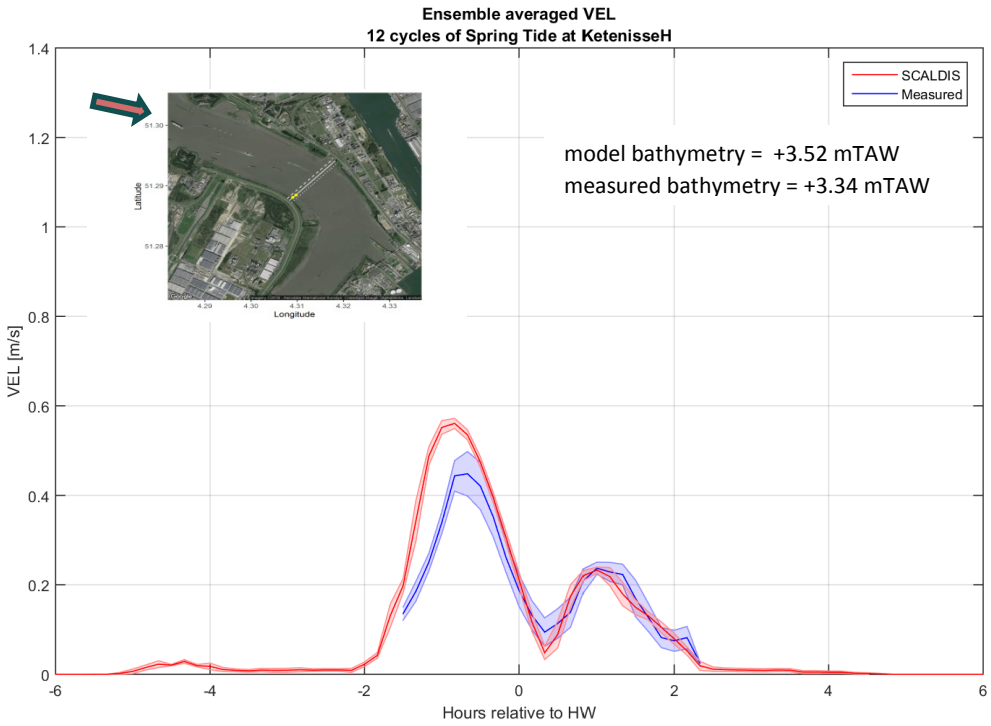

Figure 23 – Measured (blue) and computed (red) flow velocities at Ketenisse-Low (spring tide).
The orange arrow shows the flood direction.

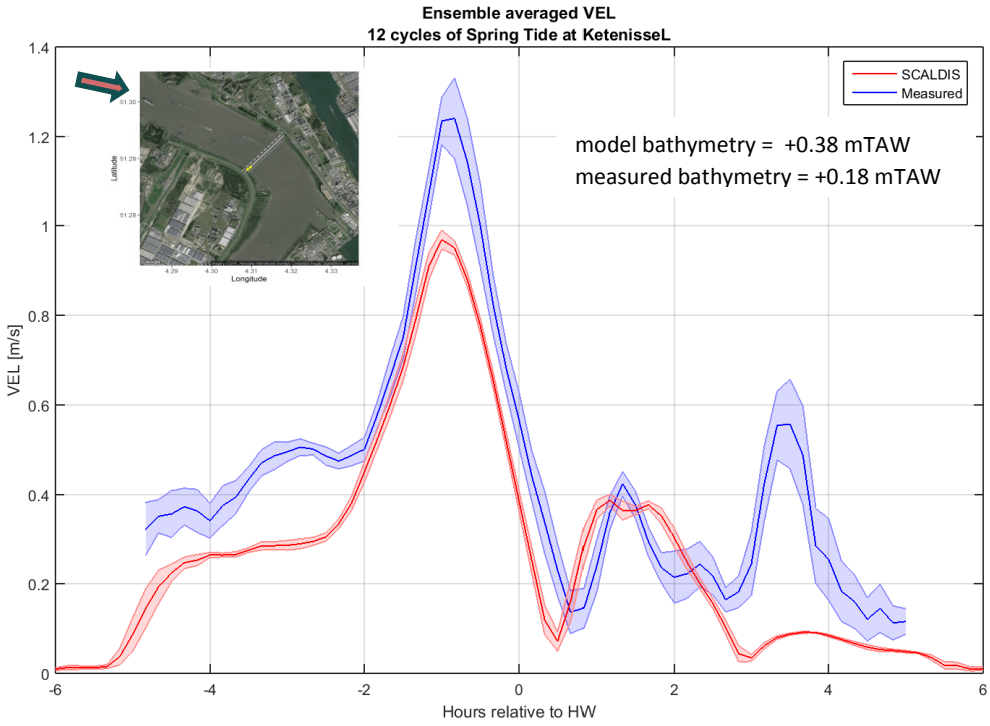

6.3.2 Water depth variation and flow velocities

Figure 24 and Figure 25 show the relation between the increase/decrease in water levels and the depth-averaged maximum flood/ebb velocities. The measured values and SCALDIS-model results are presented at the two measuring locations.

It is clear from the flood phase results that the model is underpredicting flow velocities at the low level location for all water depths. On the other hand flow velocities are slightly overpredicted by the model at the high level location. The SCALDIS-model shows a reasonably good agreement with the measurements during the ebb phase (Figure 25) except at high velocity range u > 0.5 m/s, which coincides with tidal ranges higher than 5.5 m. This is due to the recirculation velocity, which is only on tides with a high tidal range, and is clearly shown in Figure 23.

Figure 24 – Relation between water depth variation and depth-averaged maximum flow velocities as measured and computed by SCALDIS-model during flood at Ketenisse, Ketenisse-Low (orange) and Ketenisse-High (purple).

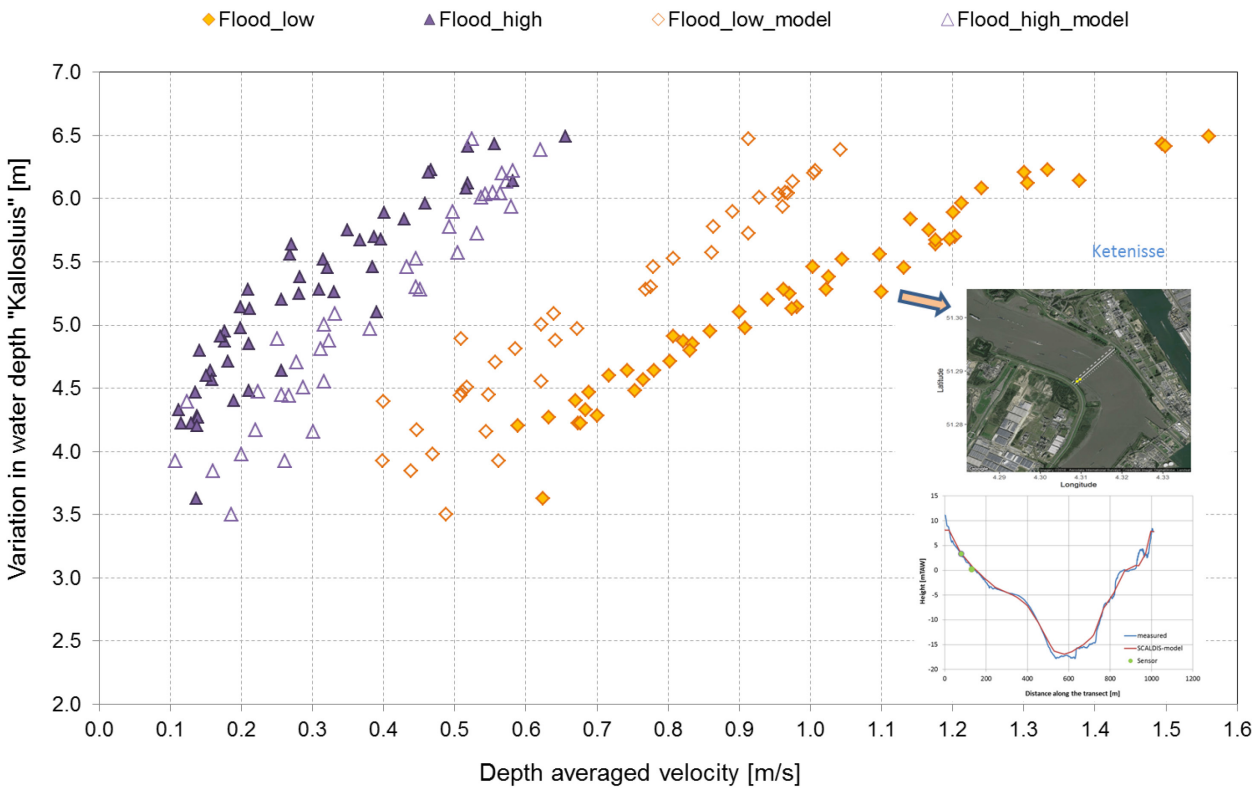

Figure 25 – Relation between water depth variation and depth-averaged maximum flow velocities as measured and computed by SCALDIS-model during ebb at Ketenisse, Ketenisse-Low (orange) and Ketenisse-High (purple).

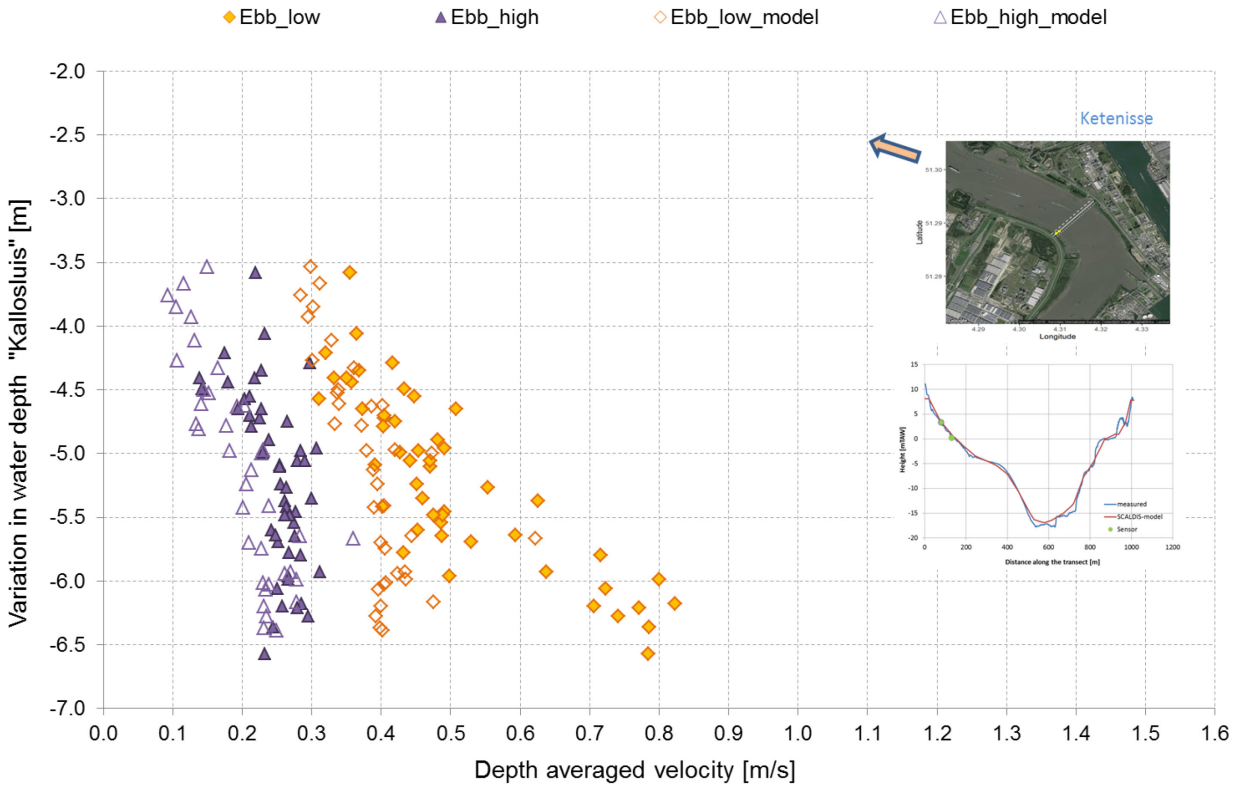

6.4 Plaat van Boomke

Boomke plate is situated on the right bank of the Scheldt estuary, almost opposite of the tidal gauge of Oosterweel. The locations of the measurements at Boomke are shown in Figure 26. These two measuring locations are on the same cross-section, one is located on Boomke-low (+ 0.09 m TAW) and the second one Boomke-high on (+ 2.41 m TAW). The distance between the two points is approximately 10 m.

The measured cross-section profiles at Boomke are presented in the upper panel of Figure 26. The lower panel includes the cross-section profile as used in the SCALDIS-model in comparison with the measured one.

Figure 26 – Measuring locations at Plaat van Boomke (yellow dots).

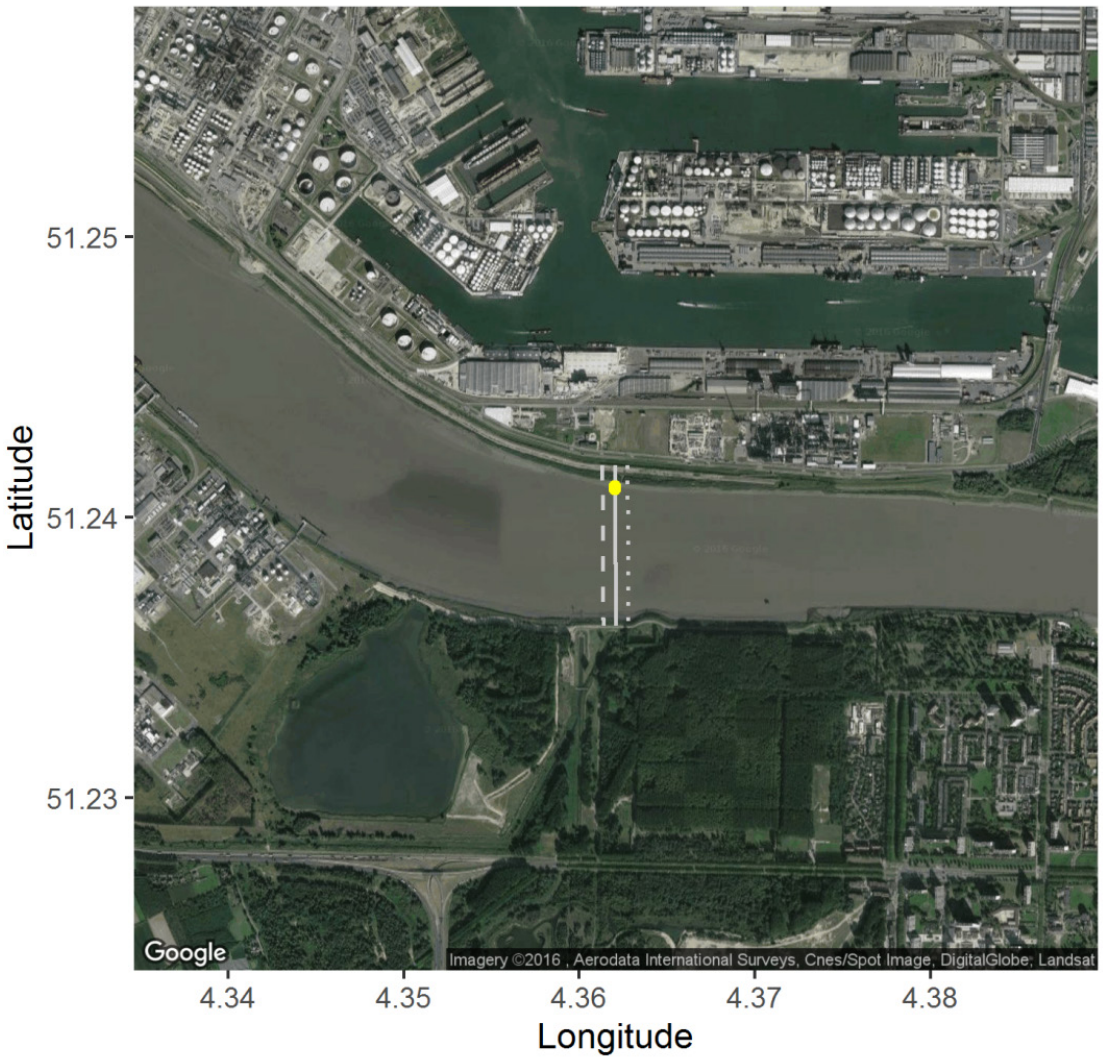

Figure 27 – Cross-section profiles at the measuring points, Boomke 50 m up- and down-stream.
The position of the measuring sensors is marked with a red circle. SCALDIS-model cross-section in the lower panel.

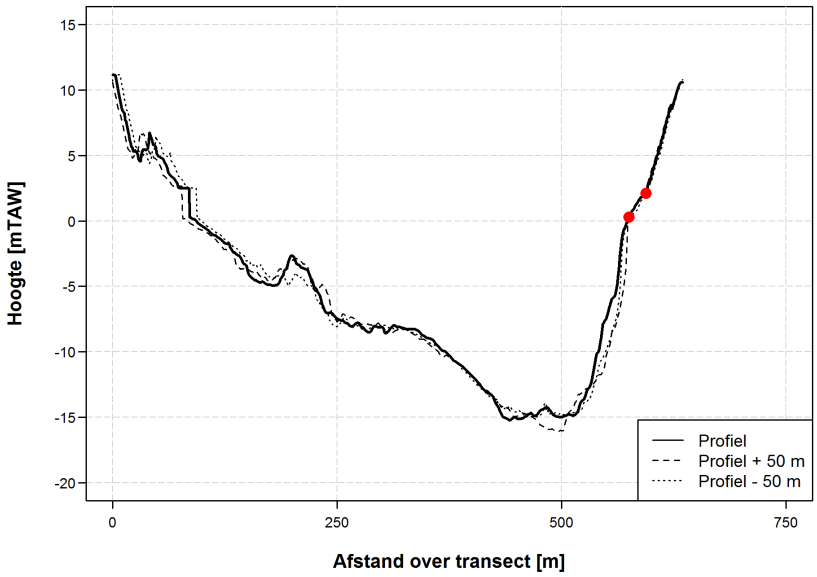

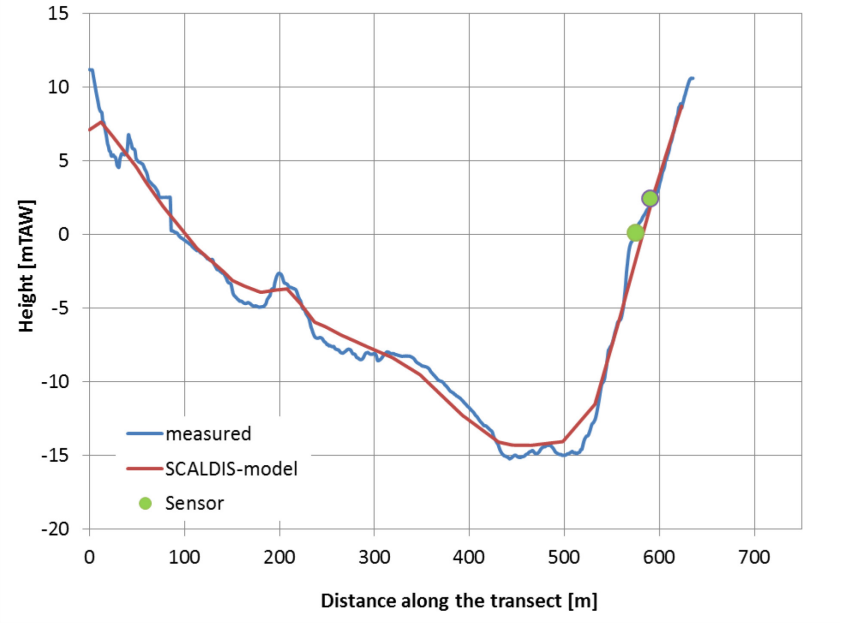

6.4.1 Ensemble-averaged velocities

Ensemble-averaged velocities of the spring tides as measured and computed using SCALDIS-model are presented in Figure 28 and Figure 29 at Boomke-High and Boomke-Low, respectively. Results of averaged and neap tides are presented in Appendix 9.4.

The model represents the velocities at Boomke-High (Figure 28) wel, especially for the ebb phase. For the flood phase the model overestimates slightly the measured velocities (approx. 0.1 m/s). At Boomke-Low (Figure 29) both the ebb and flood peaks are underestimated by the model, with approximately 0.2 m/s. The general patterns of the flow velocities over the tide and the moments of slack are well represented by the model.

Figure 28 – Measured (blue) and computed (red) flow velocities at Boomke-High (spring tide).
The orange arrow shows the flood direction.

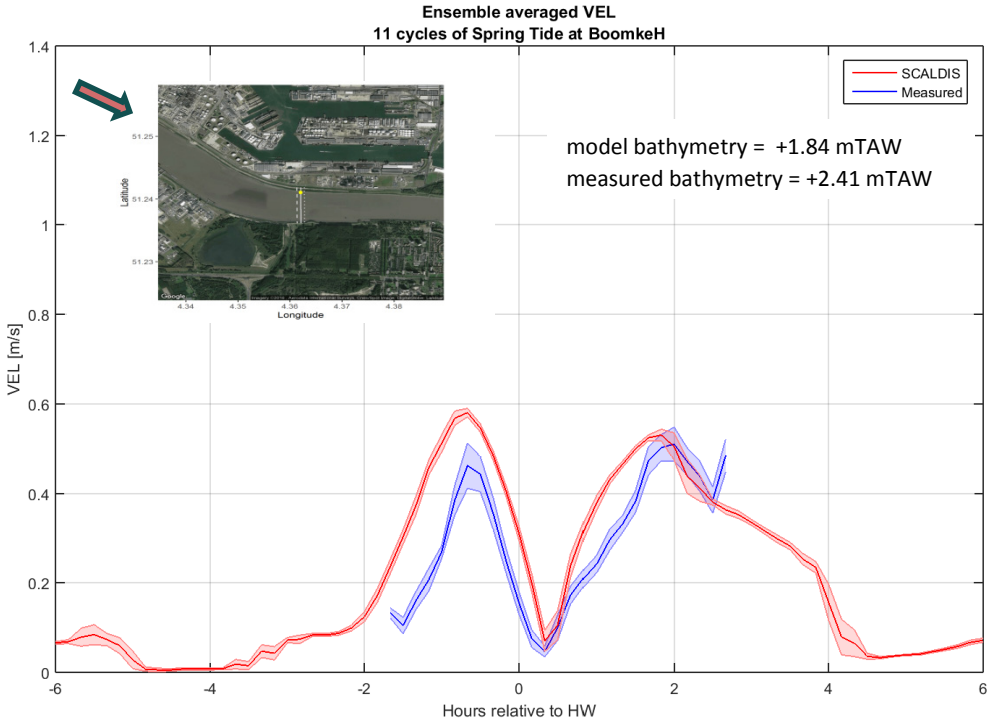

Figure 29 – Measured (blue) and computed (red) flow velocities at Boomke-Low (spring tide).
The orange arrow shows the flood direction.

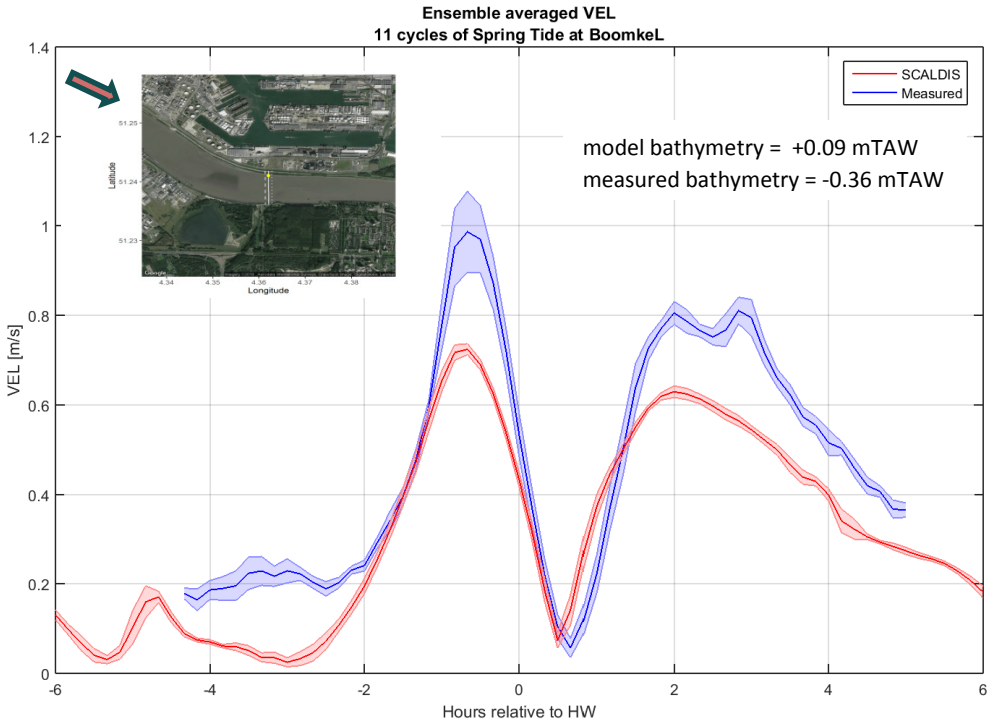

6.4.2 Water depth variation and flow velocities

Measured and computed depth-averaged velocities against the water depth variation during flood and ebb phases are presented in Figure 30 and Figure 31, respectively at Boomke-High and Boomke-Low locations. During the flood phase the model overestimates velocities at Boomke-High ($u < 0.55$ m/s). At Boomke-Low the model underpredicts flow velocity magnitudes in the high velocity range ($u > 0.7$ m/s). The measured flow velocities seem to react much more on a change in the tidal range, compared to the model.

In Figure 30 the model underpredicts flow velocities at Boomke-High and Boomke-Low. The difference between the model results and measurements is more pronounced at Boomke-Low. The curves on both locations are similar in the model and the measurements.

Figure 30 – Relation between water depth variation and depth-averaged maximum flow velocities as measured and computed by SCALDIS-model during flood at Boomke, Boomke-Low (orange) and Boomke-High (purple).

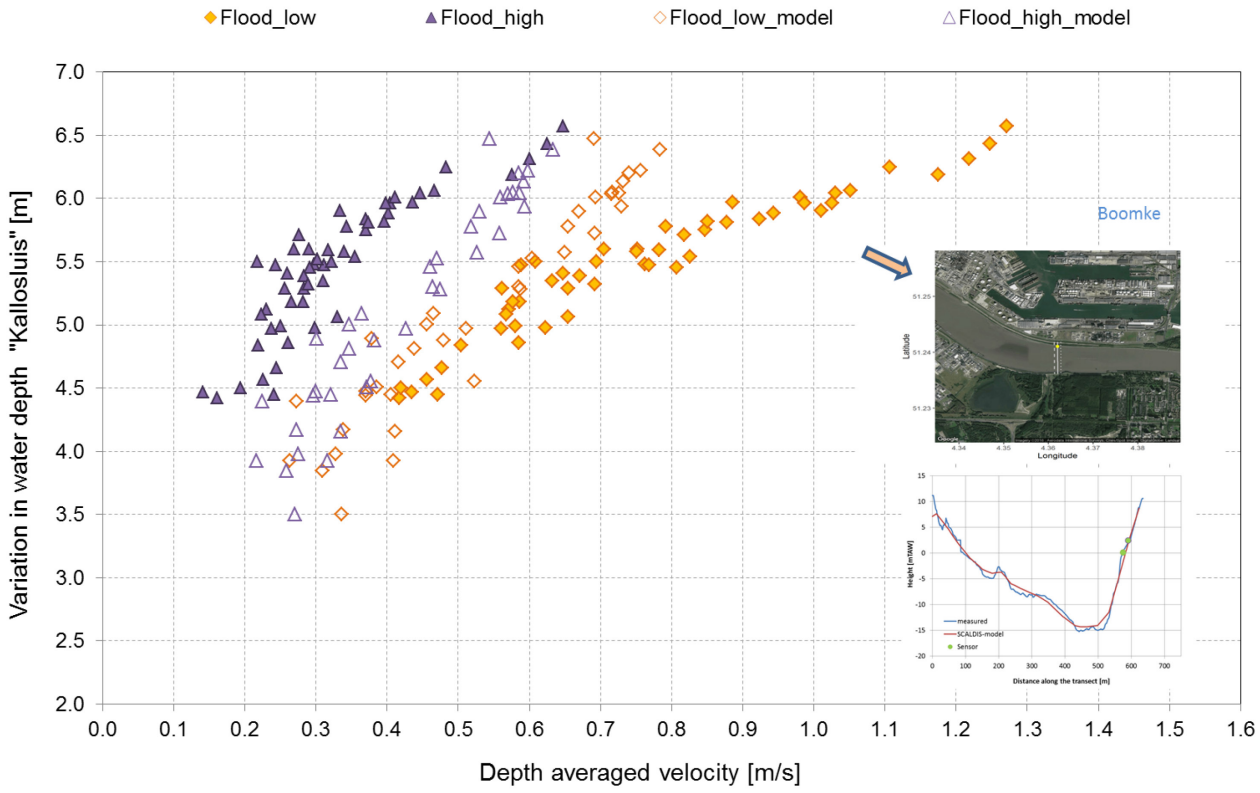

Figure 31 – Relation between water depth variation and depth-averaged maximum flow velocities as measured and computed by SCALDIS-model during ebb at Boomke, Boomke-Low (orange) and Boomke-High (purple).

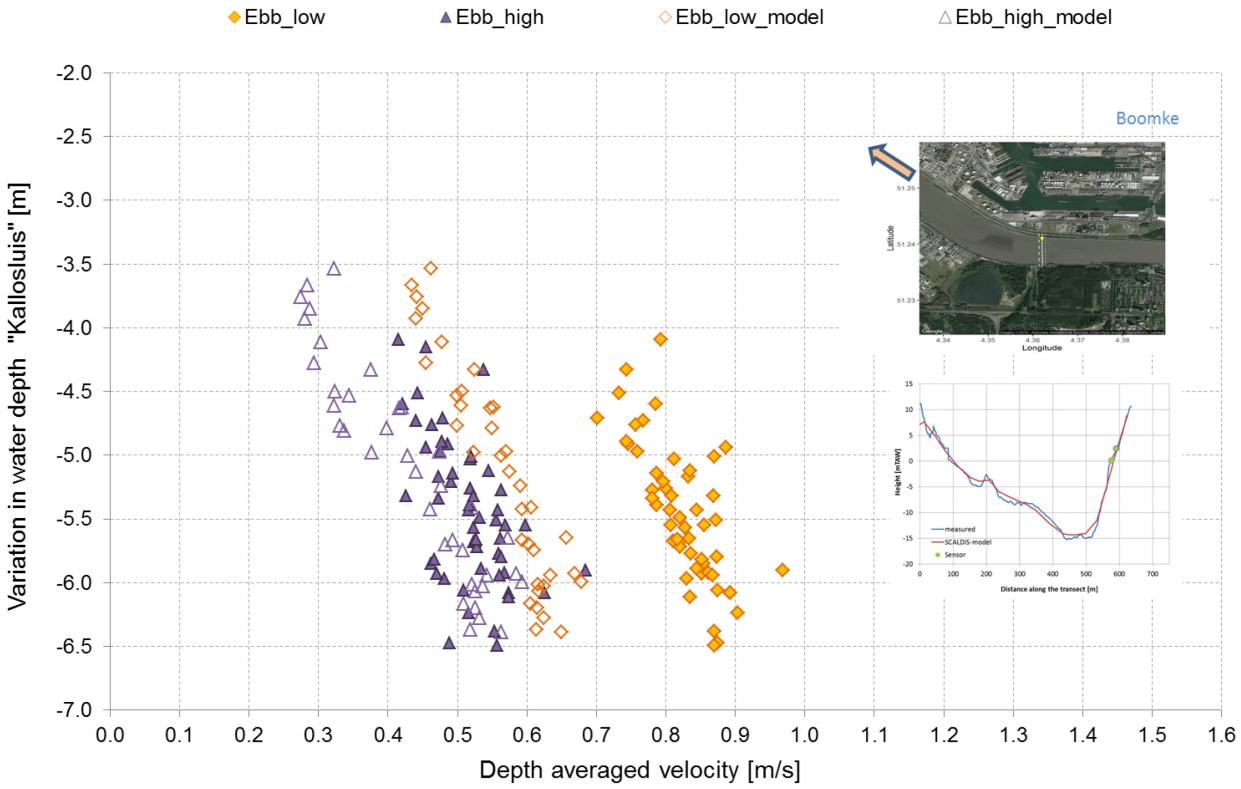

6.5 Palingplaat

The Palingplaat is situated on the left bank of the Scheldt estuary. The position of the two measuring locations at Palingplaat is shown in Figure 32, which are located on the same cross-section. One is located on low level (+ 0.85 m TAW) and the second one on high level (+ 1.76 m TAW). The distance between the two measuring points is approximately 15 m.

Cross-section profiles and the two measuring locations at Palingplaat are introduced in Figure 33.

Figure 32 – Measuring locations at Palingplaat (yellow dots).

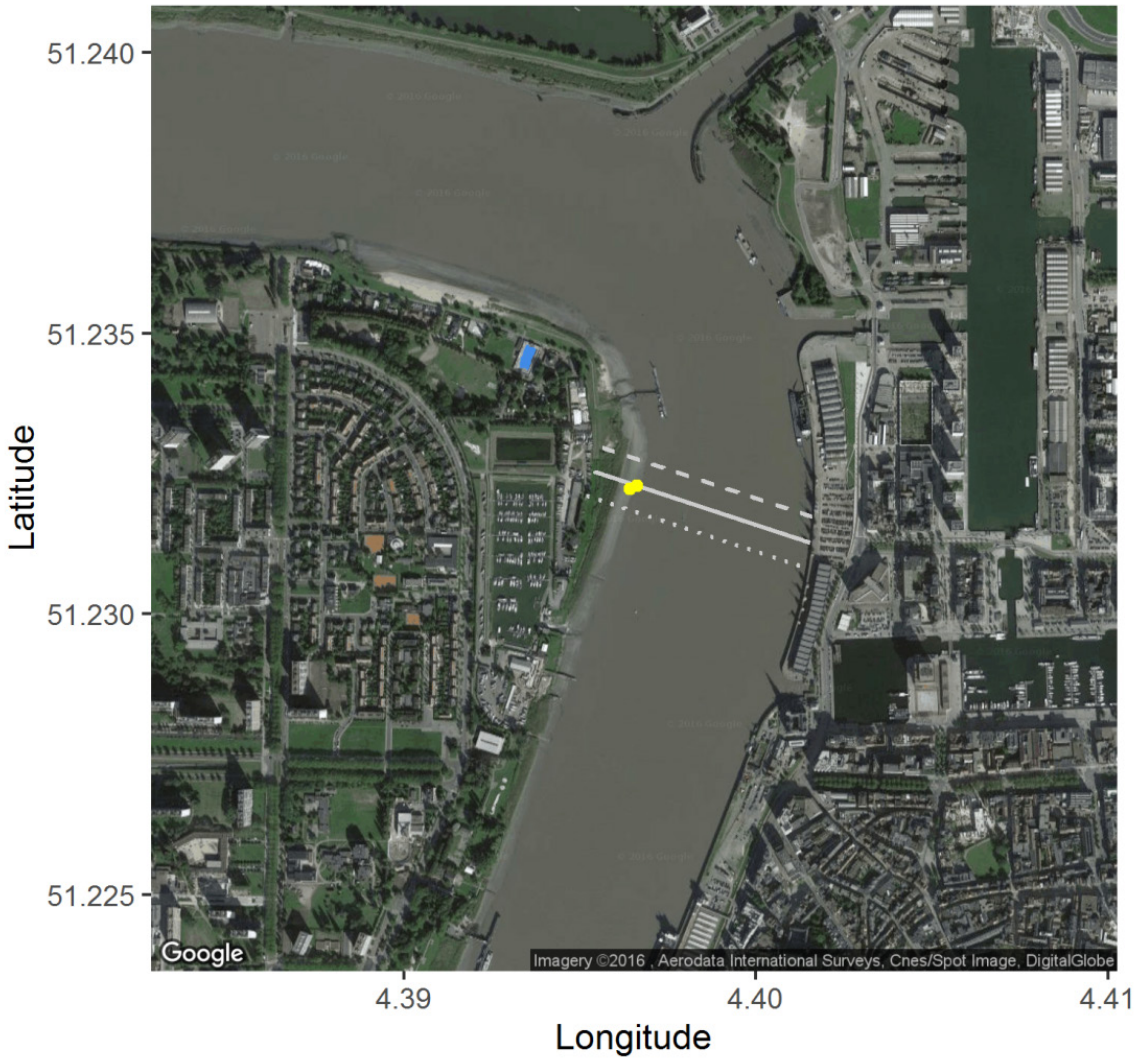

Figure 33 – Cross-section profiles at the measuring points, Palingplaat 50 m up- and down-stream.
The position of the measuring sensors is marked with a red circles. SCALDIS-model cross-section in the lower panel.

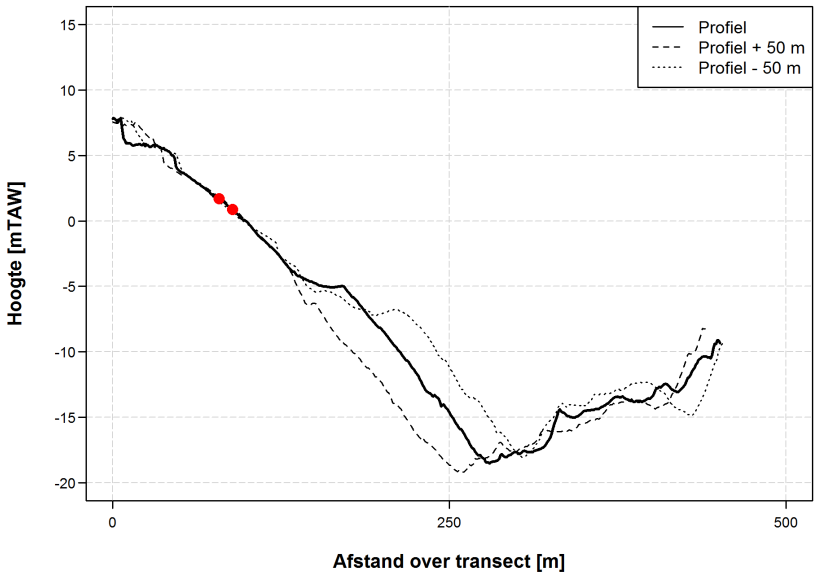

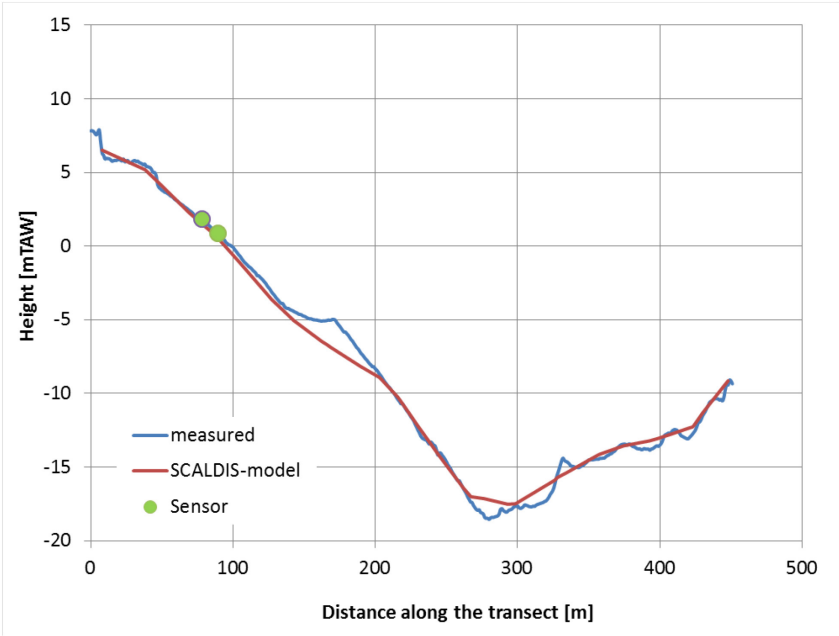

6.5.1 Ensemble-averaged velocities

Figure 34 and Figure 35 introduce the mean values of the ensemble-averaged velocities of the spring tides as measured and computed at the two locations of Palingplaat-High and Palingplaat-Low, respectively. Results of averaged and neap tides are presented in Appendix 9.5.

It is clear that at Palingplaat-High measuring location (Figure 34) the model underpredicts both the maximum flood and maximum ebb velocities. A difference of approximately 0.2 m/s is observed. Flow velocity variation during the full tidal-cycle is reasonably well produced by the model. Both in the measurements as in the model, a similar maximum velocity for the flood and ebb is found.

At Palingplaat-Low (Figure 35) the model is able to simulate flow velocities during flood phase rather good, especially during the flow acceleration part. On the other hand, flow velocities are underestimated during the ebb phase (approx. 0.15 m/s).

Figure 34 – Measured (blue) and computed (red) flow velocities at Palingplaat-High (spring tide).
The orange arrow shows the flood direction.

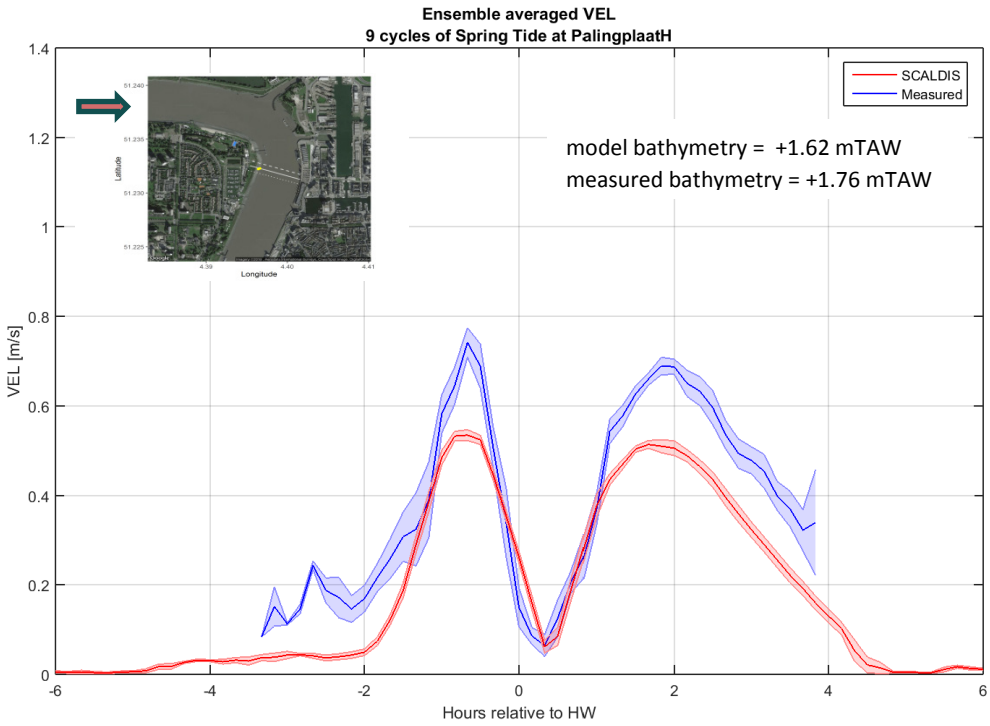

Figure 35 – Measured (blue) and computed (red) flow velocities at Palingplaat-Low (spring tide).
The orange arrow shows the flood direction.

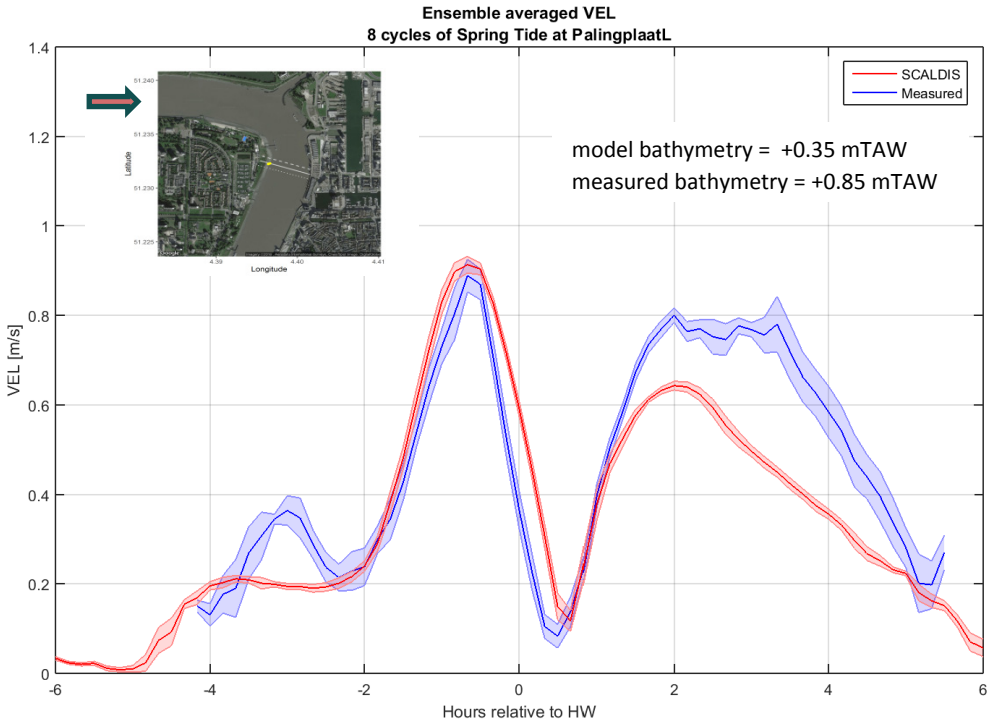

6.5.2 Water depth variation and flow velocities

SCALDIS-model validation results are presents in Figure 36 and Figure 37 during flood and ebb flows, respectively. The model is able to predict correctly depth-averaged flow velocities at Palingplaat-Low and at the lower velocity range of Palingplaat-High (u < 0.45 m/s) during flood flows. In Figure 37 results show that the model underpredicts flow velocities at the two locations, during the ebb phase of the tidal-cycles.

Figure 36 – Relation between water depth variation and depth-averaged maximum flow velocities as measured and computed by SCALDIS-model during flood at Palingplaat, Palingplaat-Low (orange) and Palingplaat-High (purple).

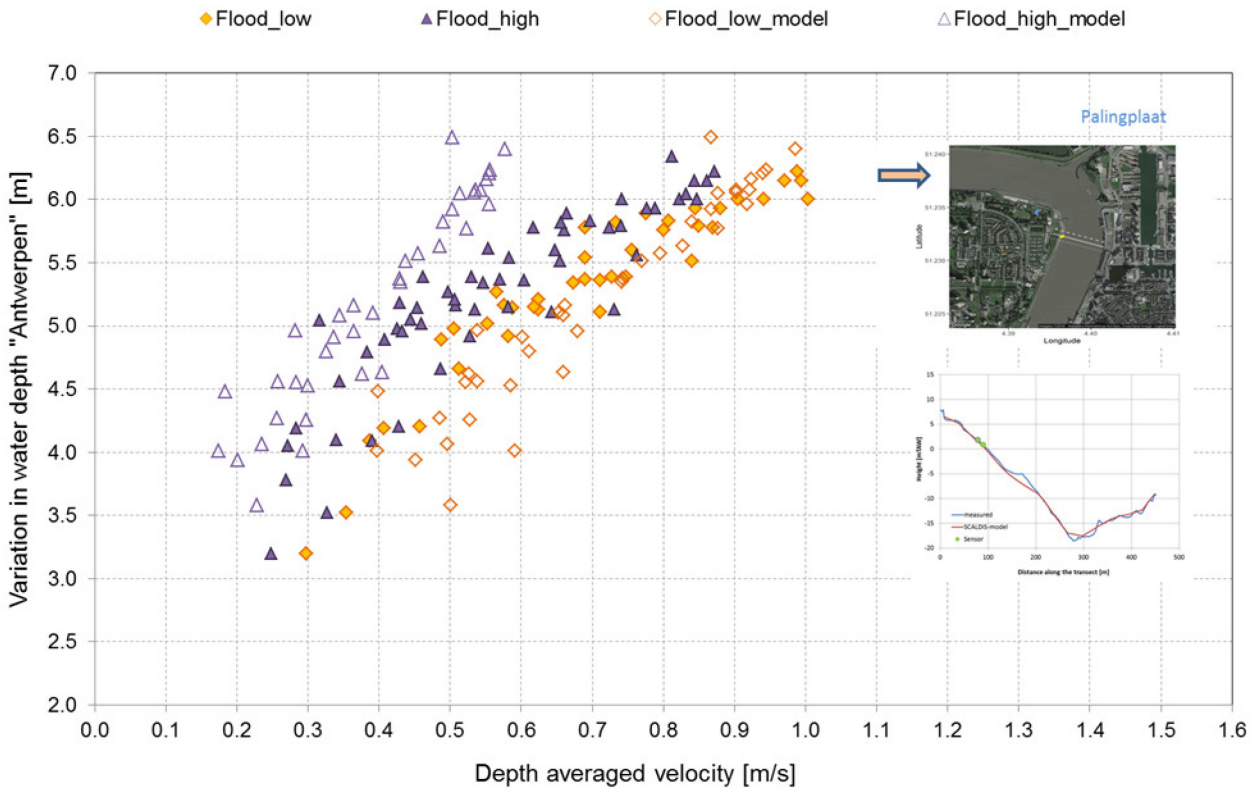

Figure 37 – Relation between water depth variation and depth-averaged maximum flow velocities as measured and computed by SCALDIS-model during ebb at Palingplaat, Palingplaat-Low (orange) and Palingplaat-High (purple).

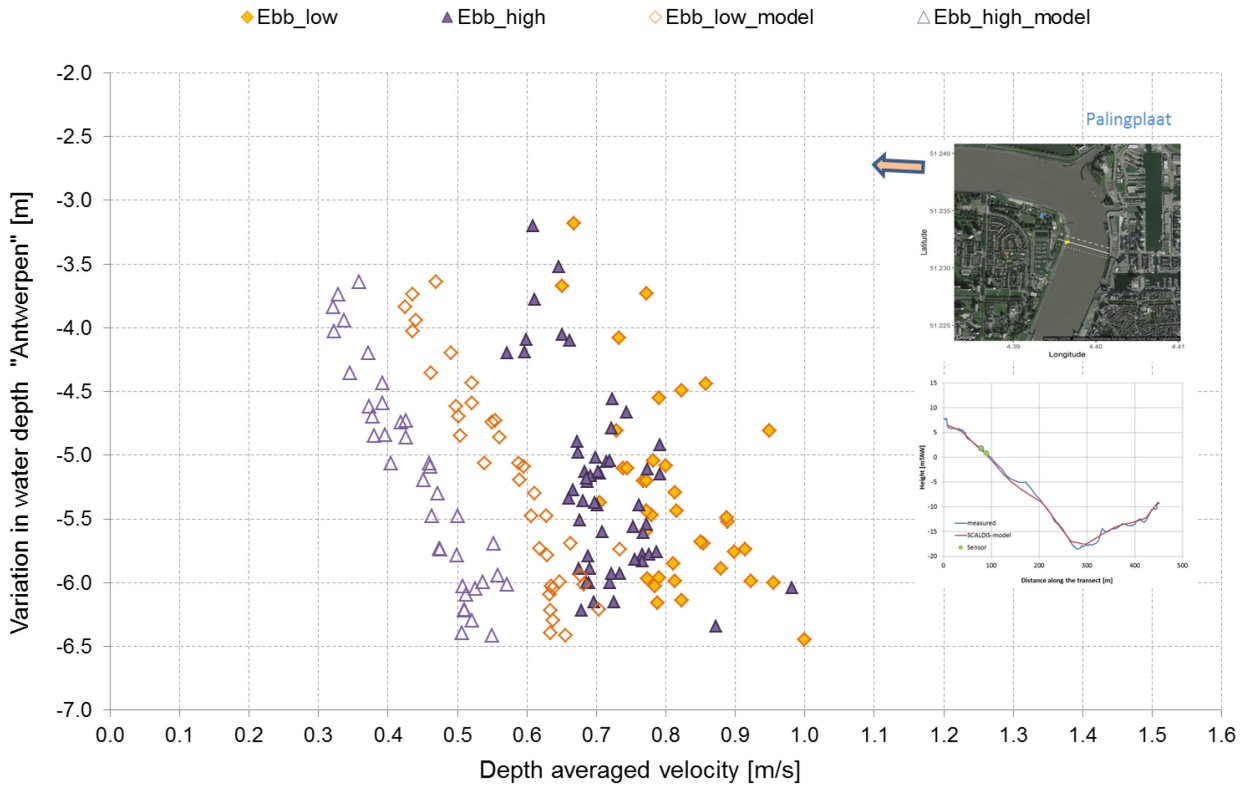

6.6 Plaat van Hoboken

The plate of Hoboken is located on the left bank of the Scheldt estuary as we can see the two measuring locations in Figure 38. The measuring positions are located on the same cross-section at two different levels, Hoboken-Low on + 0.10 m TAW and Hoboken-high on + 2.10 m TAW. The distance between the two points is approximately 45 m.

Figure 39 presents the measured cross-section profiles and the two measuring locations at Hoboken in the upper panel. The lower panel shows the cross-section profile as used in the SCALDIS-model in comparison with the measured profile.

Figure 38 – Measuring locations at Plaat van Hoboken (yellow dots).

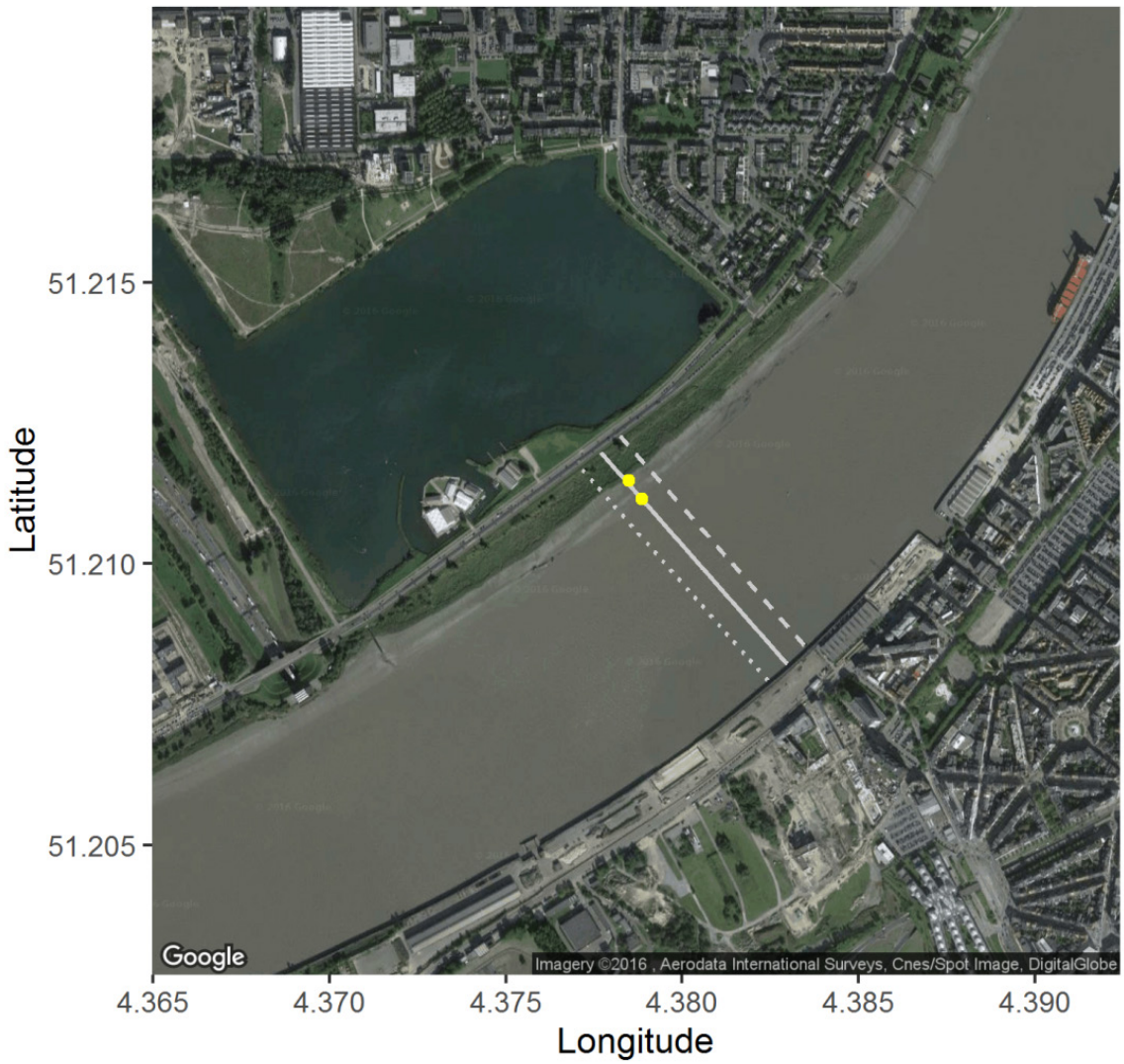

Figure 39 – Cross-section profiles at the measuring points, Hoboken 50 m up- and down-stream.
The position of the measuring sensors is marked with a red circles. SCALDIS-model cross-section in the lower panel.

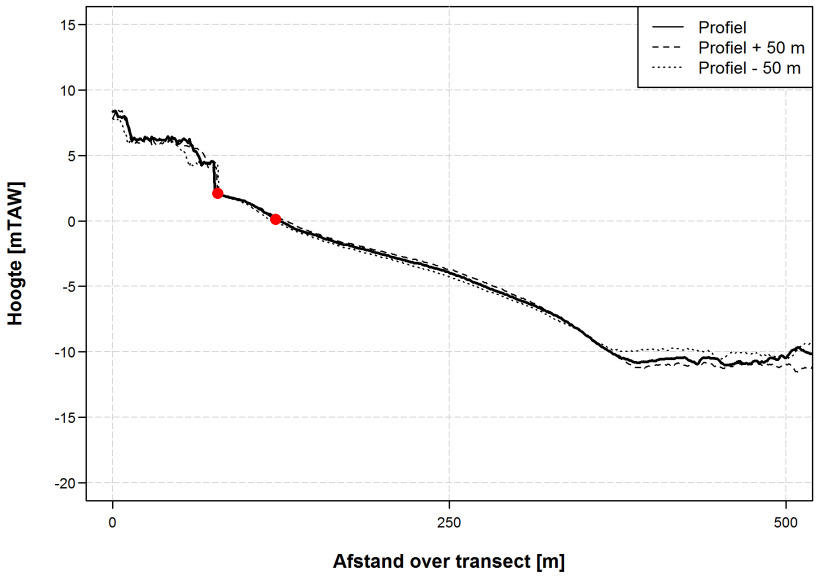

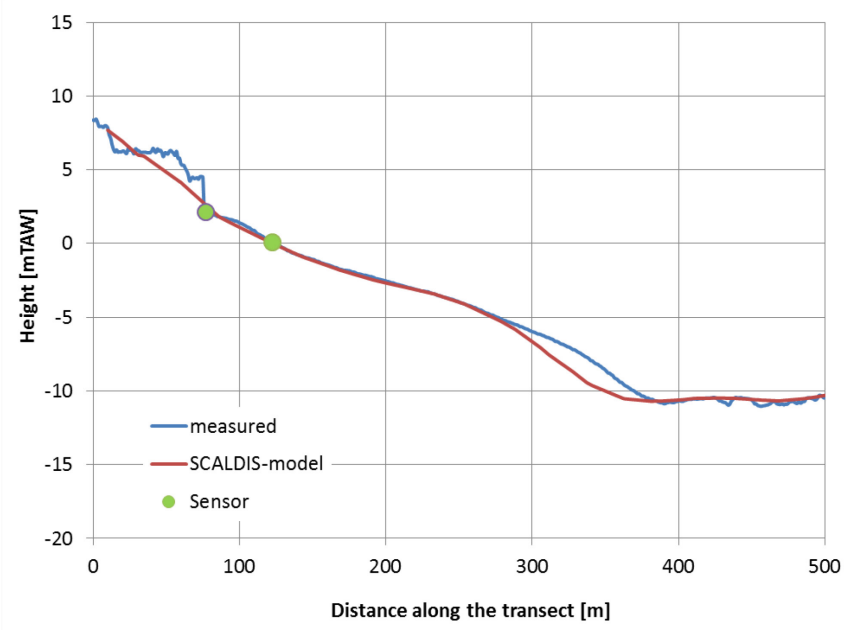

6.6.1 Ensemble-averaged velocities

Figure 40 and Figure 41 show the comparison between the measured and computed ensemble-averaged velocities of the spring tides, at the two locations of Palingplaat-High and Palingplaat-Low, respectively. Results of averaged and neap tides are presented in Appendix 9.6.

For the location on the high-tidal flat, It is clear from the results that the model is able to simulate flow velocities during flow acceleration in the flood phase accurately. During the ebb phase, a clear underestimation of the simulated flow velocities is observed (approximately 0.20 m/s difference). At the measurement location Hoboken-Low, the SCALDIS-model underpredicts both the maximum flood and maximum ebb velocities (Figure 41), with approx. 0.20 m/s. Flow velocity variation form during the full tidal-cycle is reasonably well produced by the model, both the flood and ebb maxima are in the same order of magnitude.

Figure 40 – Measured (blue) and computed (red) flow velocities at Hoboken-High (spring tide).
The orange arrow shows the flood direction.

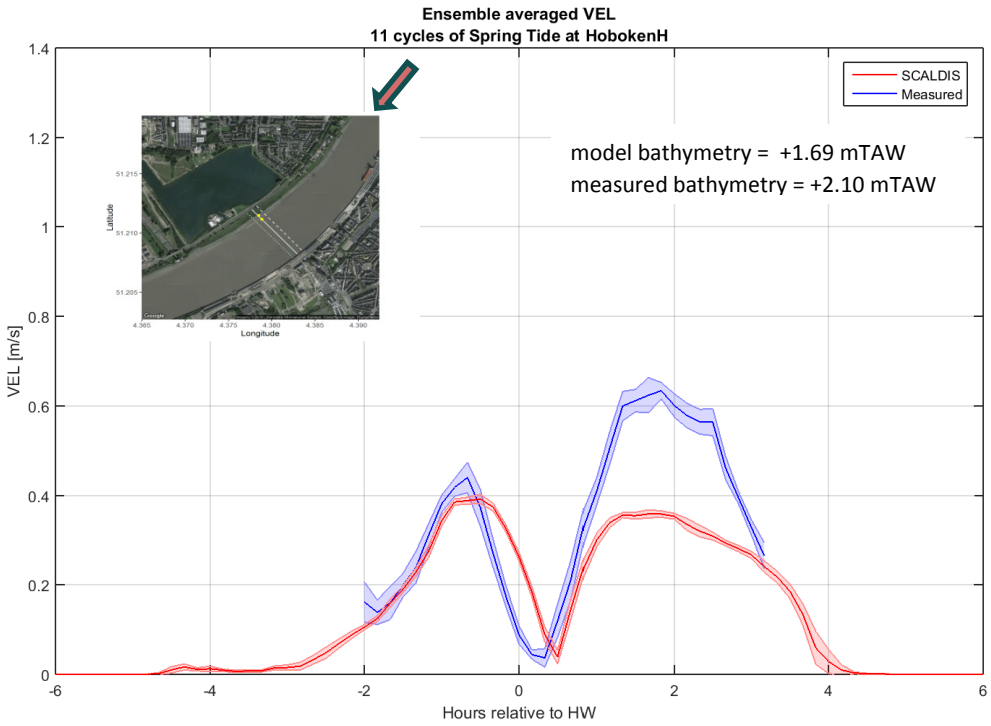

Figure 41 – Measured (blue) and computed (red) flow velocities at Hoboken-Low (spring tide).
The orange arrow shows the flood direction.

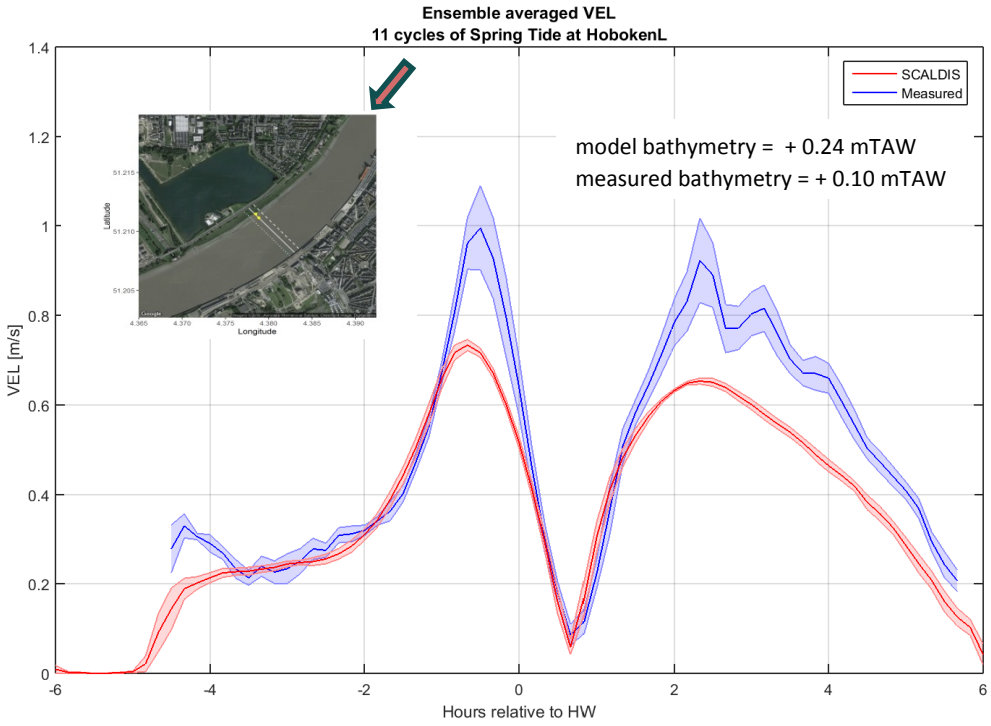

6.6.2 Water depth variation and flow velocities

Figures 42 and 43 introduce the measured and computed depth-averaged velocities at Hoboken-High and Hoboken-Low, respectively. It is clear from the results at the two locations that the model underestimates flow velocities. The differences between the model results and the measurements are increased in the high velocity range (u > 0.6 m/s) during flood flow at Hoboken-Low. For the Hoboken-High location, the model is able to represent good results during flood flow. In general flow velocities are clearly underpredicted by the model during the ebb phase at the two locations (Figure 43).

Figure 42 – Relation between water depth variation and depth-averaged maximum flow velocities as measured and computed by SCALDIS-model during flood at Hoboken, Hoboken-Low (orange) and Hoboken-High (purple).

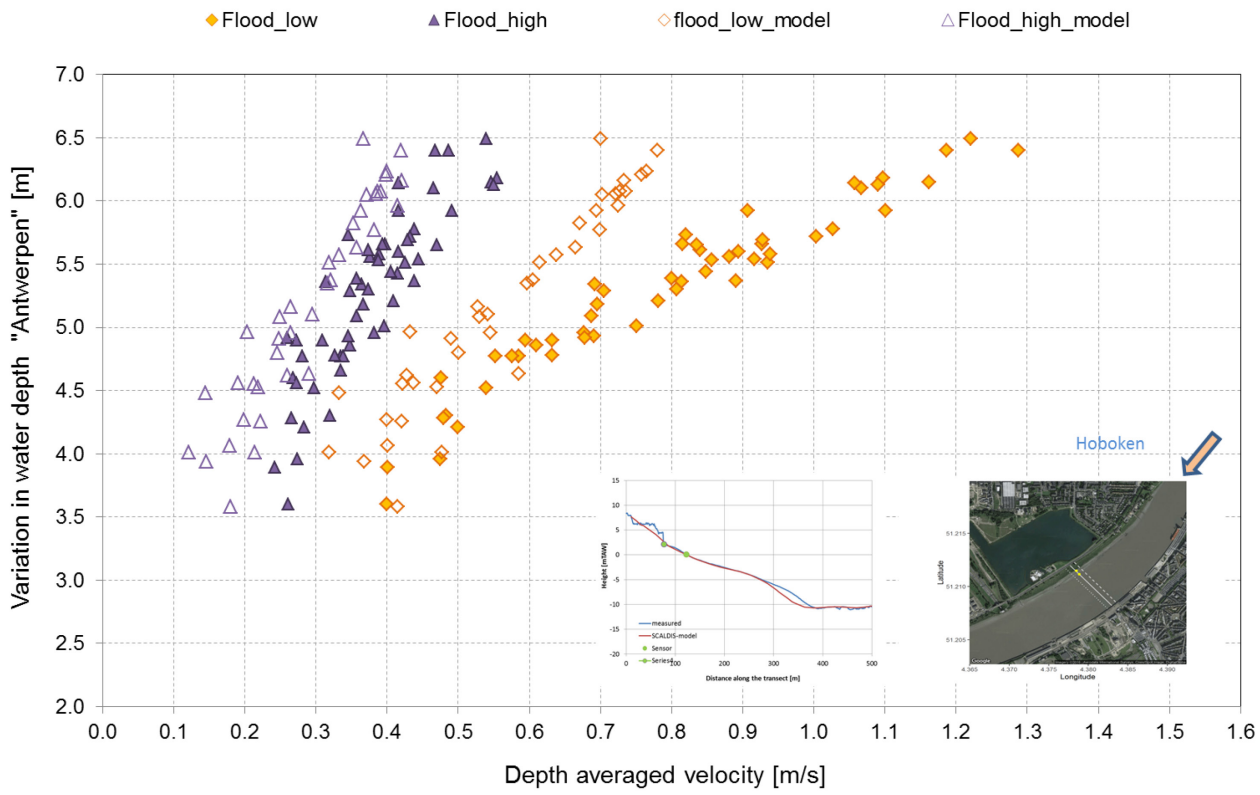

Figure 43 – Relation between water depth variation and depth-averaged maximum flow velocities as measured and computed by SCALDIS-model during ebb at Hoboken, Hoboken-Low (orange) and Hoboken-High (purple).

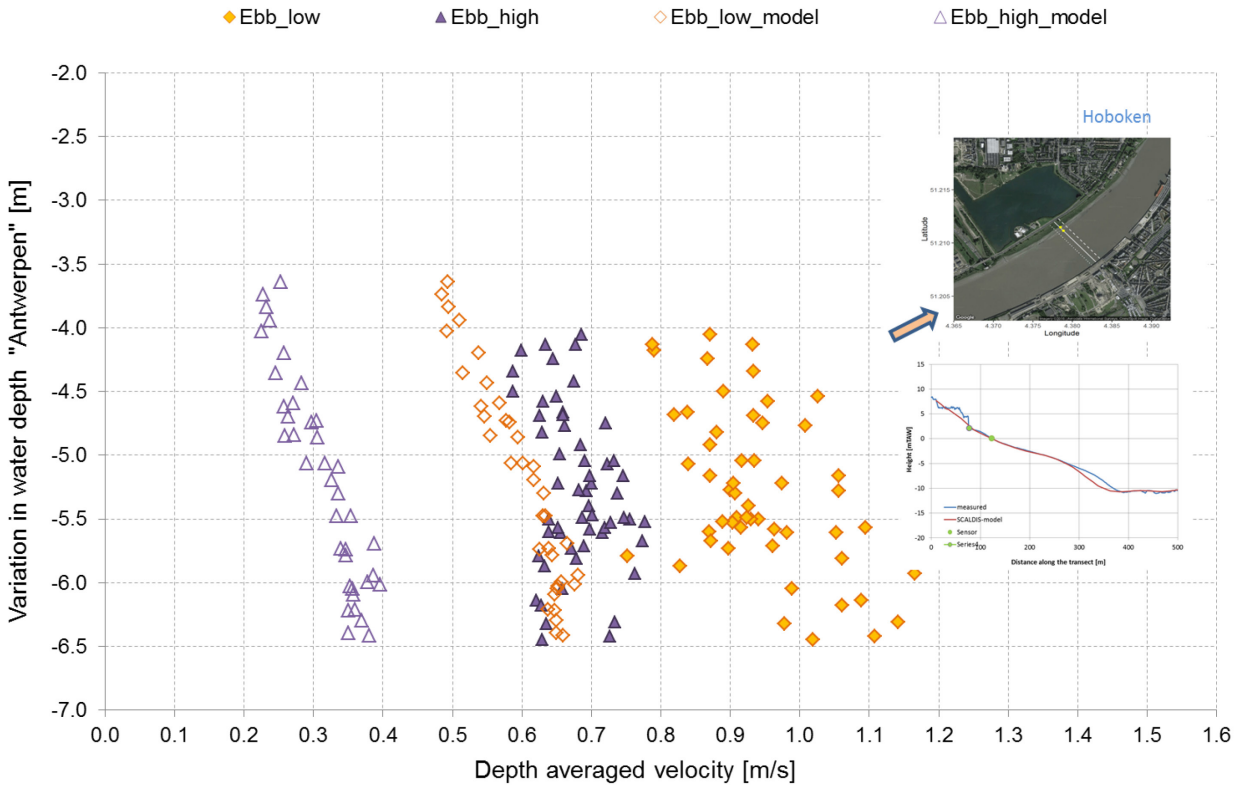

6.7 Notelaer

The measuring locations at Notelaer are located on the right bank of the Scheldt estuary as shown in Figure 44. The two measuring points are located on the same cross-section at two various levels. The Notelaer-Low is located at + 1.0 m TAW and the Notelaer-High on + 1.34 m TAW. The distance between the two points is about 10 m apart.

Cross-section profiles and the two measuring locations at Notelaer are presented in Figure 45 in m TAW. The lower panel includes the cross-section profile as used in the SCALDIS-model and as measured in the field.

Figure 44 – Measuring locations at Notelaer (yellow dots).

Figure 45 – Cross-section profiles at the measuring points, Notelaer 50 m up- and down-stream.
The position of the measuring sensors is marked with a red circles. SCALDIS-model cross-section in the lower panel.

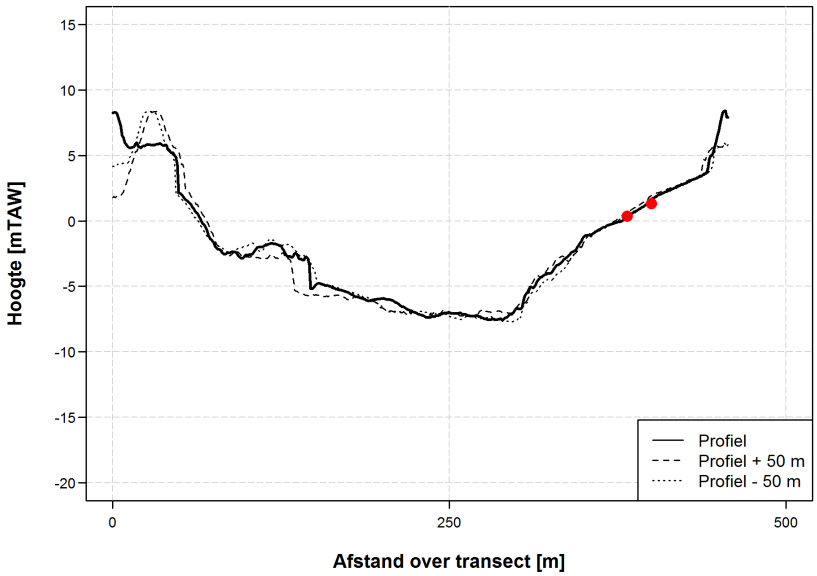

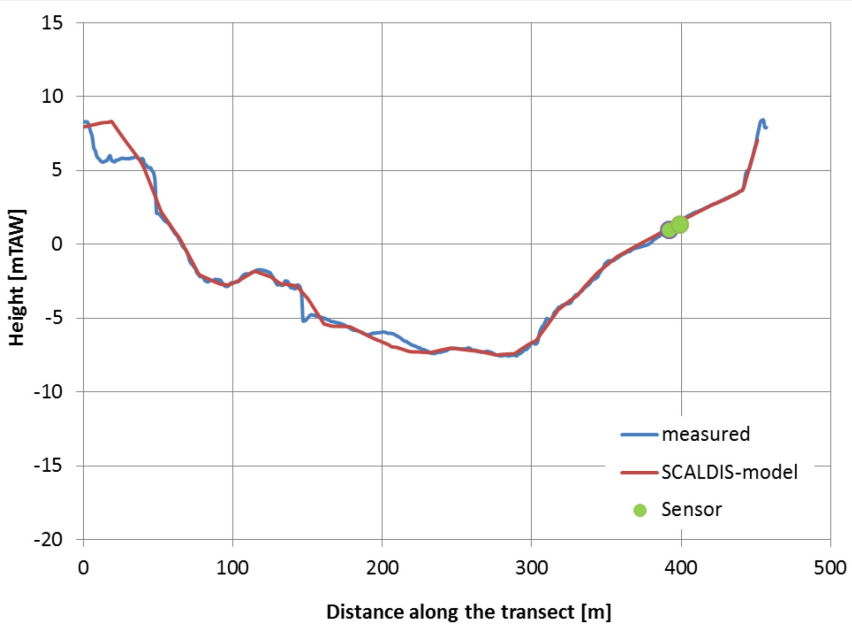

6.7.1 Ensemble-averaged velocities

Figure 46 and Figure 47 show the comparison between the measured and computed ensemble-averaged velocities of the spring tides at the two locations of Notelaer-High and Notelaer-Low, respectively. Results of averaged and neap tides are presented in Appendix 9.7.

It is clear from the results that the model is able to simulate the velocity form quite well during the tidal-cycle. On the other hand flow velocities are underpredicted by the model during most of the phases. SCALDIS-model underpredicts both the maximum flood and maximum ebb velocities at the two locations. The difference is larger for the low tidal flat (approximately 0.2 to even 0.3 m/s) compared to the high location, with differences between 0.15 and 0.10 m/s.

Figure 46 – Measured (blue) and computed (red) flow velocities at Notelaer-High (spring tide).
The orange arrow shows the flood direction.

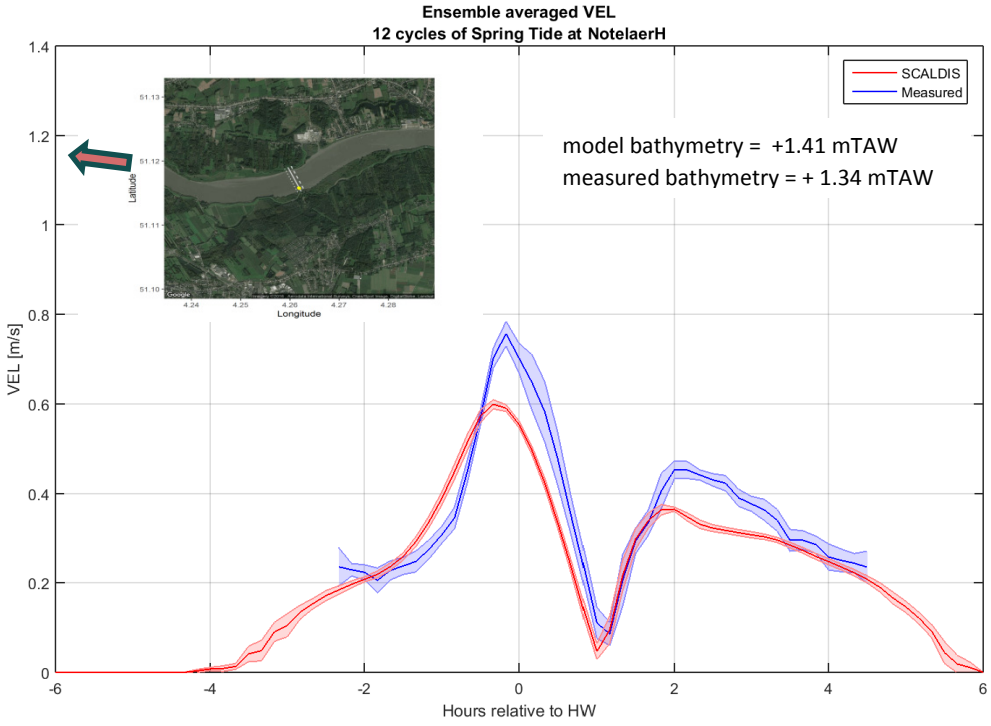

Figure 47 – Measured (blue) and computed (red) flow velocities at Notelaer-Low (spring tide).
The orange arrow shows the flood direction.

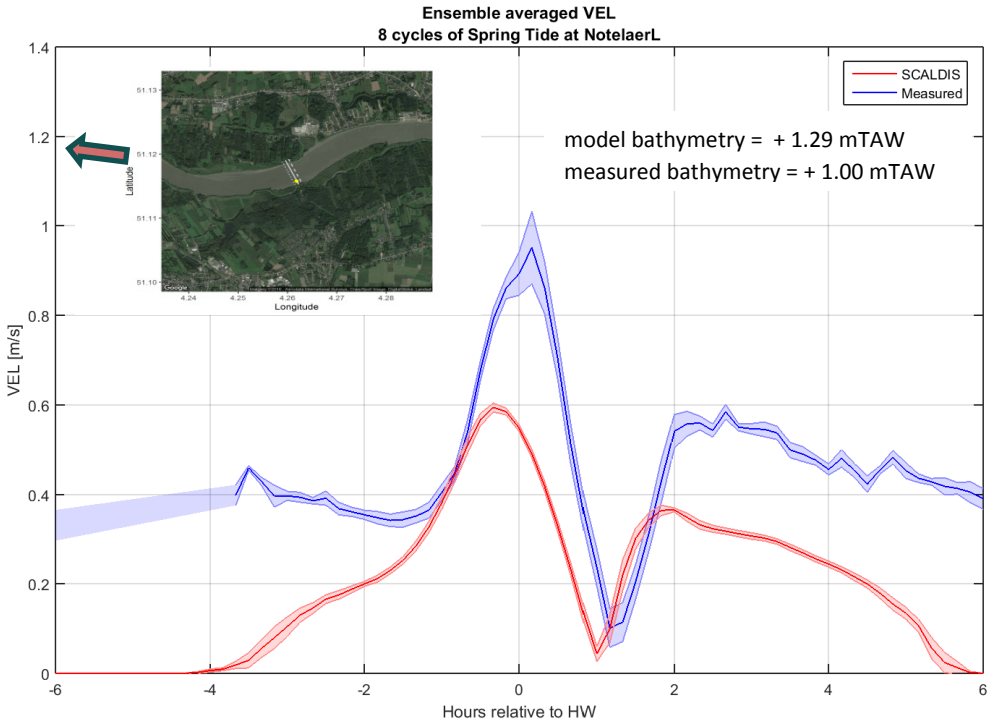

6.7.2 Water depth variation and flow velocities

Figure 48 and Figure 49 show the relation between the increase/decrease in water levels and the depth-averaged maximum flood/ebb velocities as measured and computed by the model. The measured and SCALDIS-model results are presented at the two locations.

It is clear from the flood phase results (Figure 48) that the model is underpredicting flow velocities at the two locations with the high water depth variation. The model is able to show a better performance at the low velocity range (u < 0.5 m/s). During the ebb phase (Figure 49) flow velocities are underpredicted by the model at the two locations.

The SCALDIS-model shows quite similar results at the two locations because the distance between the two locations is very small (10 m apart) and the height difference also (± 10 cm).

Figure 48 – Relation between water depth variation and depth-averaged maximum flow velocities as measured and computed by SCALDIS-model during flood at Notelaer, Notelaer-Low (orange) and Notelaer-High (purple).

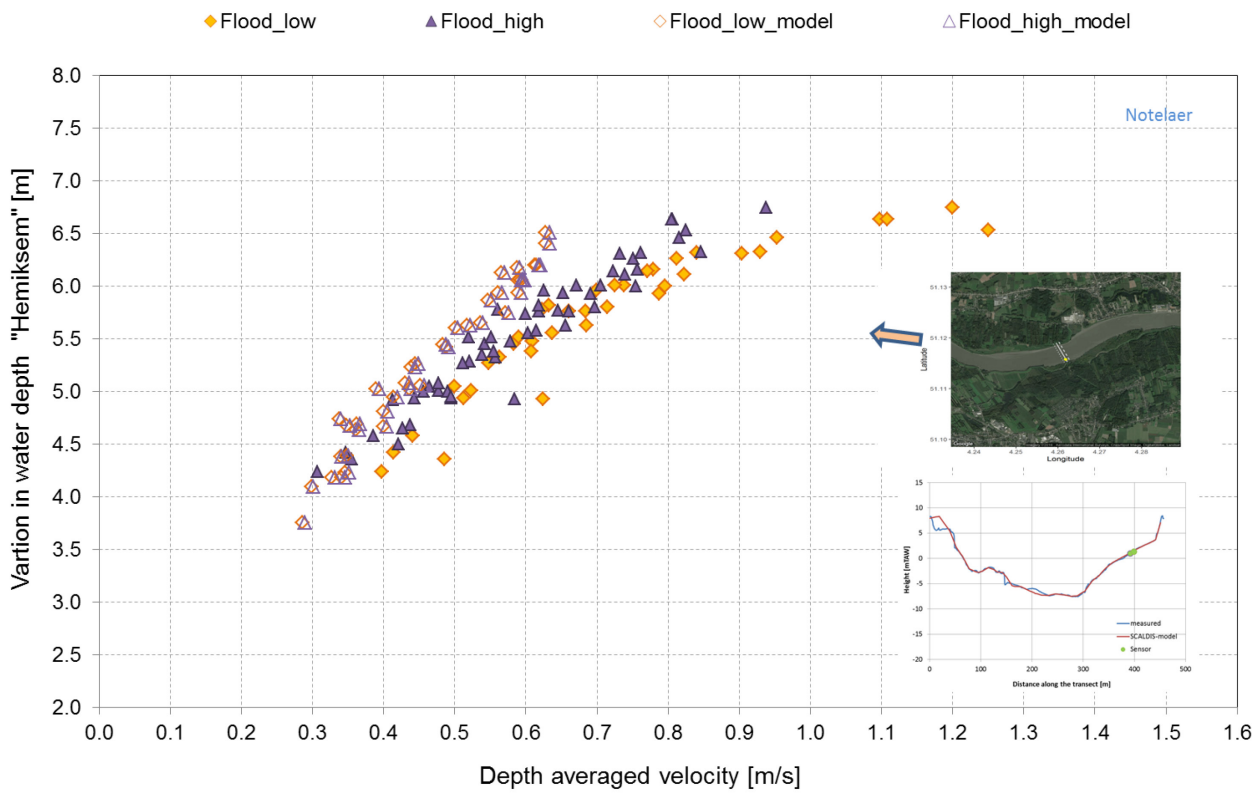

Figure 49 – Relation between water depth variation and depth-averaged maximum flow velocities as measured and computed by SCALDIS-model during ebb at Notelaer, Notelaer-Low (orange) and Notelaer-High (purple).

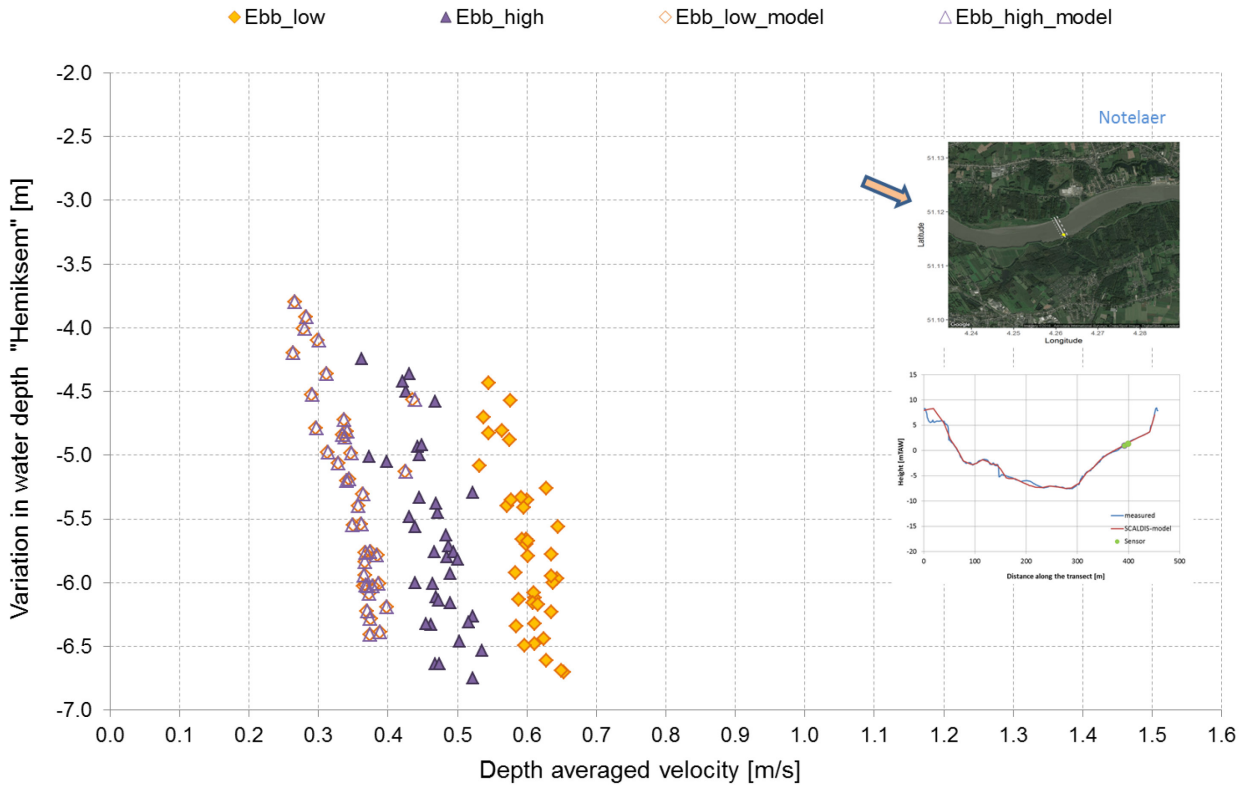

6.8 Weert

The measuring locations at Weert are located on the right bank of the Scheldt estuary as shown in Figure 50. The two measuring points are located on the same cross-section at two different levels, the lower point is located at +0.05 m TAW and the high point are located at +2.27 m TAW. The velocity measurements were carried out from 21 January to 18 February 2014.

Figure 50 – Measuring locations at Weert (yellow dots).

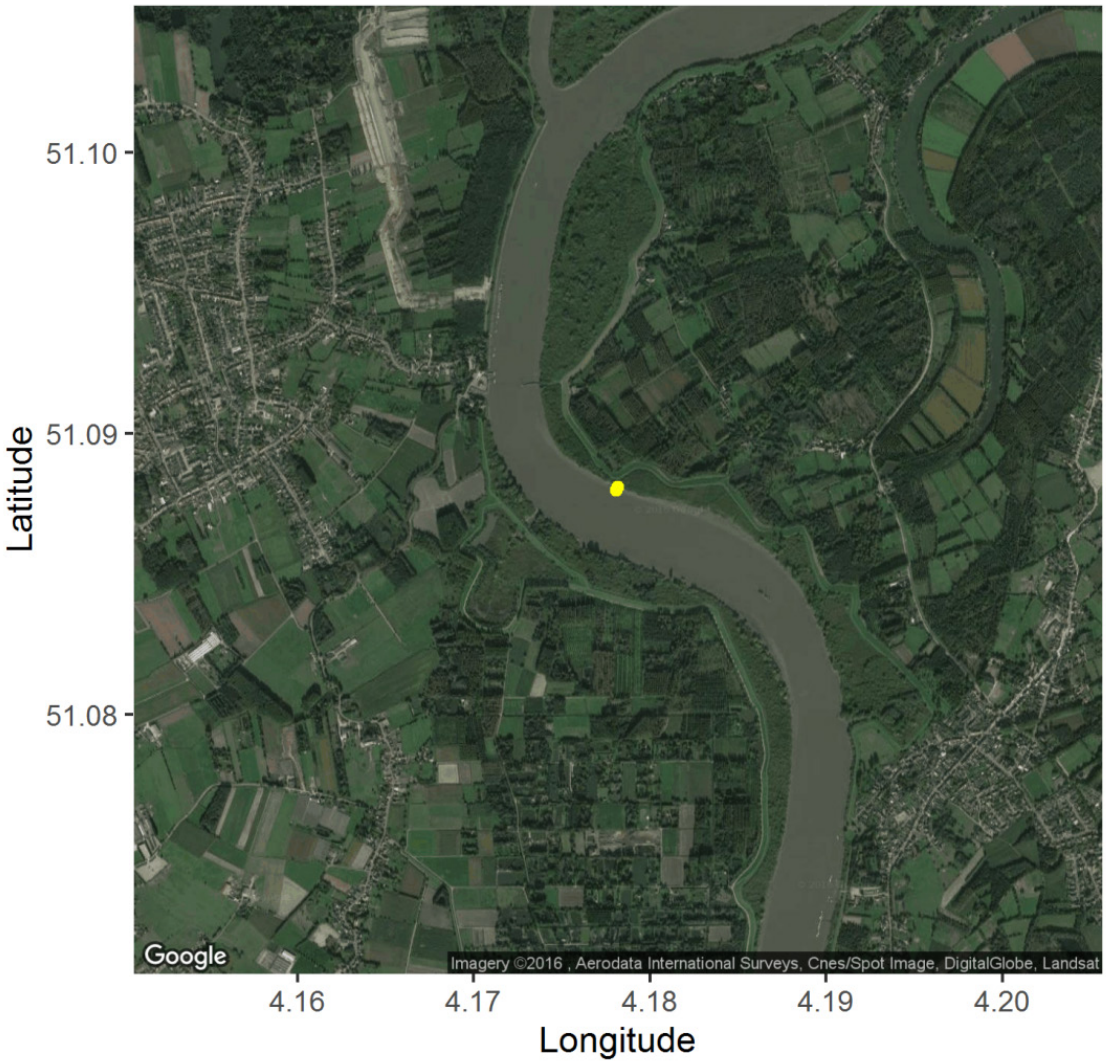

6.8.1 Ensemble-averaged velocities

The ensemble-averaged velocities in Figure 51 and Figure 52 show that the model underpredicts the measured velocities at the two measuring locations at Weert. In these two figures the ensemble-averaged velocities of the spring tides (measured and computed) are presented for the two locations, Weert-High and Weert-Low, respectively. Results of averaged and neap tides are presented in Appendix 9.8.

In Figure 51 and Figure 52 the velocity over the tide is shown, both for the simulations as the measurements, respectively for the high and low location at Weert. On the high tidal flat, the flood velocities which are simulated and measured are in a same order of magnitude. However, fot the ebb phase, a much stronger current is observed in reality compared to the model. For the low location, a similar discrepancy between measurements and model is observed in the ebb phase. In the flood phase, the velocities are doubled, both in reality as in the simulations, compared to the high location. In absolute values, the difference between model en measurements is therefore higher on the low tidal flat position.

Figure 51 – Measured (blue) and computed (red) flow velocities at Weert-High (spring tide).
The orange arrow shows the flood direction.

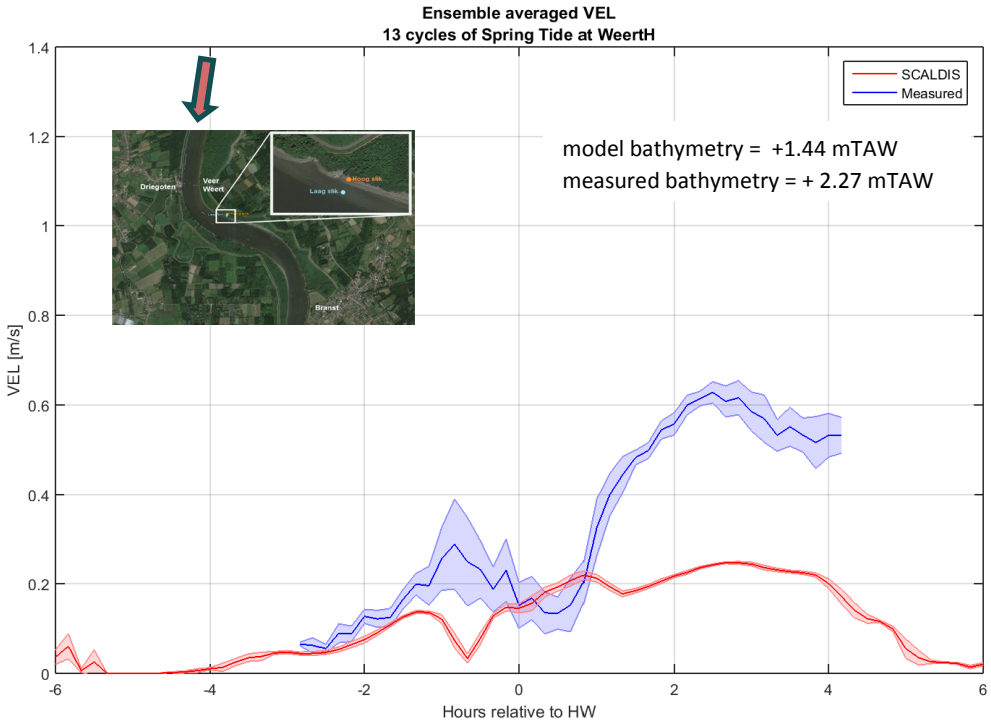

Figure 52 – Measured (blue) and computed (red) flow velocities at Weert-Low (spring tide).
The orange arrow shows the flood direction.

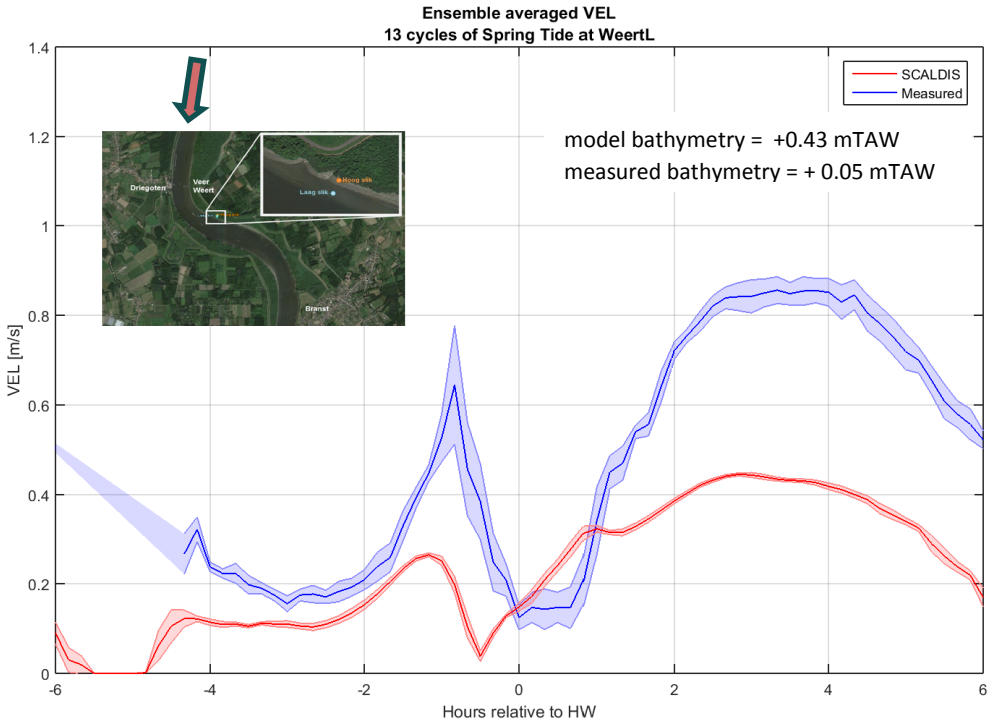

6.8.2 Water depth variation and flow velocities

In Figure 53 and Figure 54 the comparisons between the measured and computed depth-averaged velocities are presented during flood and ebb phases, respectively. Again it is clear that SCALDIS-model underpredicts the measured velocities at the two locations during flood and ebb phases. Especially for the ebb phase, the curves (not absolute values!) of measurements and model have a similar slope.

Figure 53 – Relation between water depth variation and depth-averaged maximum flow velocities as measured and computed by SCALDIS-model during flood at Weert, Weert-Low (orange) and Weert-High (purple).

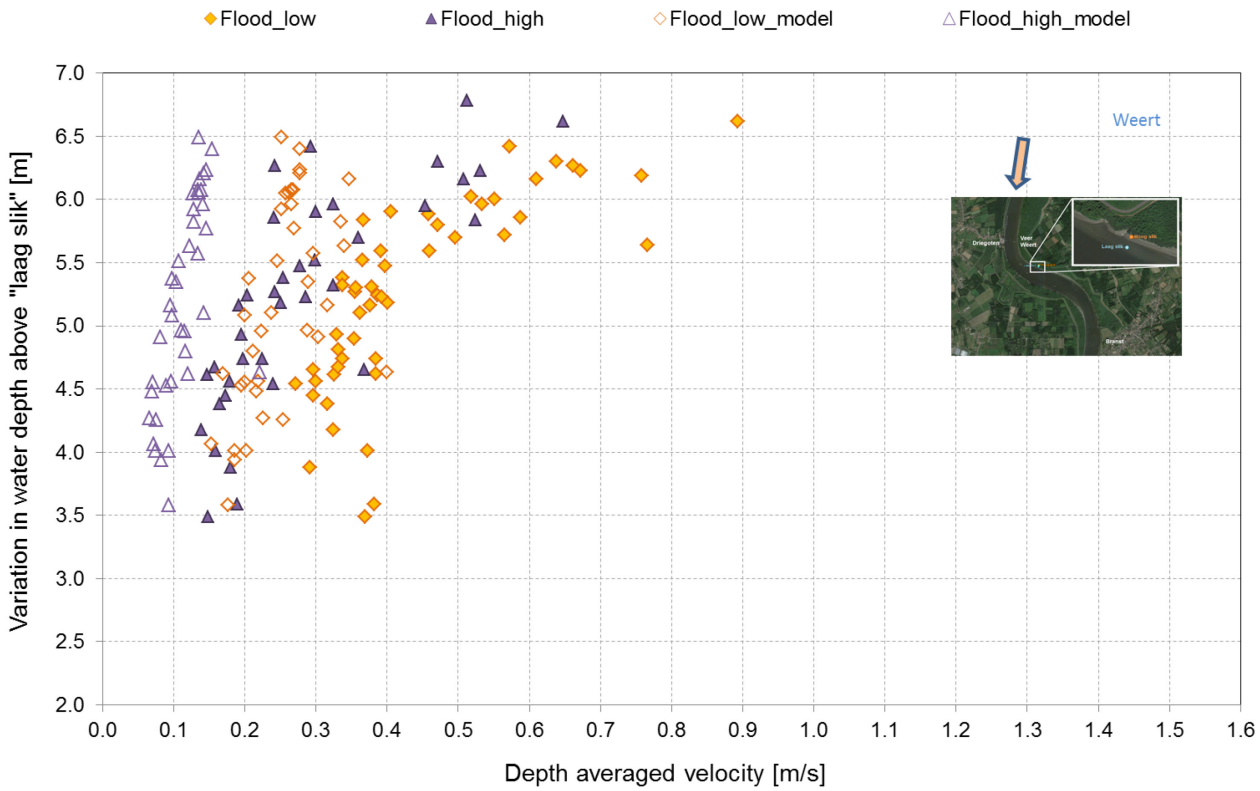

Figure 54– Relation between water depth variation and depth-averaged maximum flow velocities as measured and computed by SCALDIS-model during ebb at Weert, Weert-Low (orange) and Weert-High (purple).

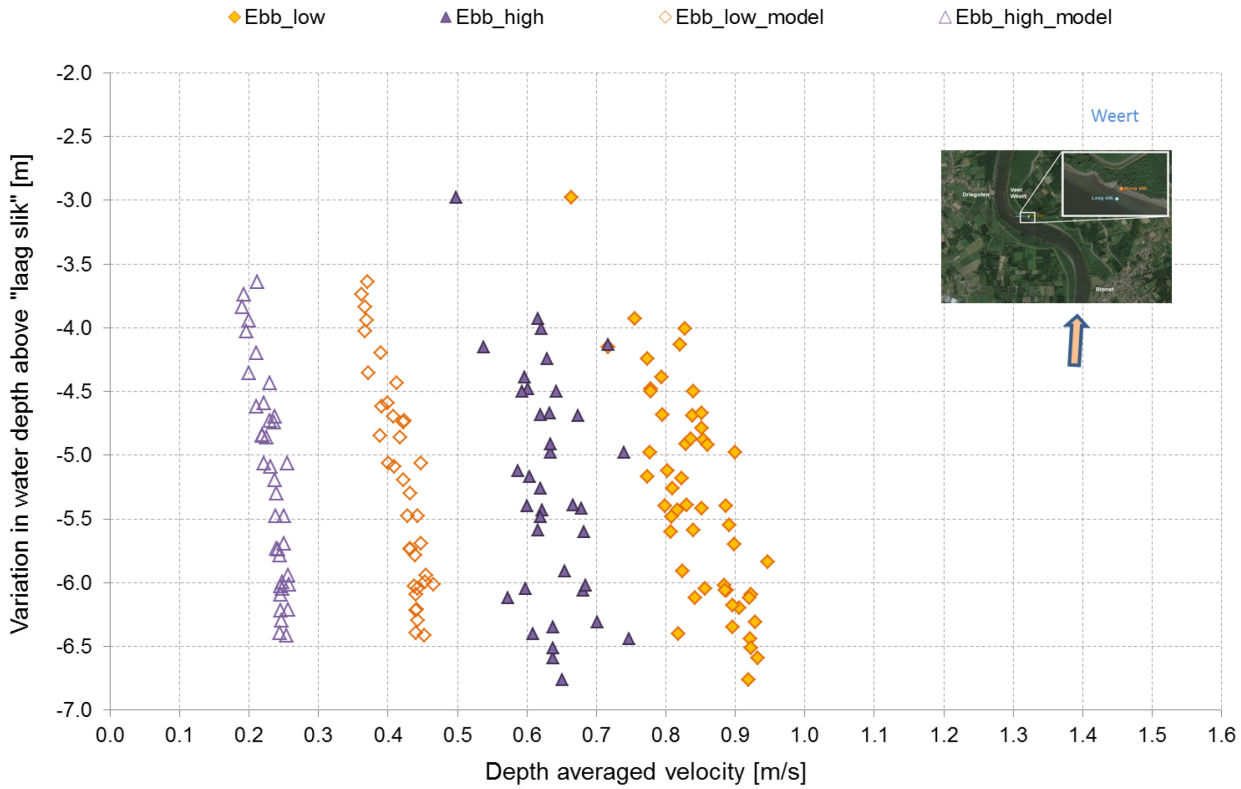

6.9 Appels

Flow velocity measurements at Appels were measured two times. The first one was carried out between 28 April and 29 May 2014 on the right bank of the estuary. The second measurements were carried out between 13 June and 22 July 2014 on the left bank. The two measuring locations at Appels are presented in Figure 55.

Figure 55 – Measuring locations at Appels.
The AppelsRO "right bank" of Scheldt is located on the lower side of the photo, the AppelsLO "left bank" on the upper side of the photo.

6.9.1 Ensemble-averaged velocities

Appels – left bank

The comparisons between the measured and computed ensemble-averaged velocities at Appels (left bank) are presented in Figure 56 and in Figure 57 during the full tidal-cycle. These results include the spring tides at the two locations of AppelsLO-High and AppelsLO-Low, respectively. Results of averaged and neap tides are presented in Appendix 9.9.

Results show that flow velocities are underpredicted by the model at the location of AppelsLO-High (Figure 56). This is especially the case for the flood phase. In the ebb phase, the velocities are low and similar, except for the small peak in the measurements, which is not found in the model. On the second location AppelsLO-Low maximum flood velocities are well predicted. On the other hand, maximum ebb velocities are overestimated by the model, especially after the moment where the measurements show a small peak.

Figure 56 – Measured (blue) and computed (red) flow velocities at AppelsLO-High (spring tide).
The orange arrow shows the flood direction.

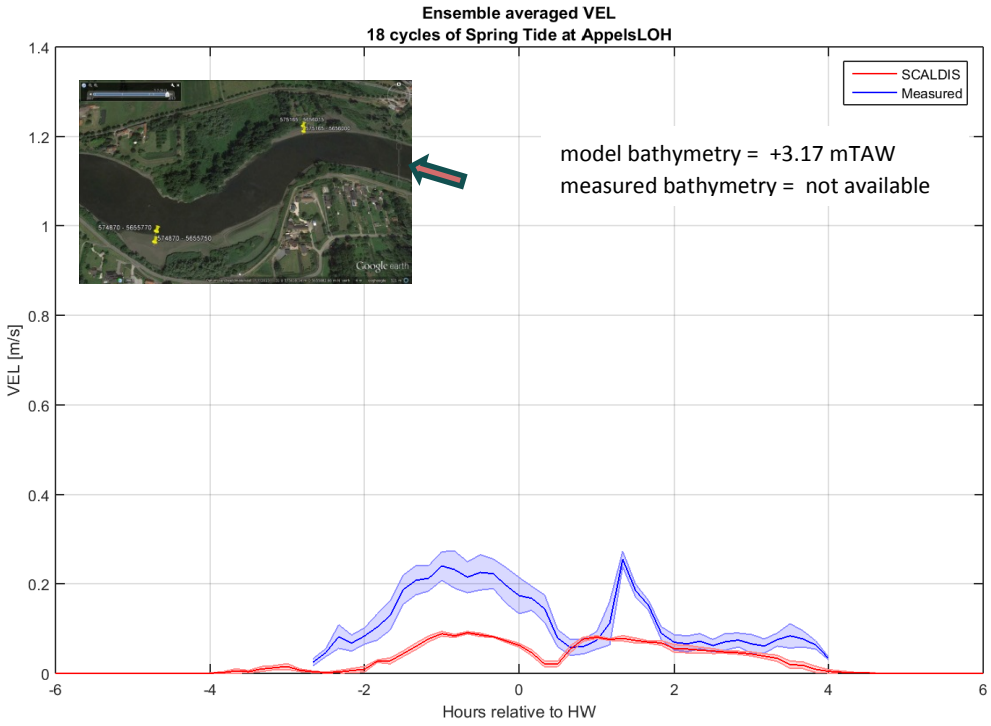

Figure 57 – Measured (blue) and computed (red) flow velocities at AppelsLO-Low (spring tide).
The orange arrow shows the flood direction.

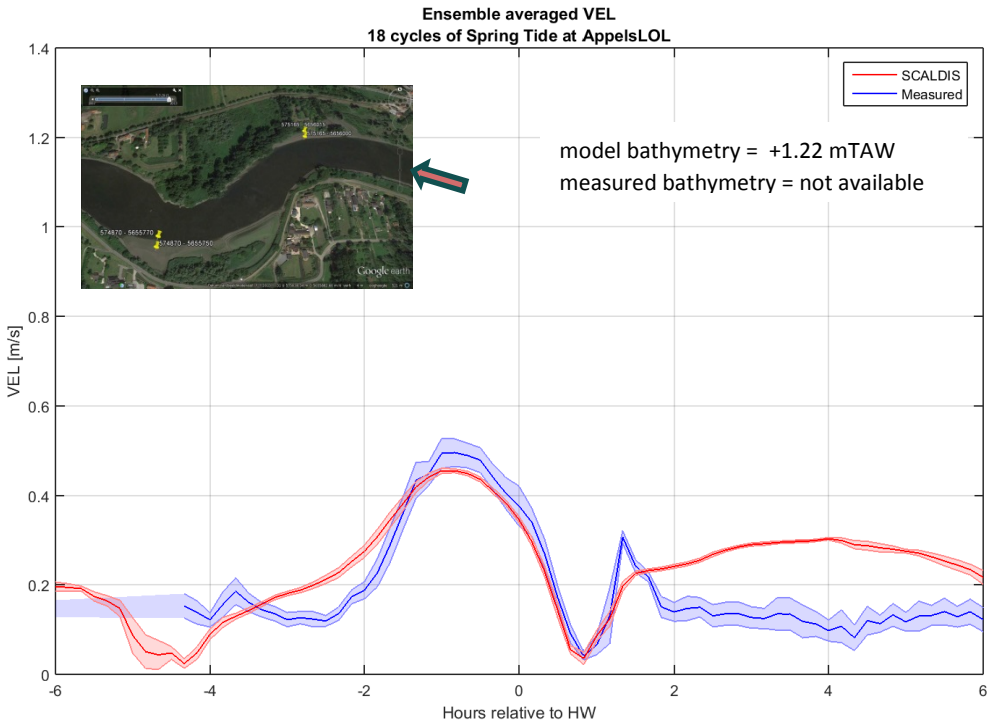

Appels – right bank

The comparisons between the measured and computed ensemble-averaged velocities at Appels (right bank) are presented in Figure 58 and in Figure 59 during the full tidal-cycle. These results include the spring tides at the two locations of AppelsRO-High and AppelsRO-Low, respectively. Results of averaged and neap tides are presented in Appendix 9.9.

Results show that flow velocities are overpredicted by the model at the location of AppelsRO-High (Figure 58). Both in the ebb and flood phase a difference of approximately 0.20 m/s can be observed. On the second location AppelsRO-Low maximum flood velocities are underpredicted, especially for the flood phase.

Figure 58 – Measured (blue) and computed (red) flow velocities at AppelsRO-High (spring tide).
The orange arrow shows the flood direction.

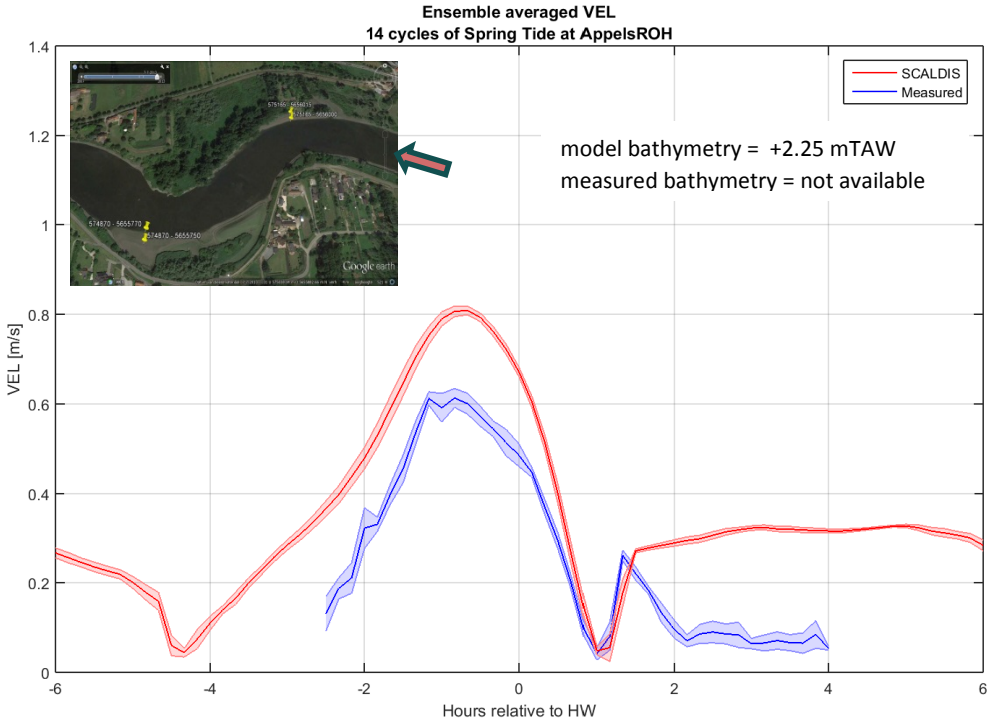

Figure 59 – Measured (blue) and computed (red) flow velocities at AppelsRO-Low (spring tide).
The orange arrow shows the flood direction.

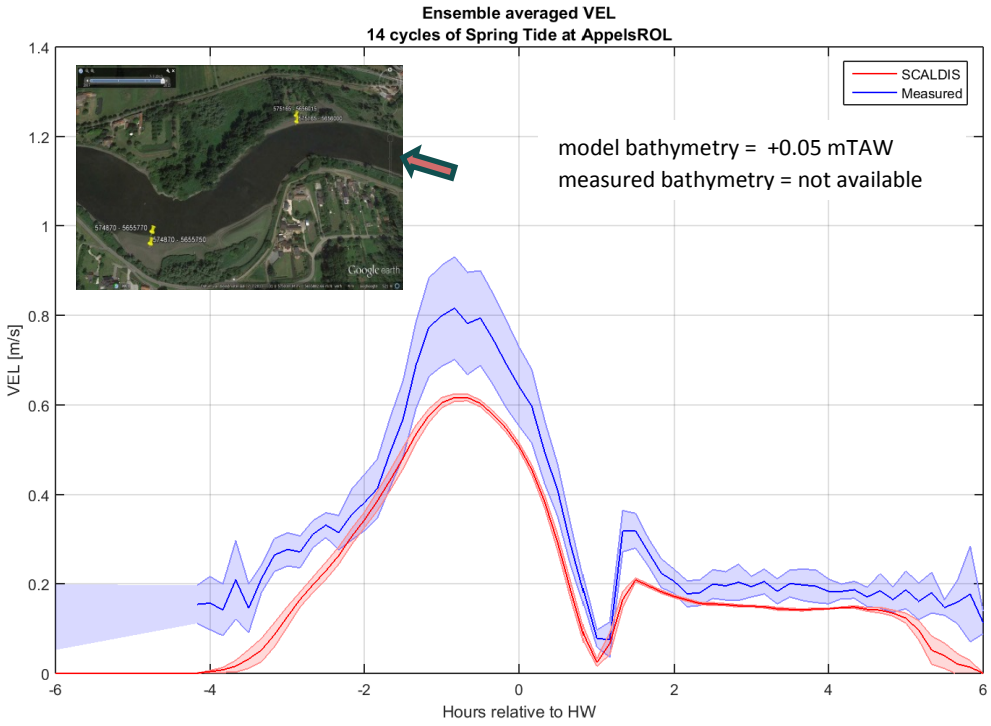

6.9.2 Water depth variation and flow velocities

Appels – left bank

In Figure 60 and Figure 61 the computed and measured velocities are presented during flood and ebb phases of the tidal-cycle at the two locations on the left bank. At the high measuring location, flow velocities are clearly underestimated by the model, during both the flood and ebb phases. The model shows a much better performance in predicting flow velocity magnitudes at the low location, both for ebb and flood. For flood, a slight underestimation of the velocities by the model can be observed for the higher tidal ranges.

Figure 60 – Relation between water depth variation and depth-averaged maximum flow velocities as measured and computed by SCALDIS-model during flood at AppelsLO, at AppelsLO-Low (orange) and at AppelsLO-High (purple).

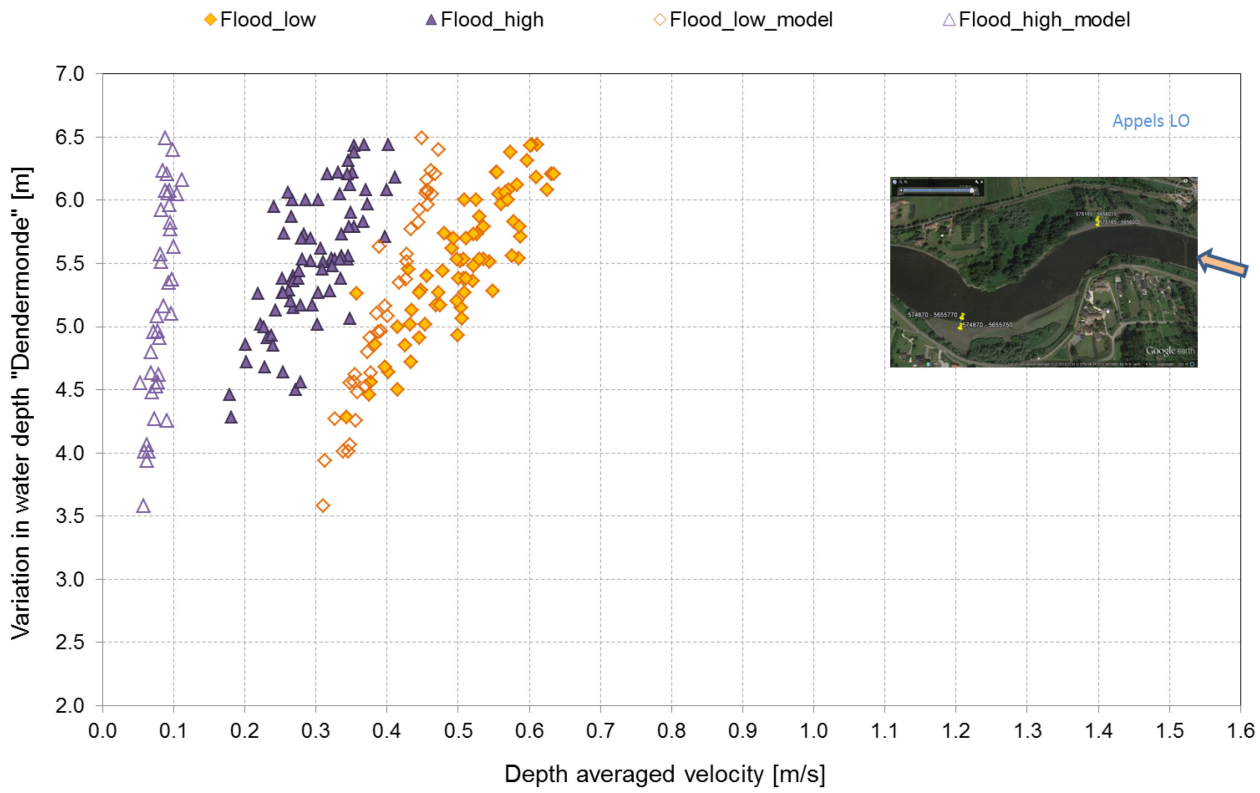

Figure 61 – Relation between water depth variation and depth-averaged maximum flow velocities as measured and computed by SCALDIS-model during ebb at AppelsLO, at AppelsLO-Low (orange) and at AppelsLO-High (purple).

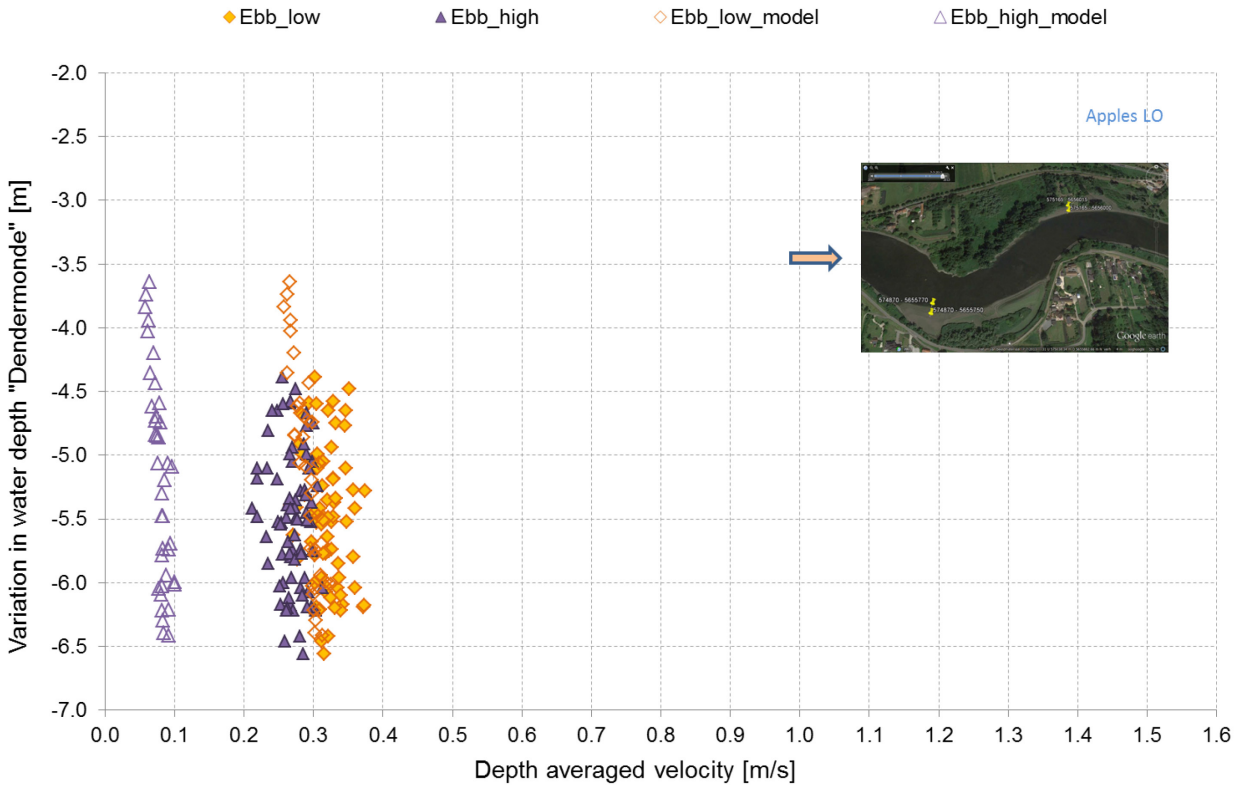

Appels – right bank

Figure 62 and Figure 63 present the model results and the measured velocities during flood and ebb phases of the tidal-cycle at the two locations of Appels on the right bank. In Figure 62 measured flow velocities are slightly underpredicted by the model at AppelsRO-Low and well predicted by the model at AppelsRO-High for various water depths. SCALDIS-model showed a good performance during the ebb phase as shown in Figure 63. The measured velocities are predicted well by the model at the two locations.

Figure 62 – Relation between water depth variation and depth-averaged maximum flow velocities as measured and computed by SCALDIS-model during flood at AppelsRO, at AppelsRO-Low (orange) and at AppelsRO-High (purple).

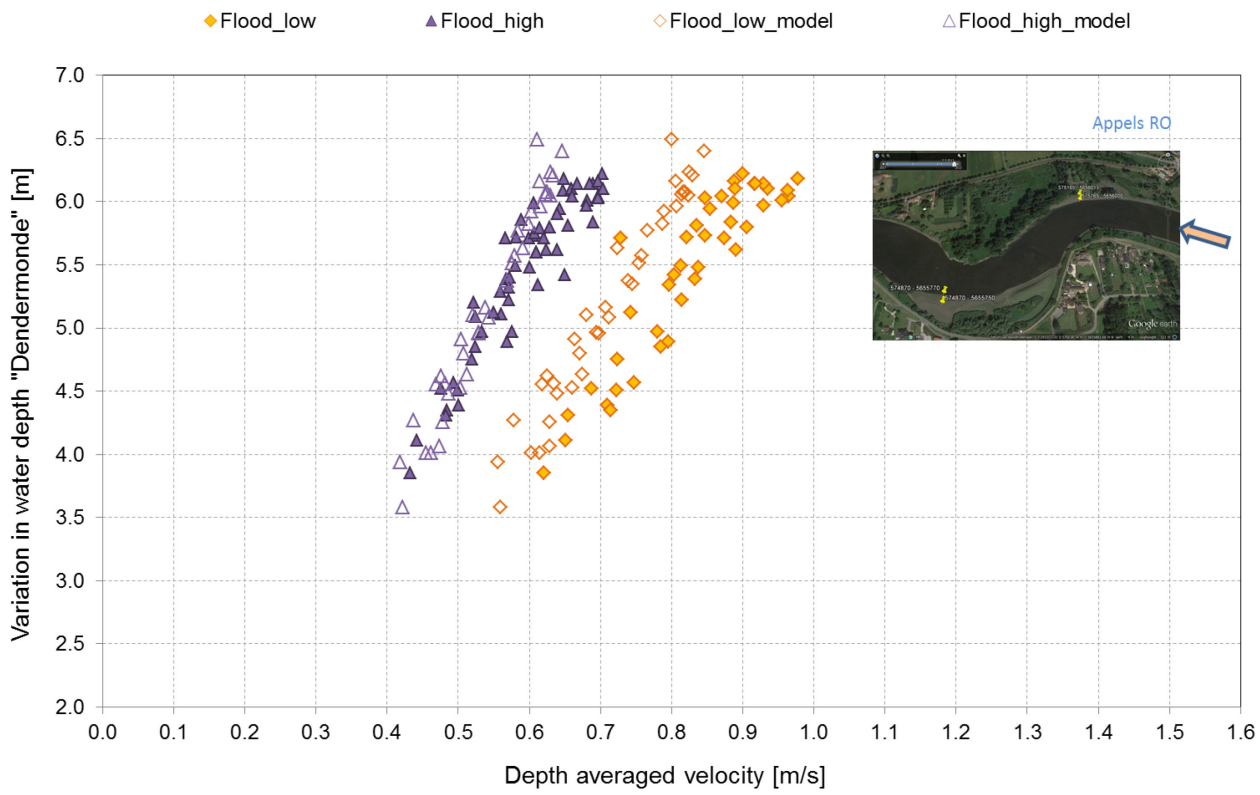

Figure 63 – Relation between water depth variation and depth-averaged maximum flow velocities as measured and computed by SCALDIS-model during ebb at AppelsRO, at AppelsRO-Low (orange) and at AppelsRO-High (purple).

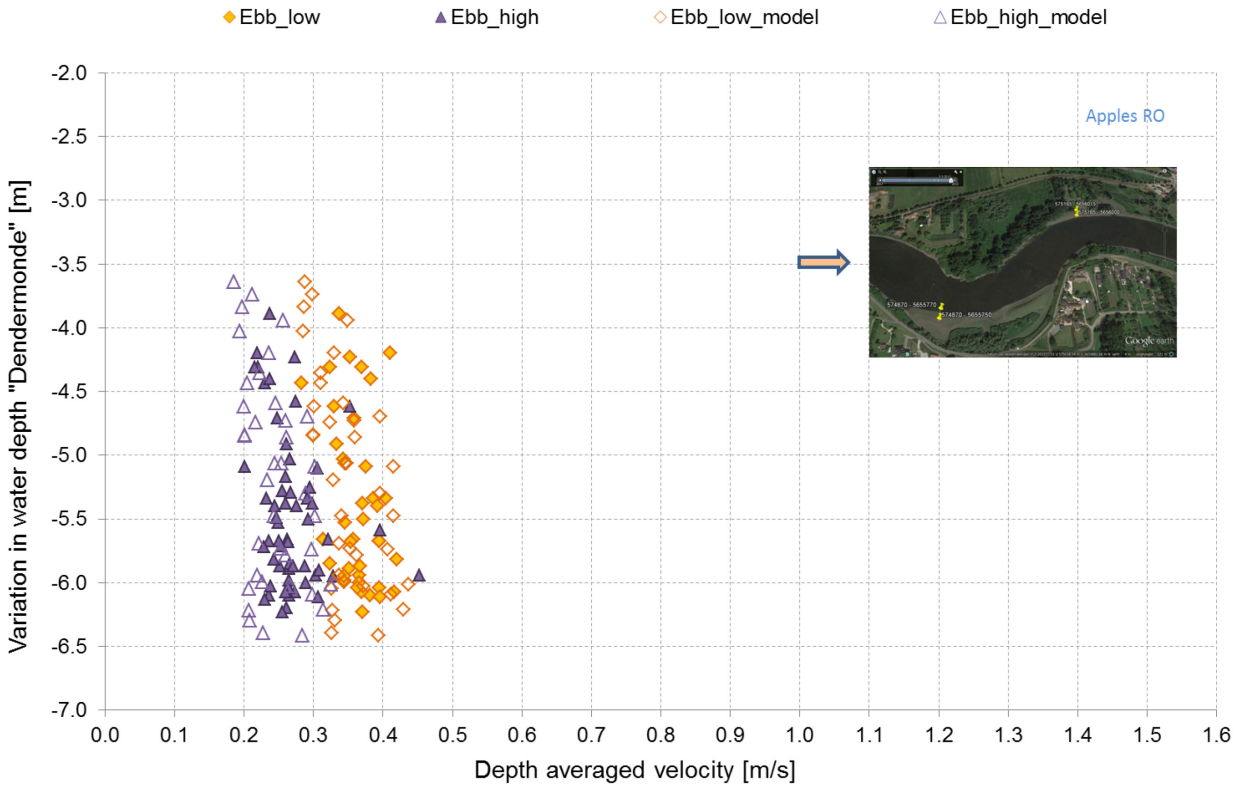

7 Summary and discussion

The main objective of the present study is to validate the calibrated 3D SCALDIS-model with new intertidal flow velocity data, measured in 2014, 2015 and 2016. For validation purposes, an independent set of Aquadopp® measurements was used for the model validation. The model validation focuses mainly on testing the model performance in the upstream part of the estuary. Bed roughness and other model parameters are not changed during the model validation.

For the analysis of flow velocities in the shallow zones it is very important that the measurement point and the analyzed point in the model have similar depths. It was not always possible to find a model node with a similar depth close to the measurement location. This may have resulted in differences between the calculated and measured velocities. At some locations the model output in different points was tested. The model results using the points with the real coordinates of the measurement locations (as an average of the 3 closest points) are very similar to the model results using the nearest node to the real location.

In general the model is validated with measured velocities at 20 different locations along the Scheldt estuary. The model and data analysis were carried out during flood and ebb phases of the tidal-cycle. The present model validation shows the following main results:

- In general the model underpredicts most of the measured flow velocities, which occurs at 16 locations out of the 20 locations;
- Flow velocities during flood phase are well predicted by the model at 5 locations out of the tested 20 locations. On the other hand velocities at 13 locations are underpredicted and only 2 locations are overpredicted by the model;
- During ebb phase, velocities are underpredicted by the model at 16 locations and overpredicted at 3 locations. Only one location is well predicted by the model;
- Although the model underpredicts most of the measured velocities at various locations, the shape of the velocity variation during the full tide-cycle is well predicted for most locations.

It is important to state that the differences between the model results and the measurements can be due to various sources. The model calibration and verification was carried out with data from 2013 and older. Changes in bathymetry are expected during the new measured velocities from 2014 to 2016.

In general the model is calibrated both on water levels in the measurement gauges, but also on the discharge data from 13 hour measurements. As such, it can be supposed that the water balances in the model are well simulated and the differences are mainly due to different velocity profiles within the considered sections.

On one hand this differences can be caused by different bathymetrical representation in the model compared to reality. On the other hand are cross-sections containing the intertidal flats, and as such the places where the new velocity measurements are performed, mostly situated in bends of the river. The cross-sections for 13 hour measurements are typically situated in straight sections of the river. As such it can be suggested to perform some additional measurement of velocity profiles in cross-sections characterized by the presence of tidal flats, to be able to calibrate the model better for these regions.

8 References

Jentink, R.; de Klerk, J.; Schrijver, M. (2013) Opvolging effectern flexibel storten. Datarapportage 2013. Rijkswaterstaat Centrale Informatievoorziening. 7210A/DR-2014-01.

Meire, D.; Vereecken, H.;Plancke, Y.;Verwaest, T.; Mostaert, F. (2017). Agenda voor de Toekomst – Stroming ter hoogte van intergetijdgebieden: Analyse van uitgevoerde metingen. Versie 4.0. WL Rapporten, 14_024_4. Waterbouwkundig Laboratorium: Antwerpen.

Plancke, Y.; Vereecken, H.; Deschamps, M.; Mostaert, F. (2014). Habitatmapping Zeeschelde: Deelrapport 5a–Stromingsmetingen op intergetijdengebieden Zone Weert - Branst. Versie 4.0. WL Rapporten, 00_028. Waterbouwkundig Laboratorium Antwerpen, België.

Smolders, S.; Maximova, T.; Vanlede, J.; Plancke, Y.; Verwaest, T.; Mostaert, F. (2016). Integraal Plan Bovenzeeschelde: Subreport 1 – SCALDIS: a 3D Hydrodynamic Model for the Scheldt Estuary. Version 5.0. WL Rapporten, 13_131. Flanders Hydraulics Research: Antwerp, Belgium.

Vanlierde, E.; Ferket, B.; Pauwaert, Z.; Michielsen, S.; Van De Moortel, I.; Levy, Y.; Plancke, Y.; Meire, D.; Deschamps, M.; Verwaest, T.; Mostaert, F. (2016). MONEOS - jaarboek monitoring WL 2015: factual data rapportage van monitoring hydrodynamiek en fysische parameters zoals gemeten door WL in het Zeescheldebekken in 2015. Versie 3.0. *WL Rapporten*, 12_070. Waterbouwkundig Laboratorium: Antwerpen.

Appendix

Saeftinghe

Figure 64 – Measured (blue) and computed (red) flow velocities at Saeftinghe-North (averaged tide)

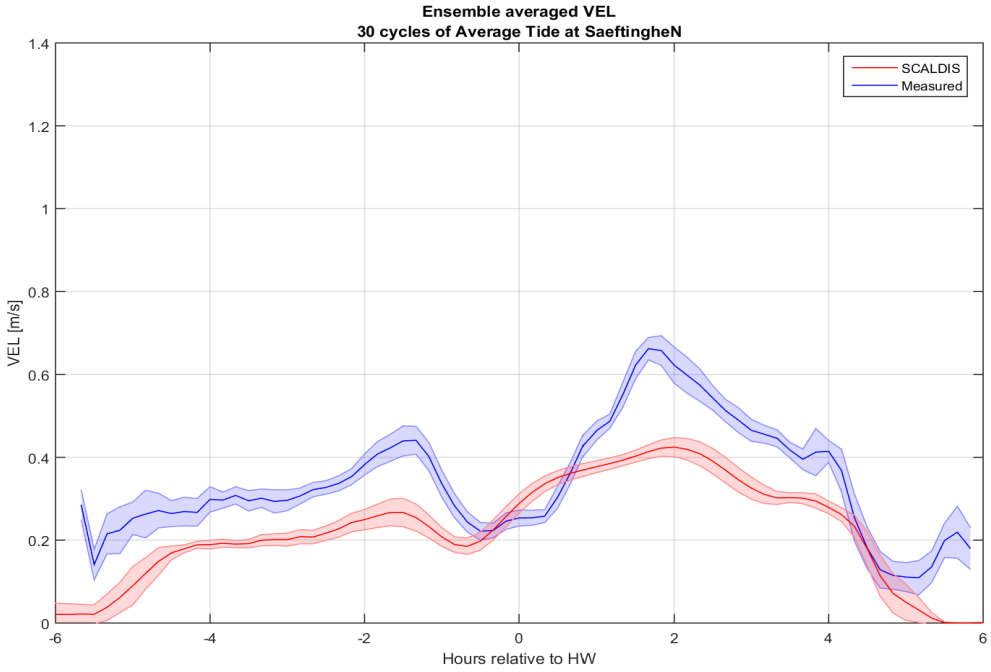

Figure 65 – Measured (blue) and computed (red) flow velocities at Saeftinghe-North (neap tide)

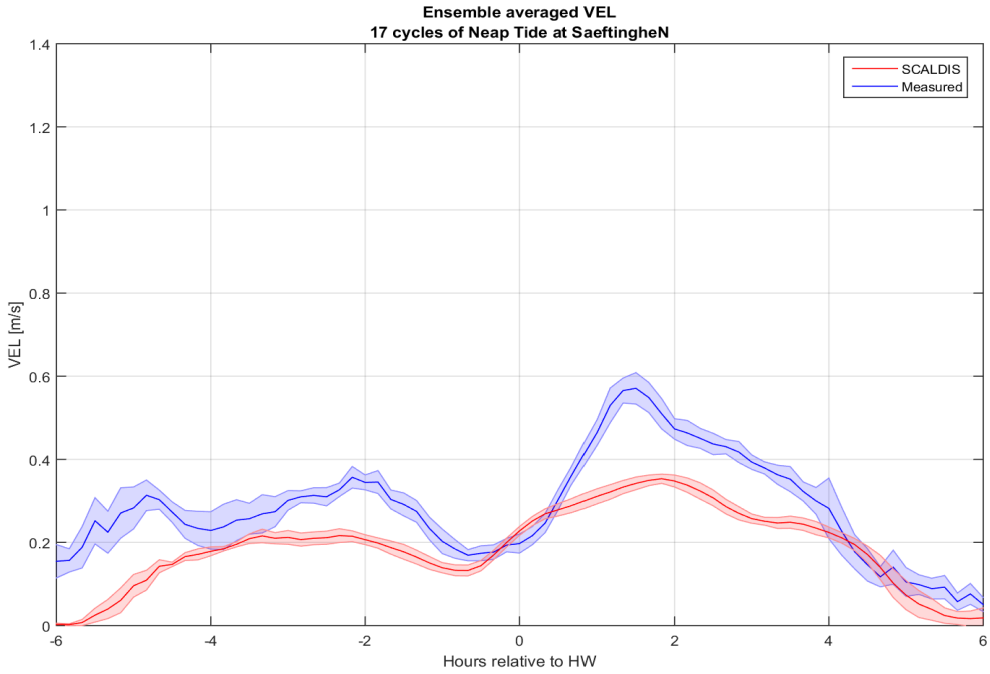

Figure 66 – Measured (blue) and computed (red) flow velocities at Saeftinghe-South (averaged tide)

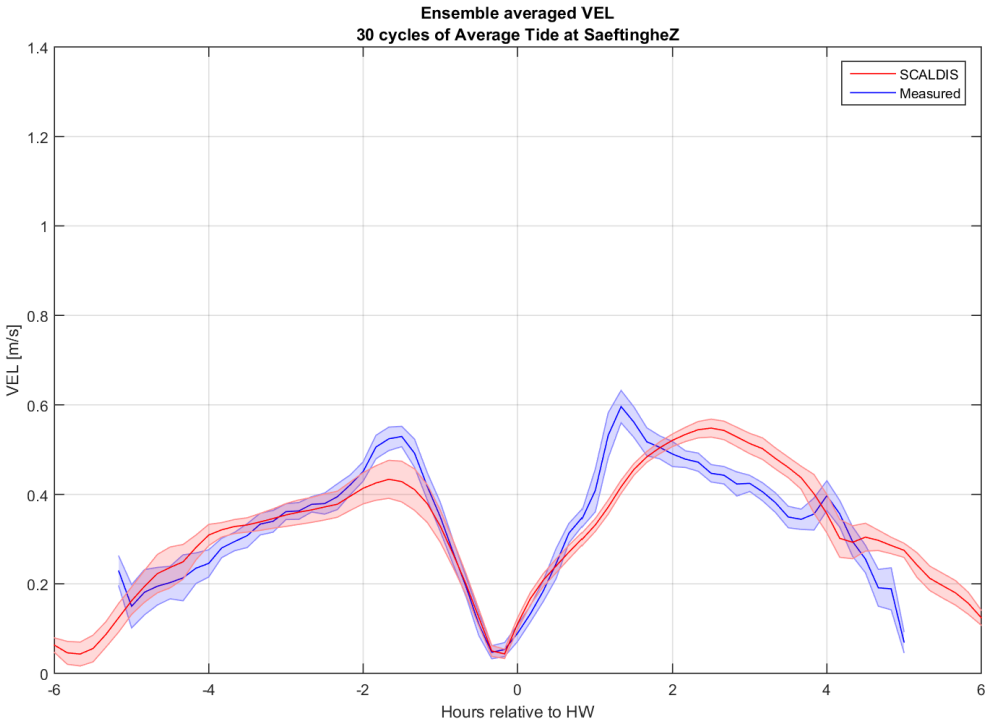

Figure 67 – Measured (blue) and computed (red) flow velocities at Saeftinghe-South (neap tide)

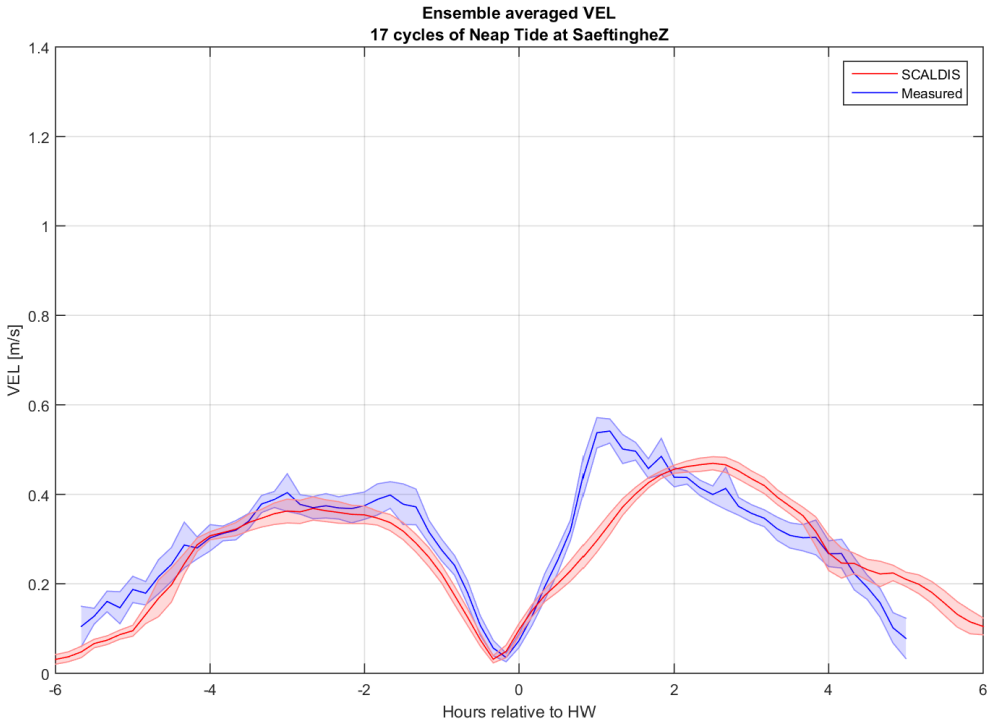

Galgeschoor

Figure 68 – Measured (blue) and computed (red) flow velocities at Galgeschoor-North (averaged tide)

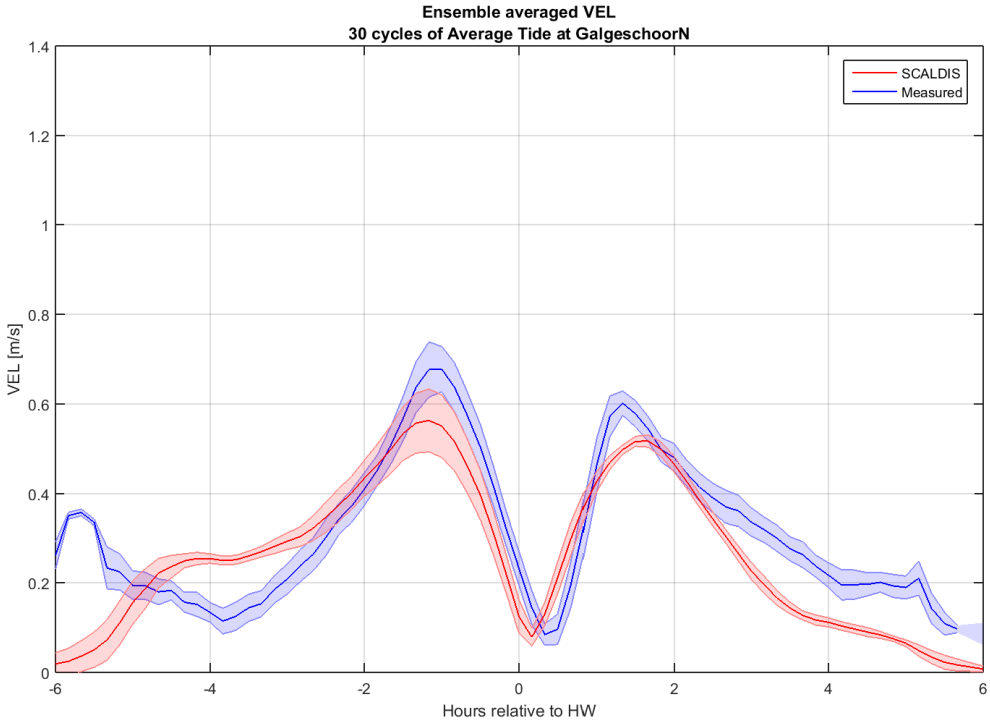

Figure 69 – Measured (blue) and computed (red) flow velocities at Galgeschoor-North (neap tide)

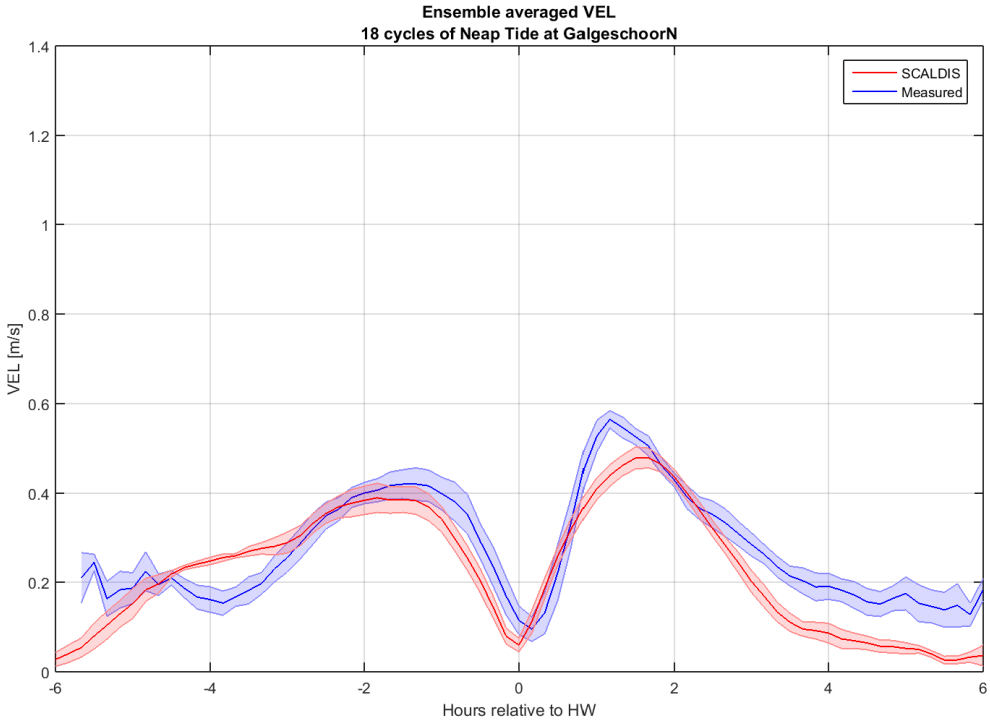

Figure 70 – Measured (blue) and computed (red) flow velocities at Galgeschoor-South (averaged tide)

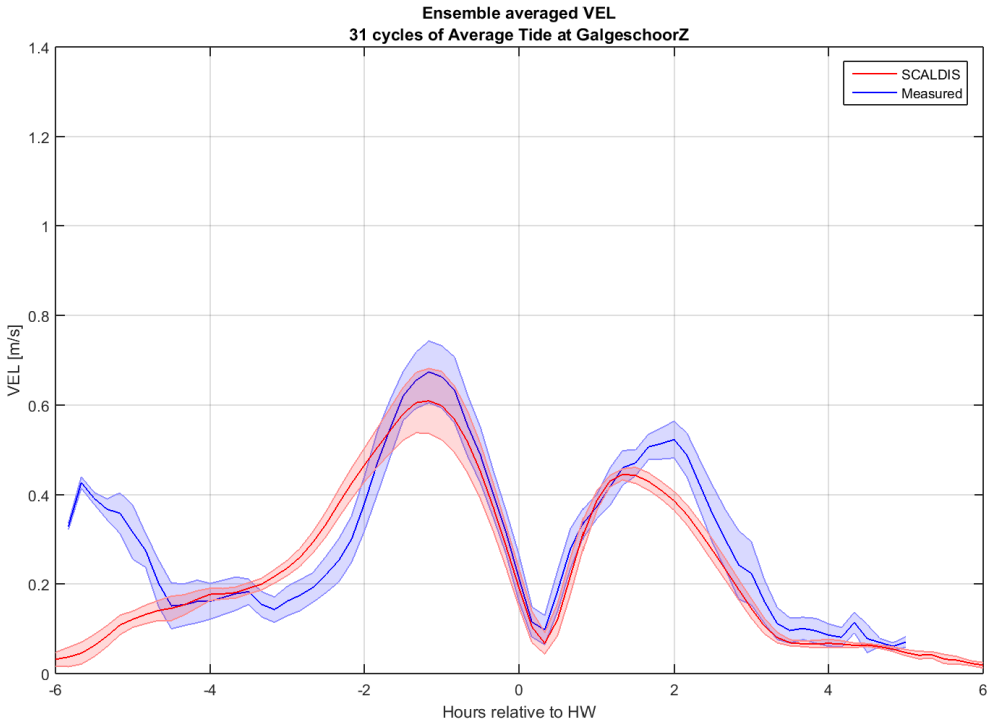

Figure 71 – Measured (blue) and computed (red) flow velocities at Galgeschoor-South (neap tide)

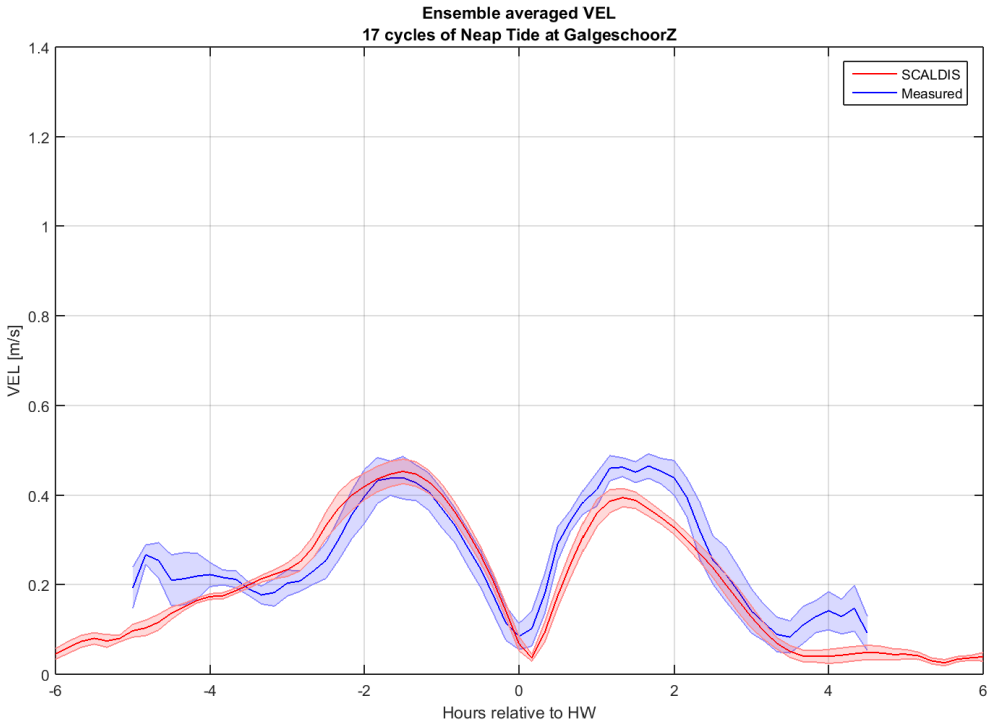

Ketenisse

Figure 72 – Measured (blue) and computed (red) flow velocities at Ketenisse-High (averaged tide)

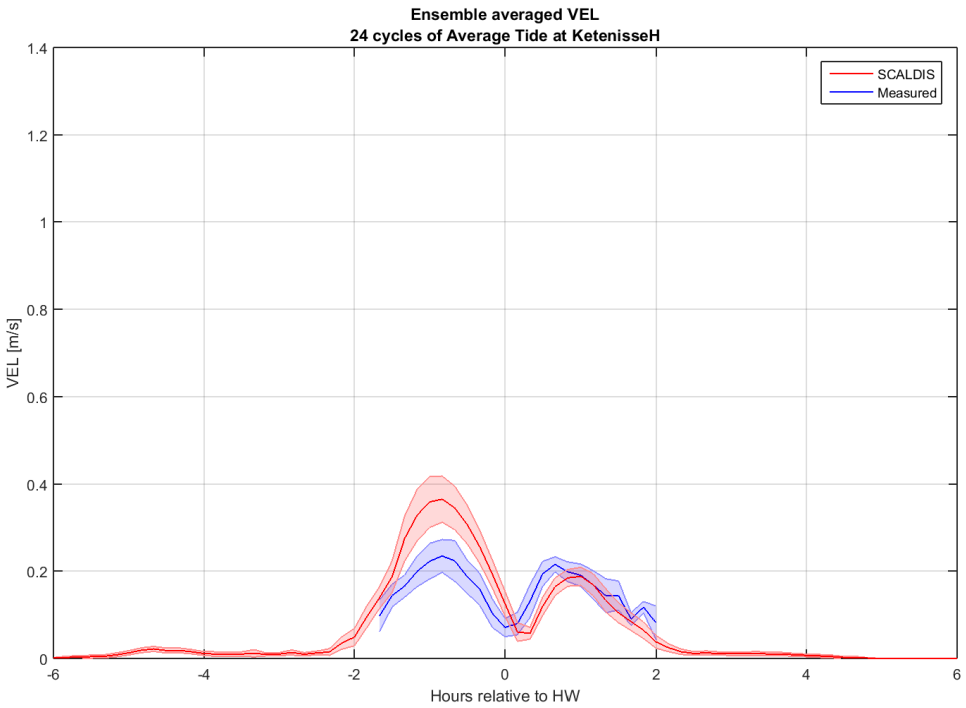

Figure 73 – Measured (blue) and computed (red) flow velocities at Ketenisse-High (neap tide)

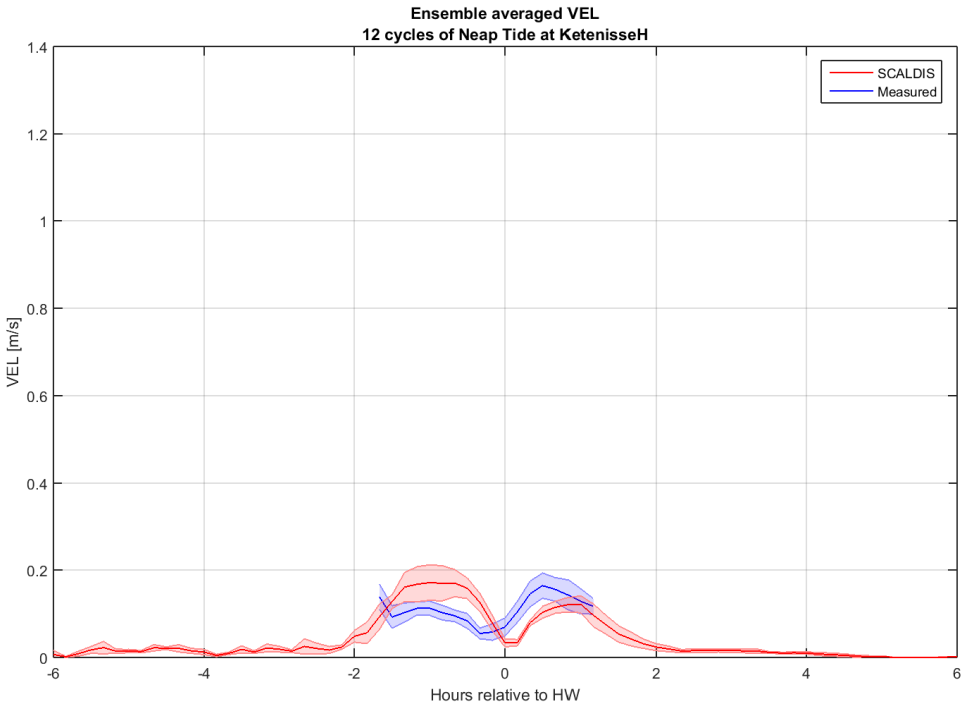

Figure 74 – Measured (blue) and computed (red) flow velocities at Ketenisse-Low (averaged tide)

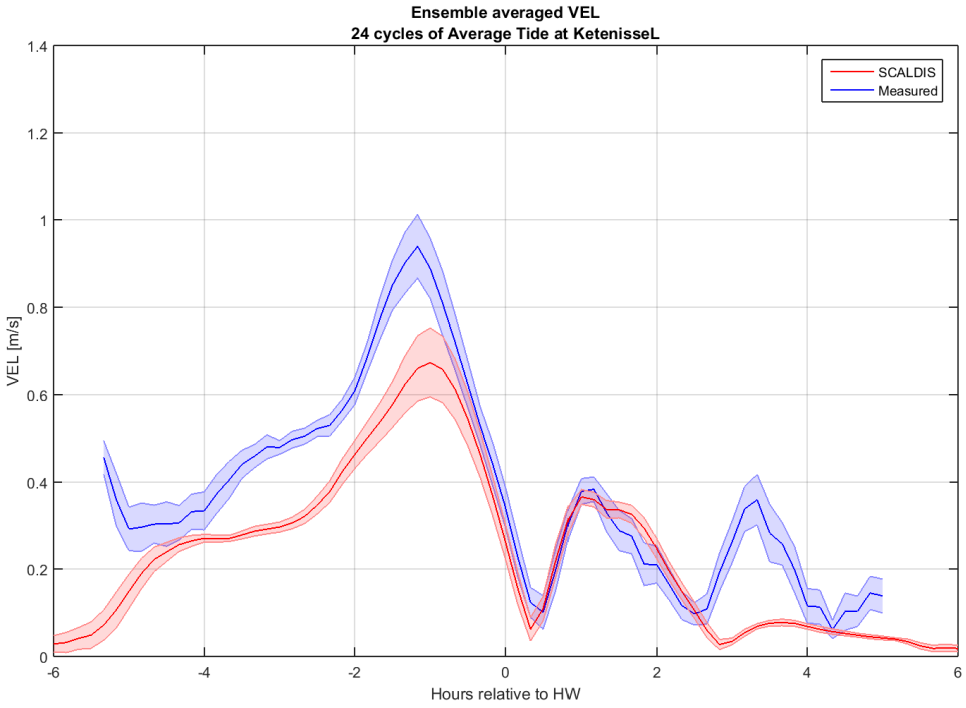

Figure 75 – Measured (blue) and computed (red) flow velocities at Ketenisse-Low (neap tide)

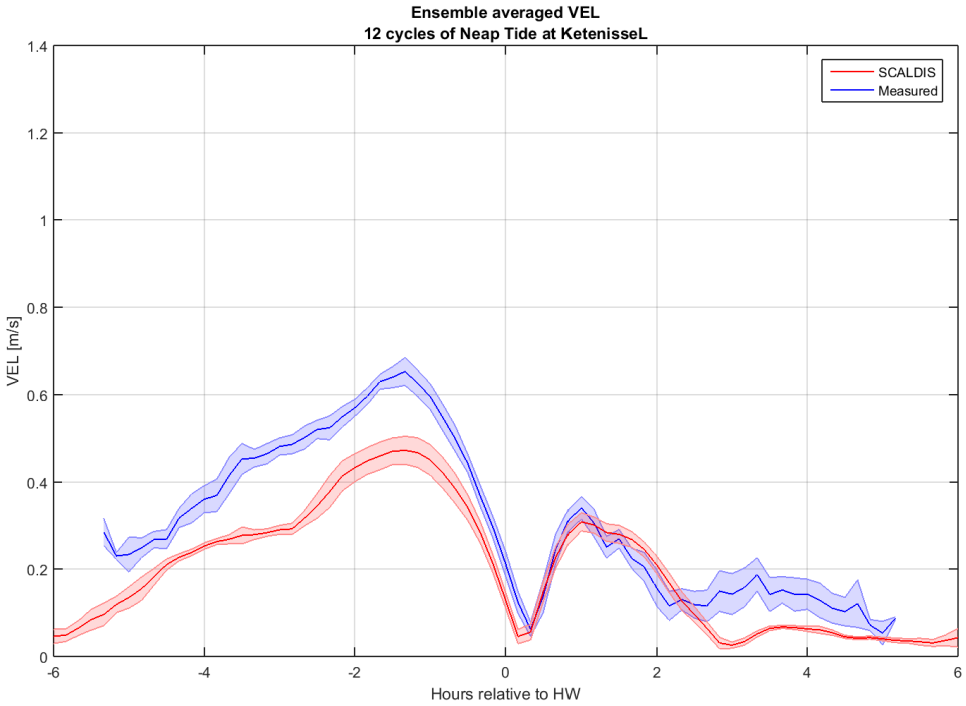

Plaat van Boomke

Figure 76 – Measured (blue) and computed (red) flow velocities at Boomke-High (averaged tide)

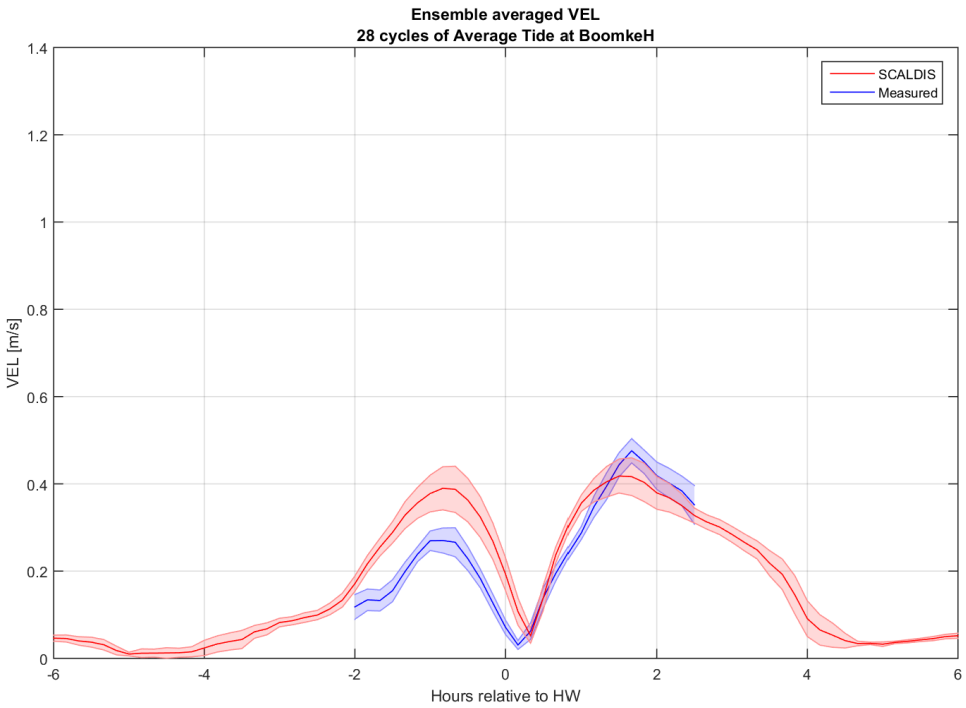

Figure 77 – Measured (blue) and computed (red) flow velocities at Boomke-High (neap tide)

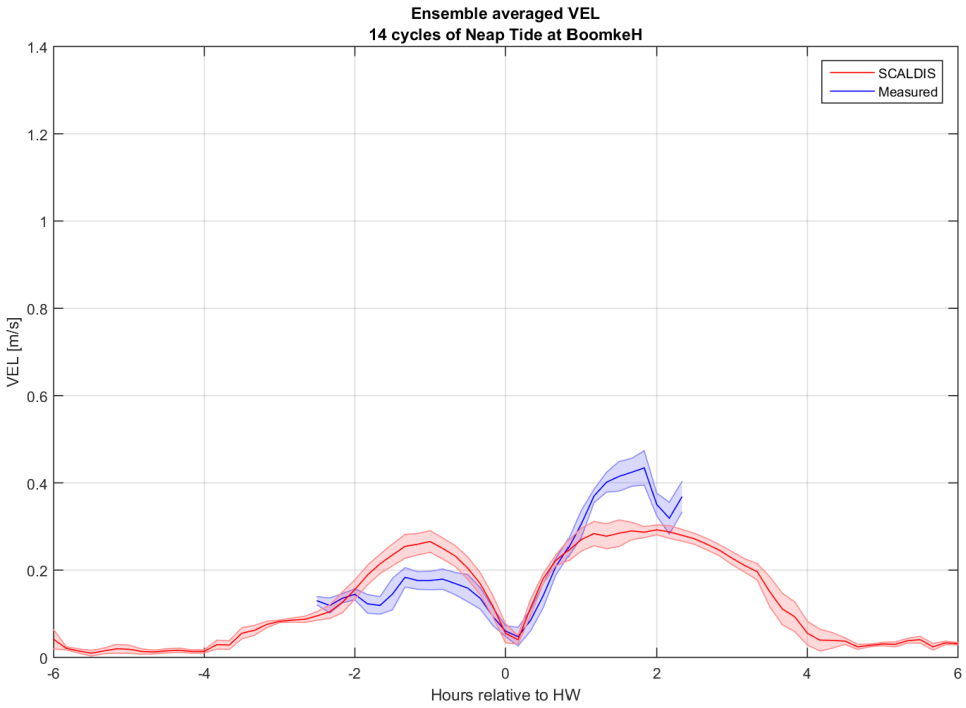

Figure 78 – Measured (blue) and computed (red) flow velocities at Boomke-Low (averaged tide)

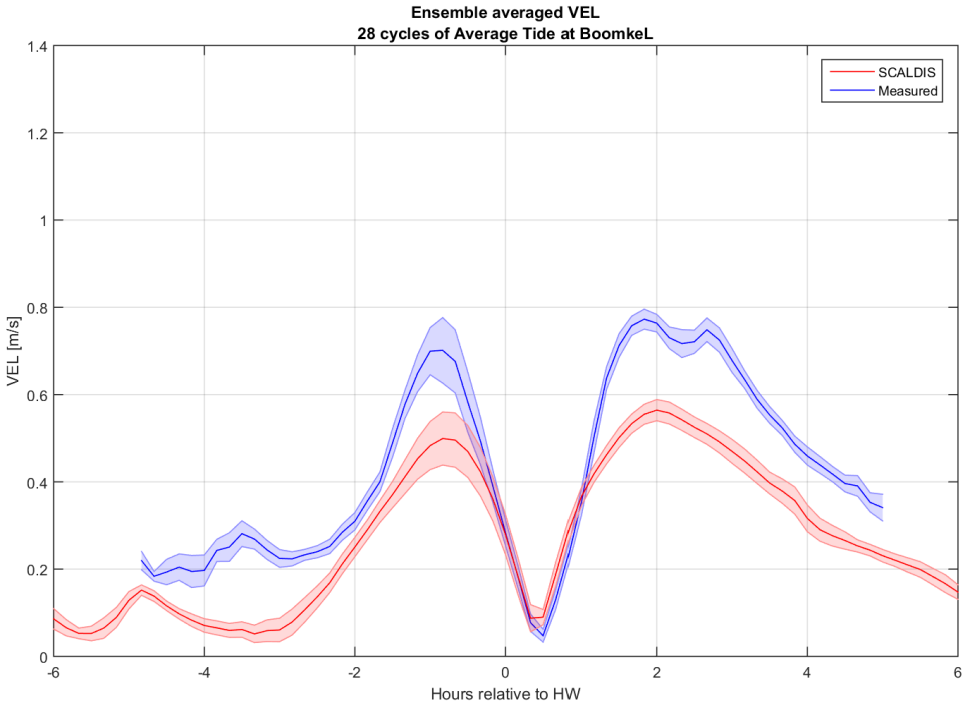

Figure 79 – Measured (blue) and computed (red) flow velocities at Boomke-Low (neap tide)

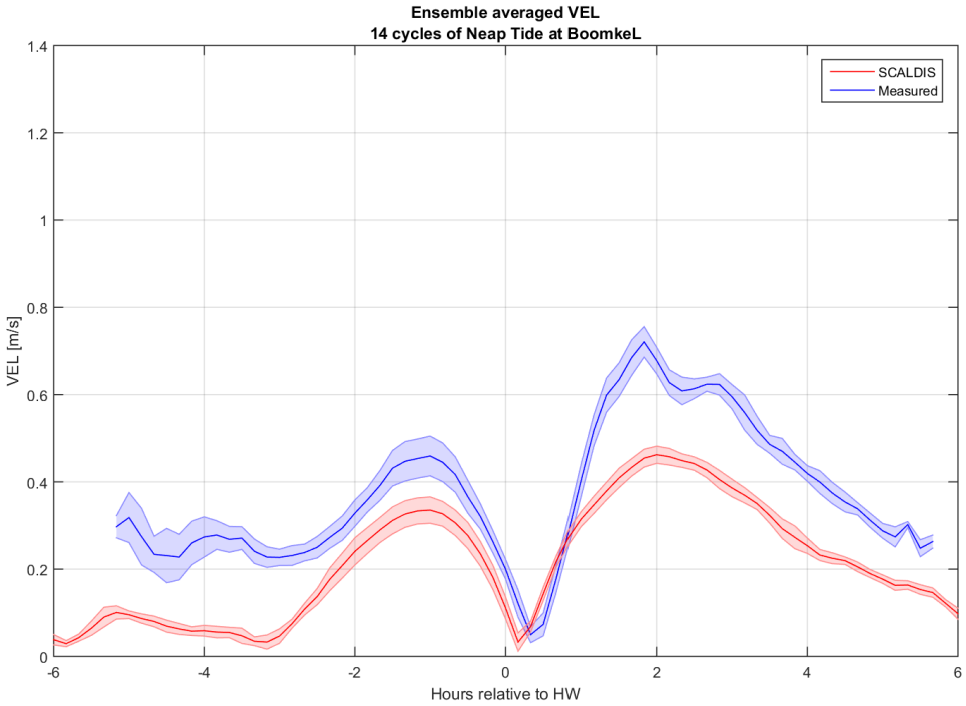

Palingplaat

Figure 80 – Measured (blue) and computed (red) flow velocities at Palingplaat-High (averaged tide)

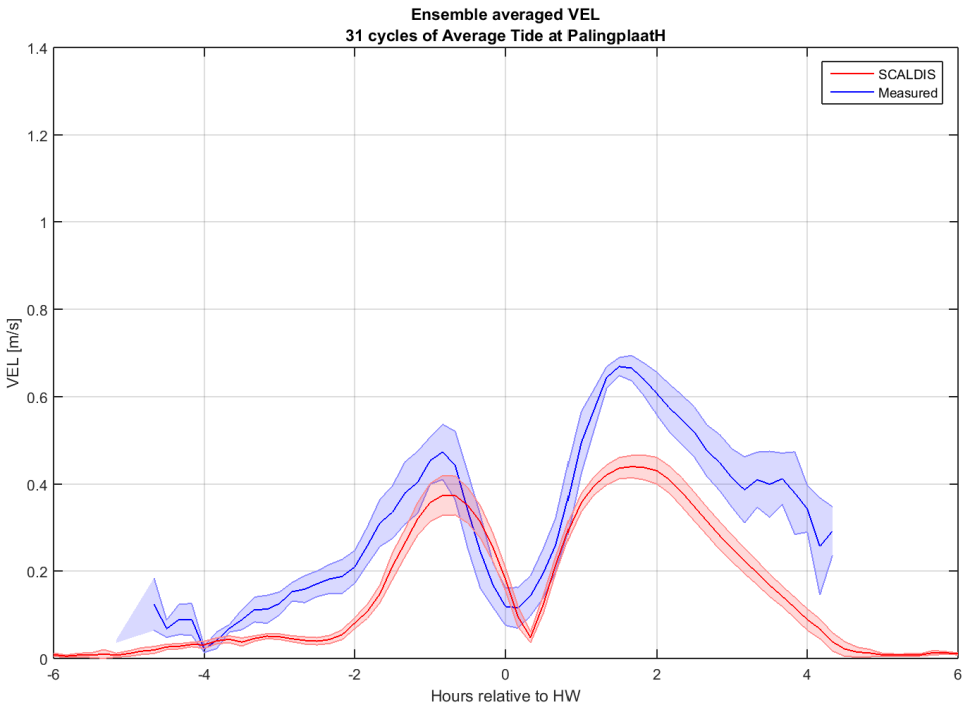

Figure 81 – Measured (blue) and computed (red) flow velocities at Palingplaat-High (neap tide)

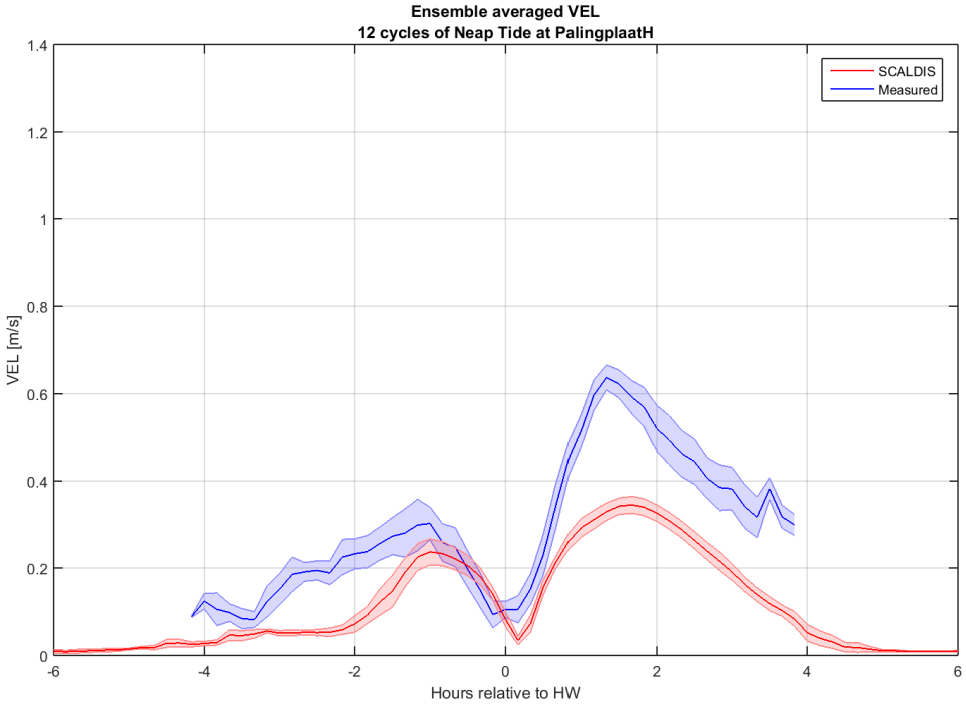

Figure 82 – Measured (blue) and computed (red) flow velocities at Palingplaat-Low (averaged tide)

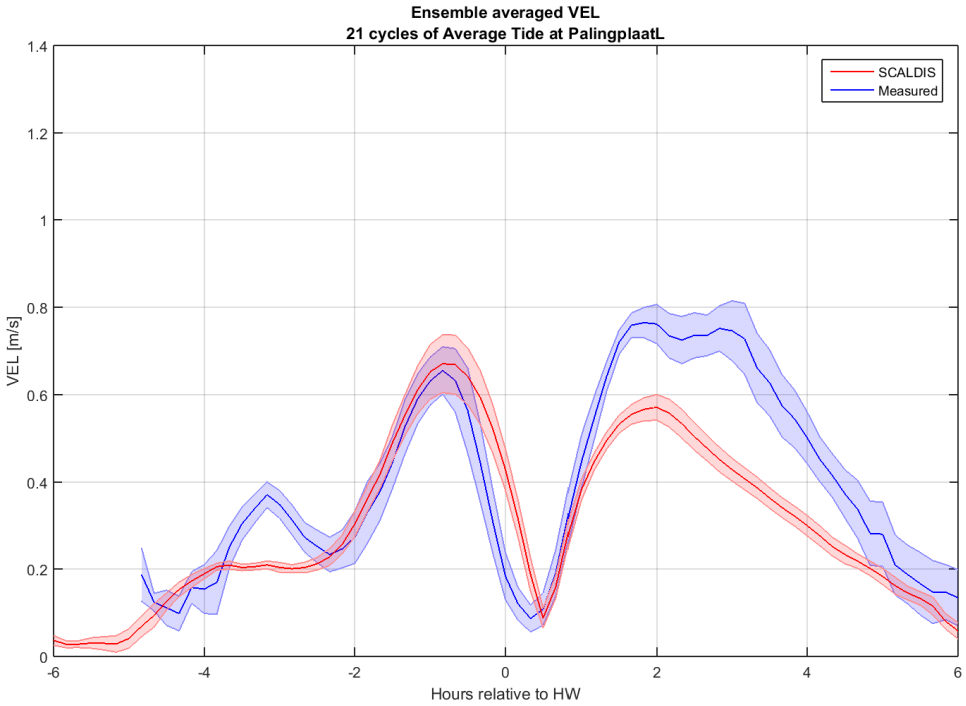

Figure 83 – Measured (blue) and computed (red) flow velocities at Palingplaat-Low (neap tide)

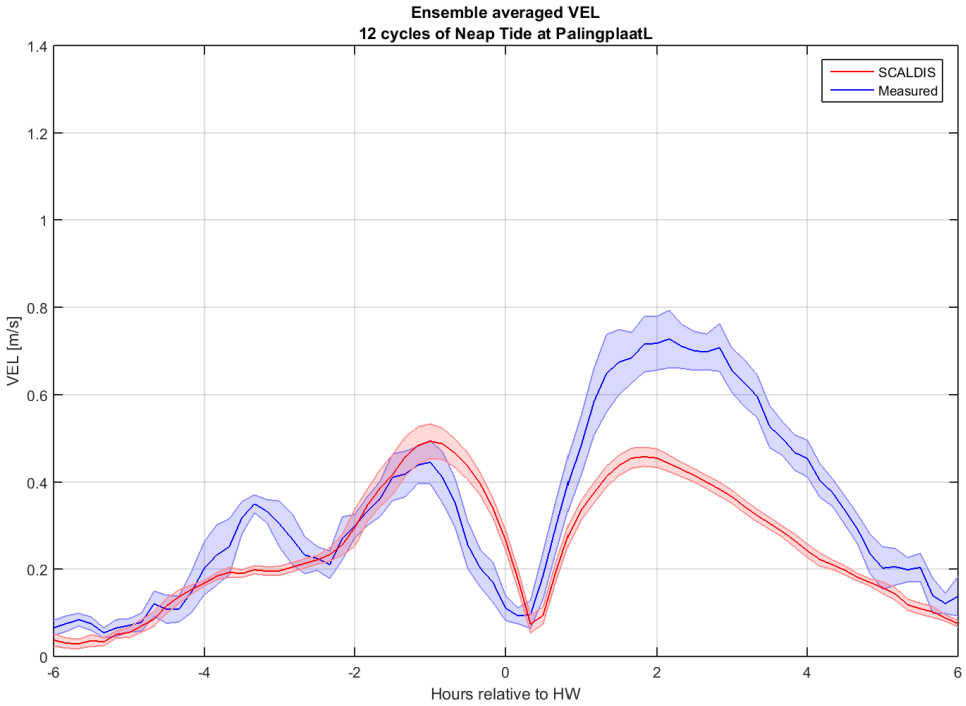

Plaat van Hoboken

Figure 84 – Measured (blue) and computed (red) flow velocities at Hoboken-High (averaged tide)

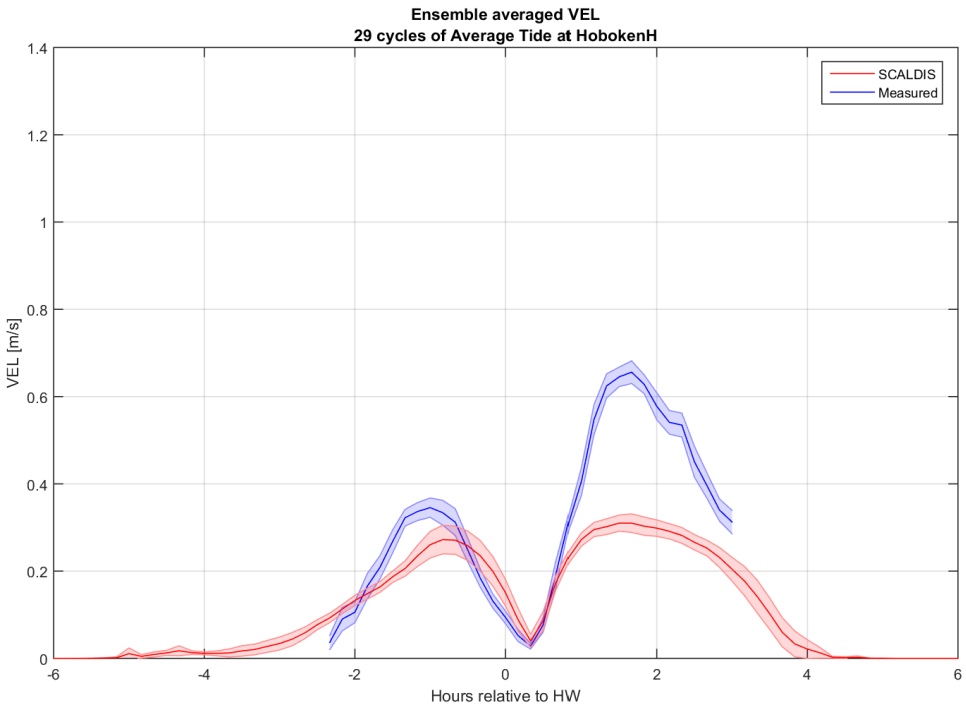

Figure 85 – Measured (blue) and computed (red) flow velocities at Hoboken-High (neap tide)

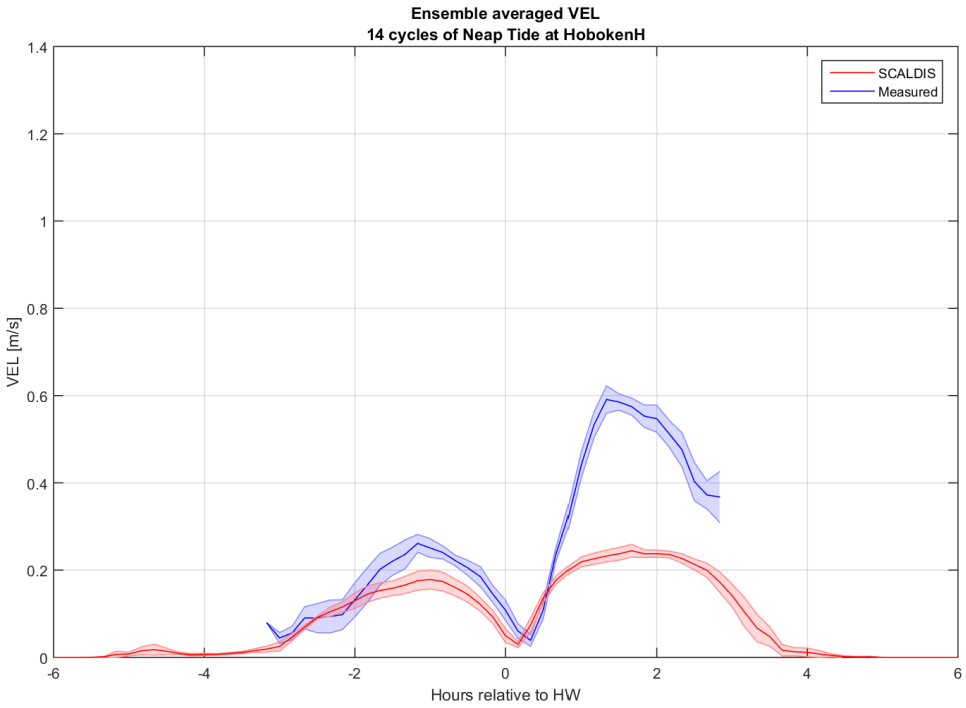

Figure 86 – Measured (blue) and computed (red) flow velocities at Hoboken-Low (averaged tide)

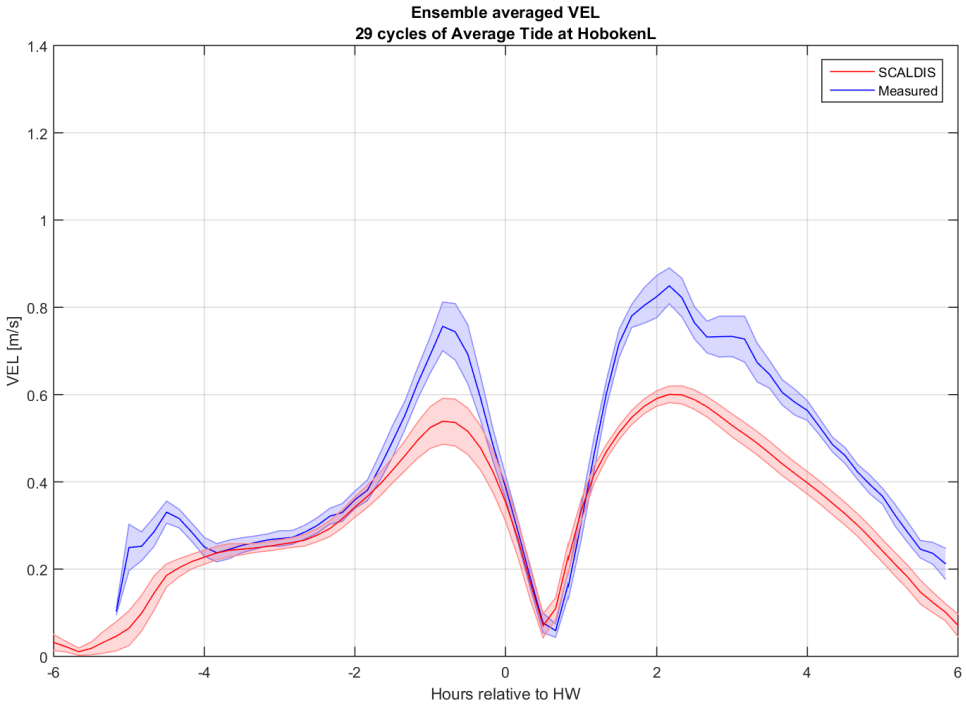

Figure 87 – Measured (blue) and computed (red) flow velocities at Hoboken-Low (neap tide)

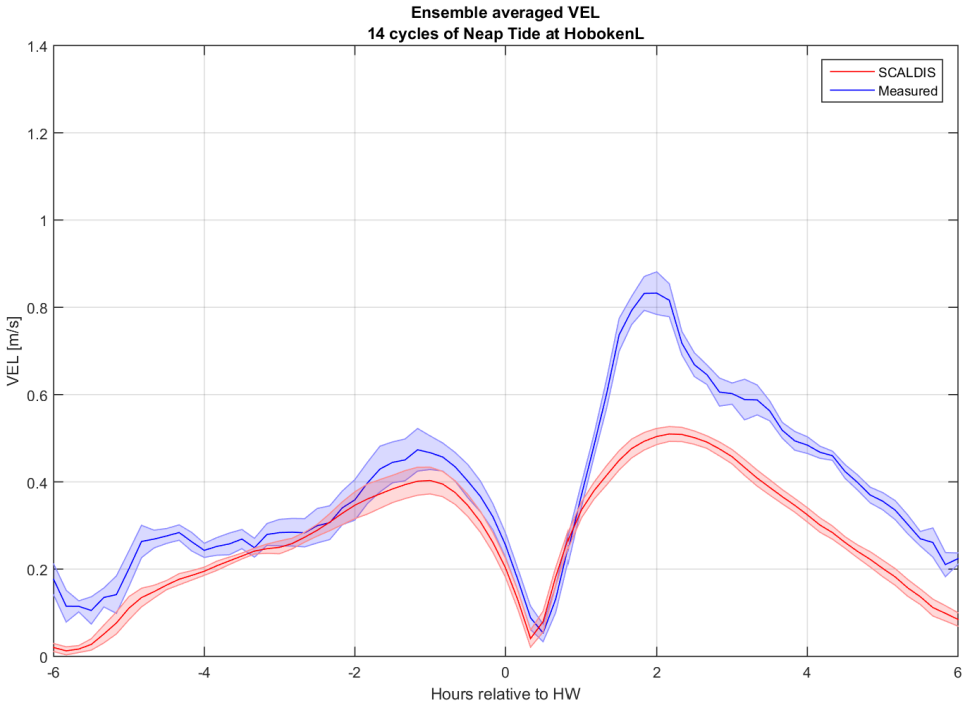

Notelaer

Figure 88 – Measured (blue) and computed (red) flow velocities at Notelaer-High (averaged tide)

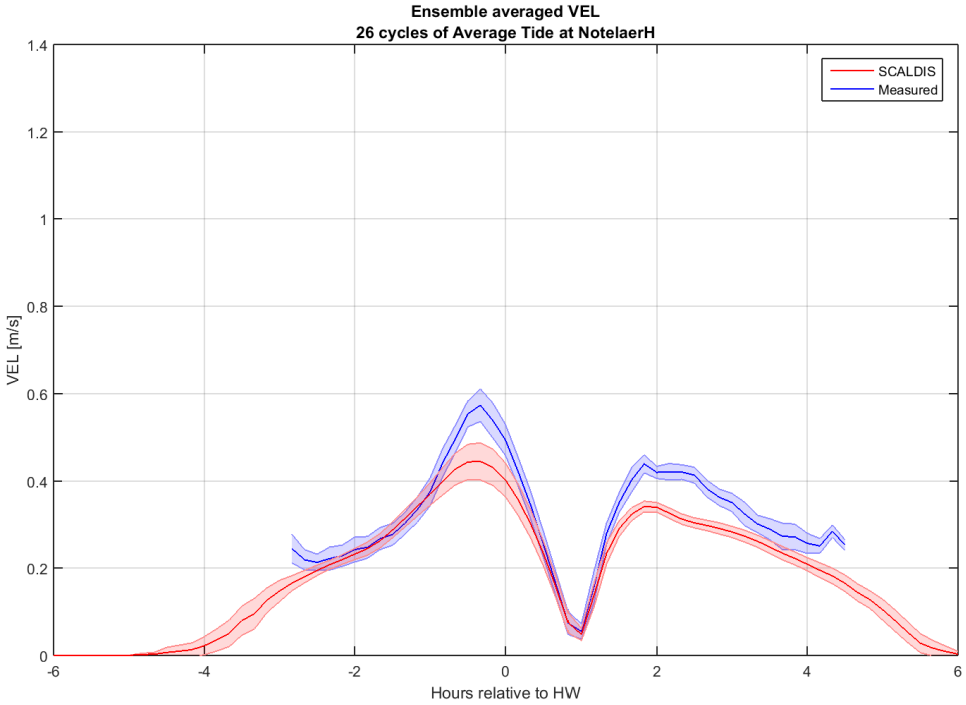

Figure 89 – Measured (blue) and computed (red) flow velocities at Notelaer-High (neap tide)

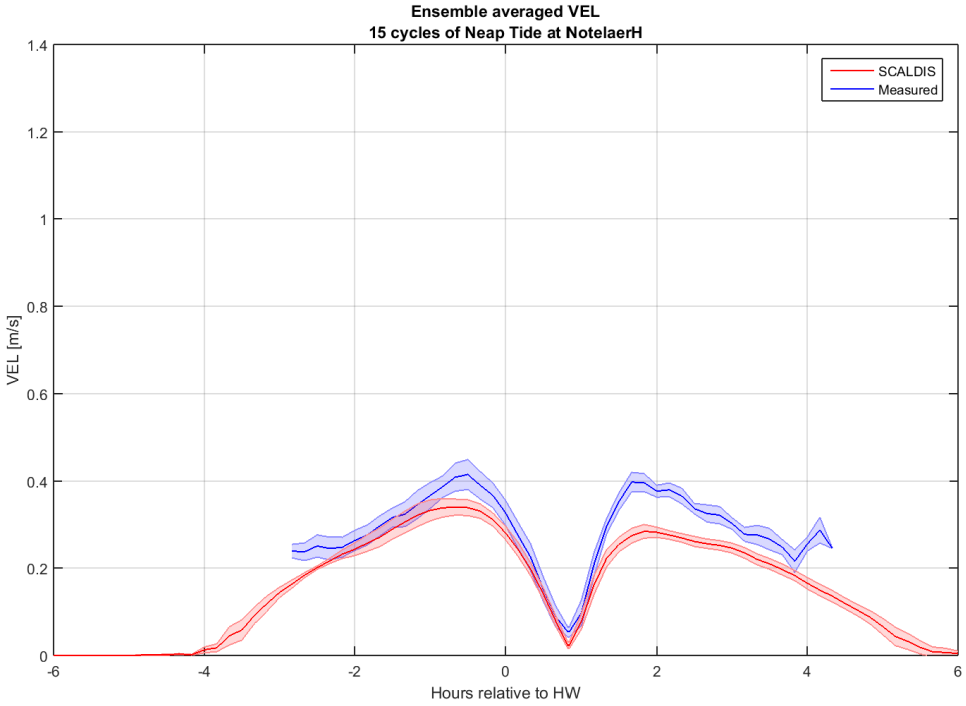

Figure 90 – Measured (blue) and computed (red) flow velocities at Notelaer-Low (averaged tide)

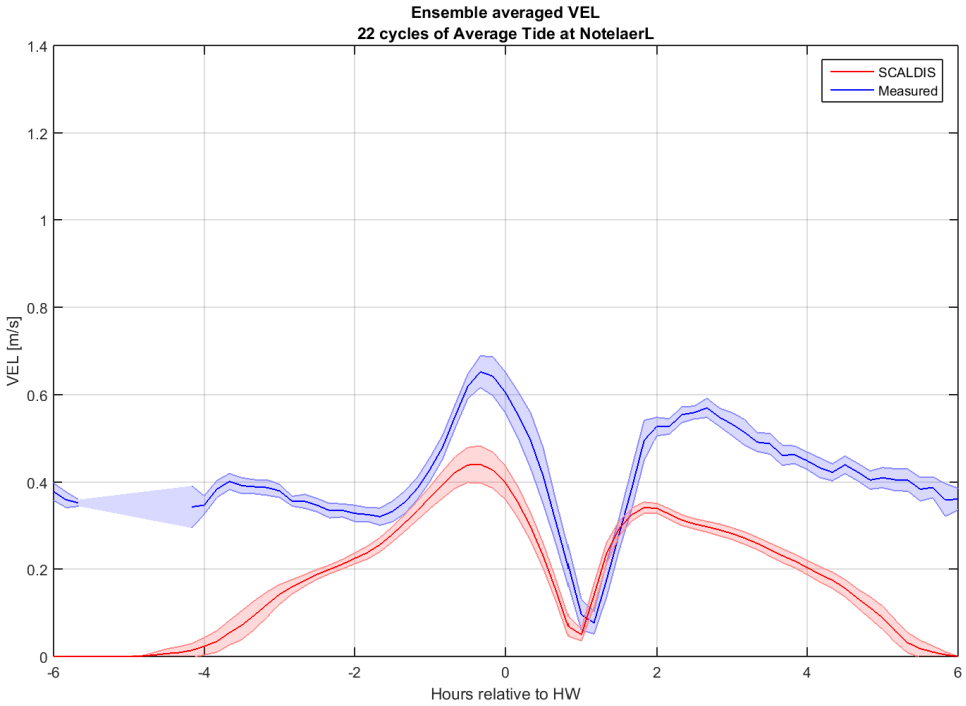

Figure 91 – Measured (blue) and computed (red) flow velocities at Notelaer-Low (neap tide)

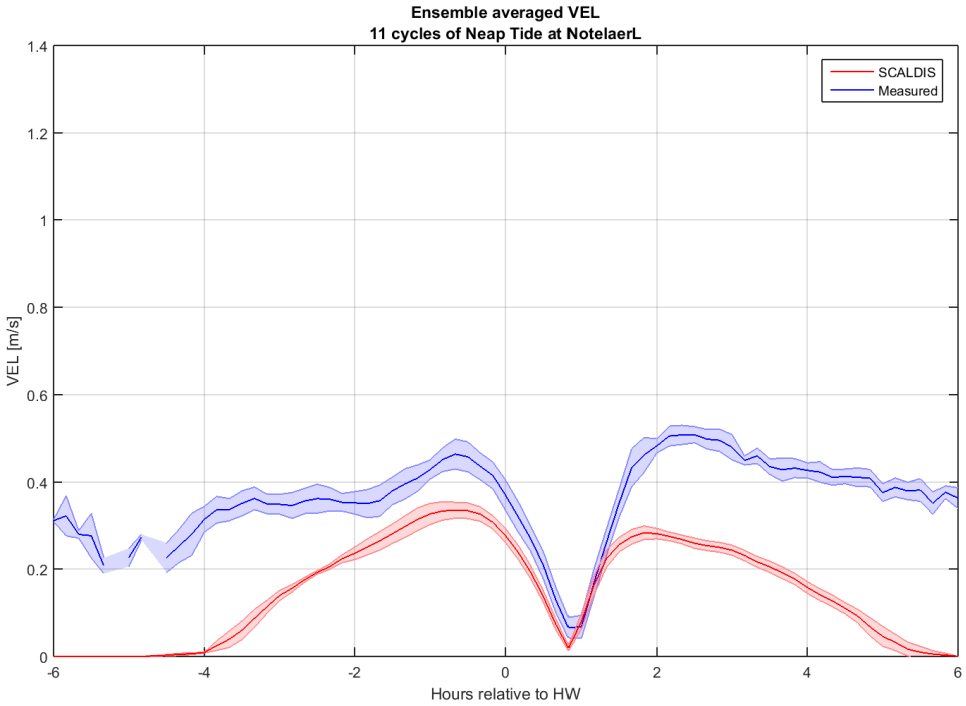

Weert

Figure 92 – Measured (blue) and computed (red) flow velocities at Weert-High (averaged tide)

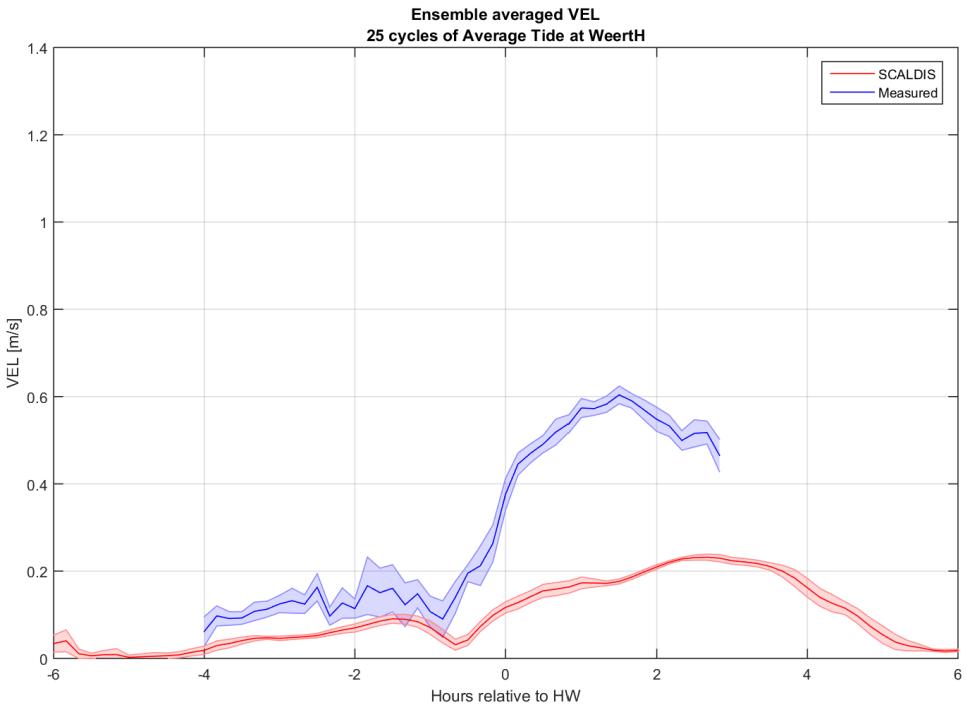

Figure 93 – Measured (blue) and computed (red) flow velocities at Weert-High (neap tide)

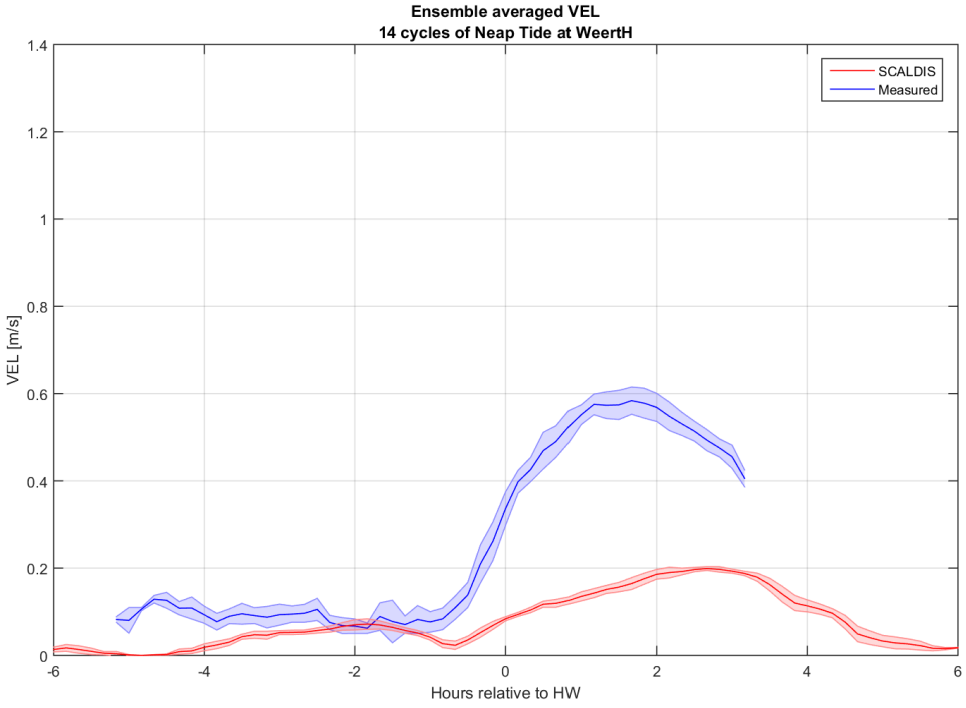

Figure 94 – Measured (blue) and computed (red) flow velocities at Weert-Low (averaged tide)

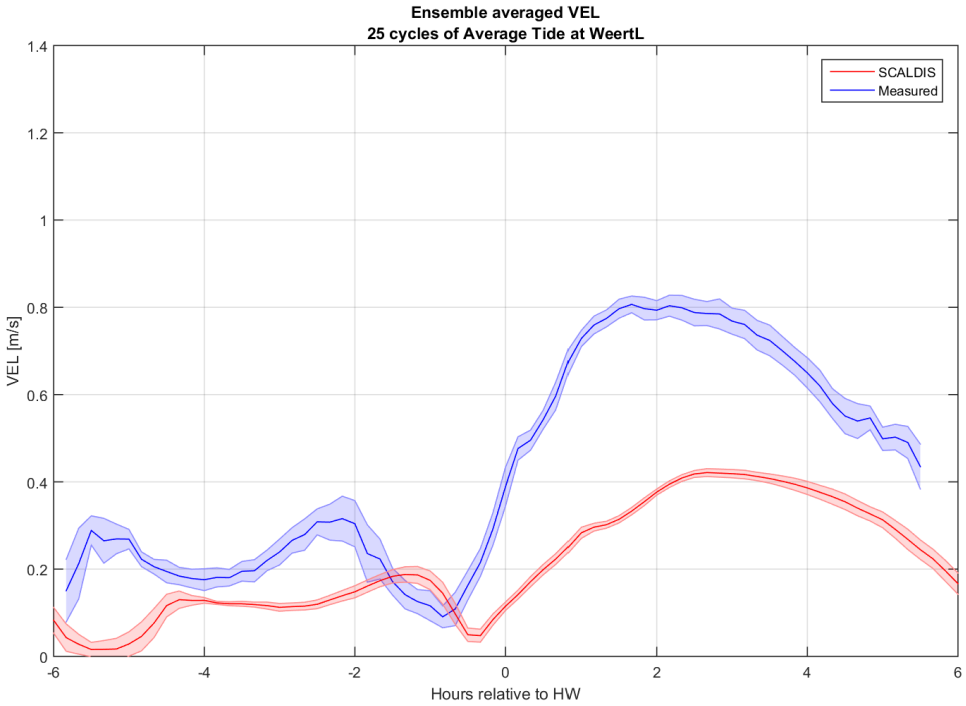

Figure 95 – Measured (blue) and computed (red) flow velocities at Weert-Low (neap tide)

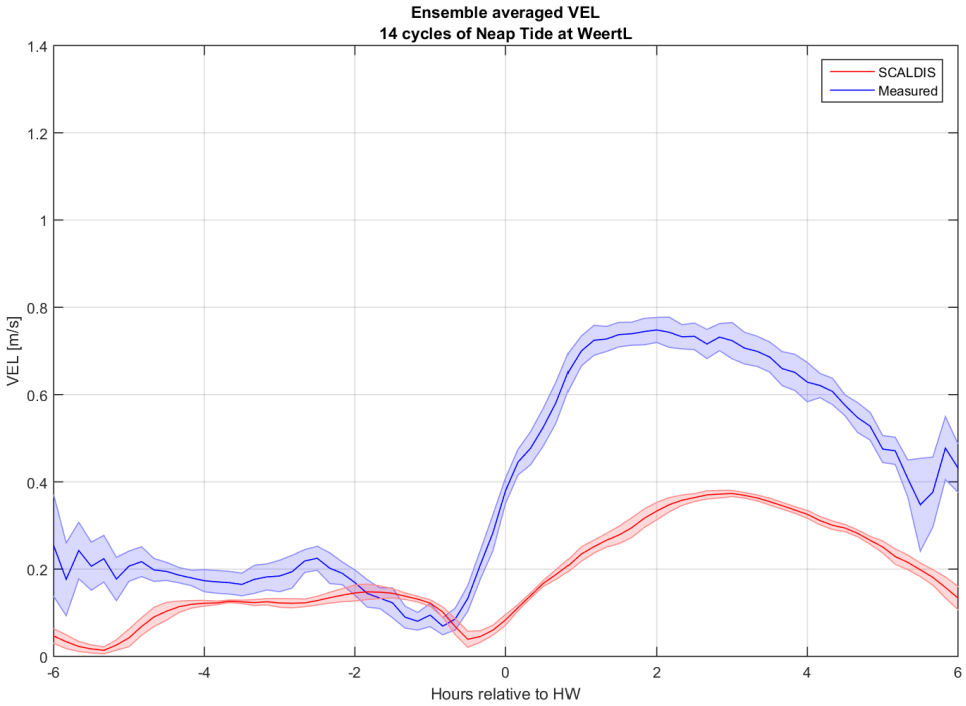

Appels

Appels – left bank

Figure 96 – Measured (blue) and computed (red) flow velocities at AppelsLO-High (averaged tide).

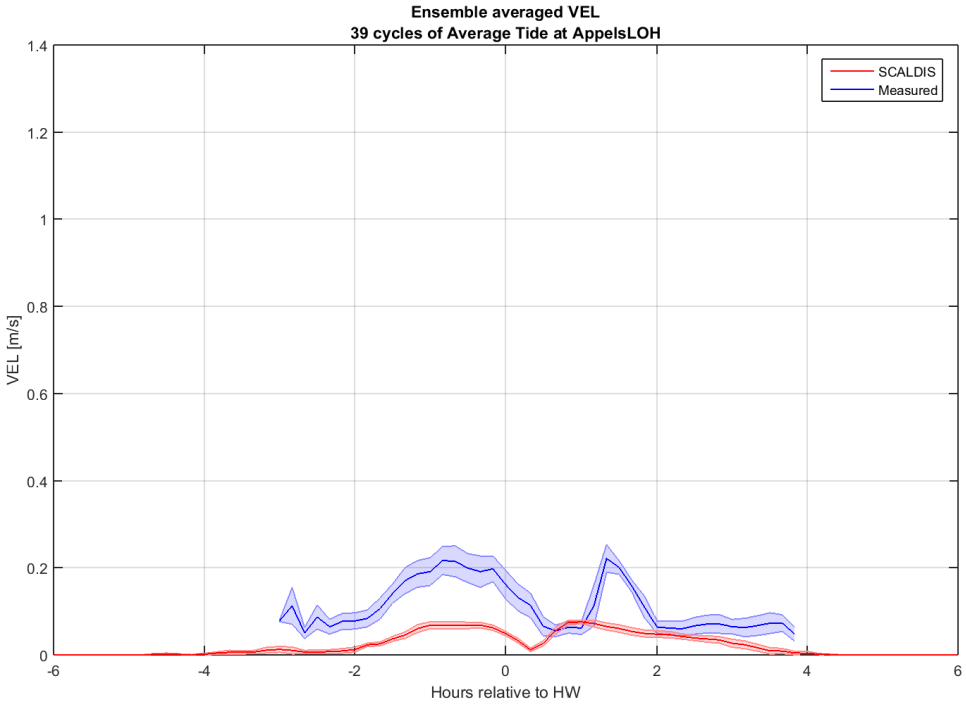

Figure 97 – Measured (blue) and computed (red) flow velocities at AppelsLO-High (neap tide).

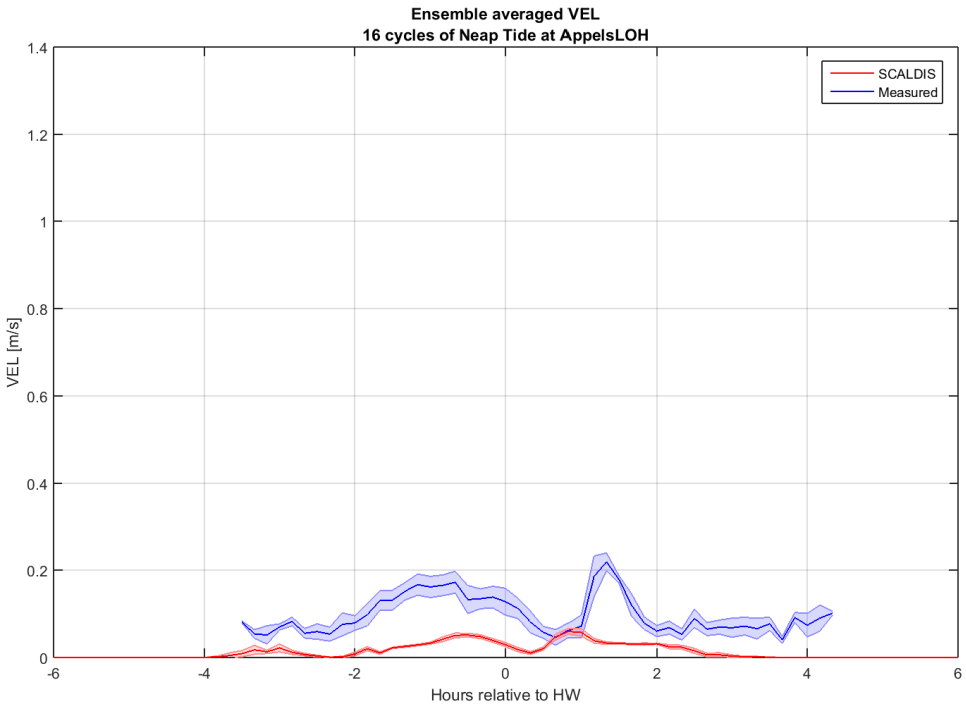

Figure 98 – Measured (blue) and computed (red) flow velocities at AppelsLO-Low (averaged tide).

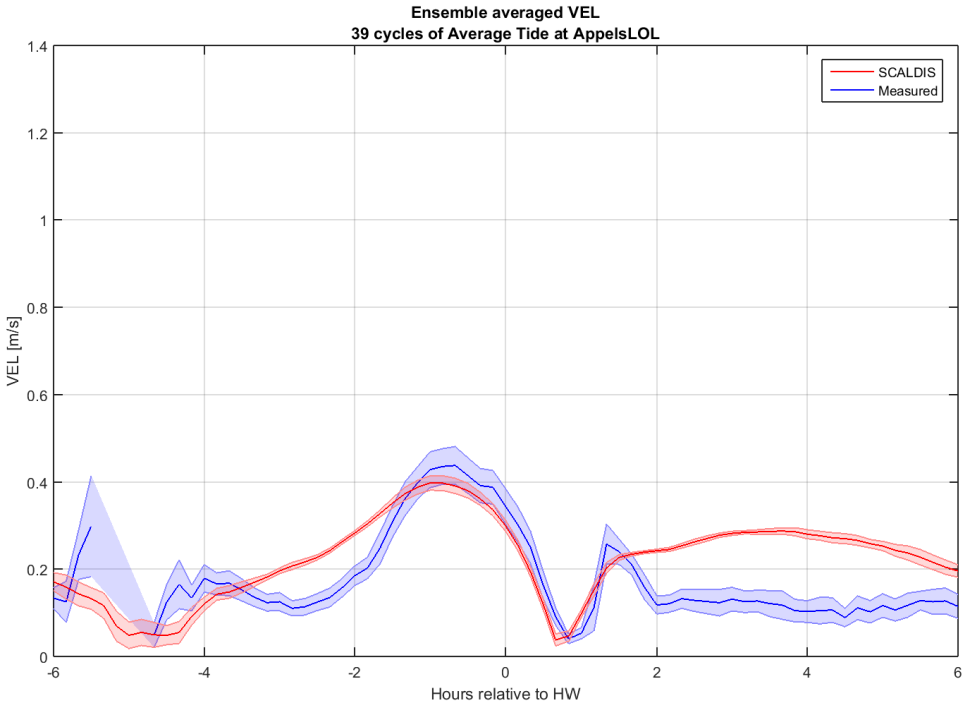

Figure 99 – Measured (blue) and computed (red) flow velocities at AppelsLO-Low (neap tide).

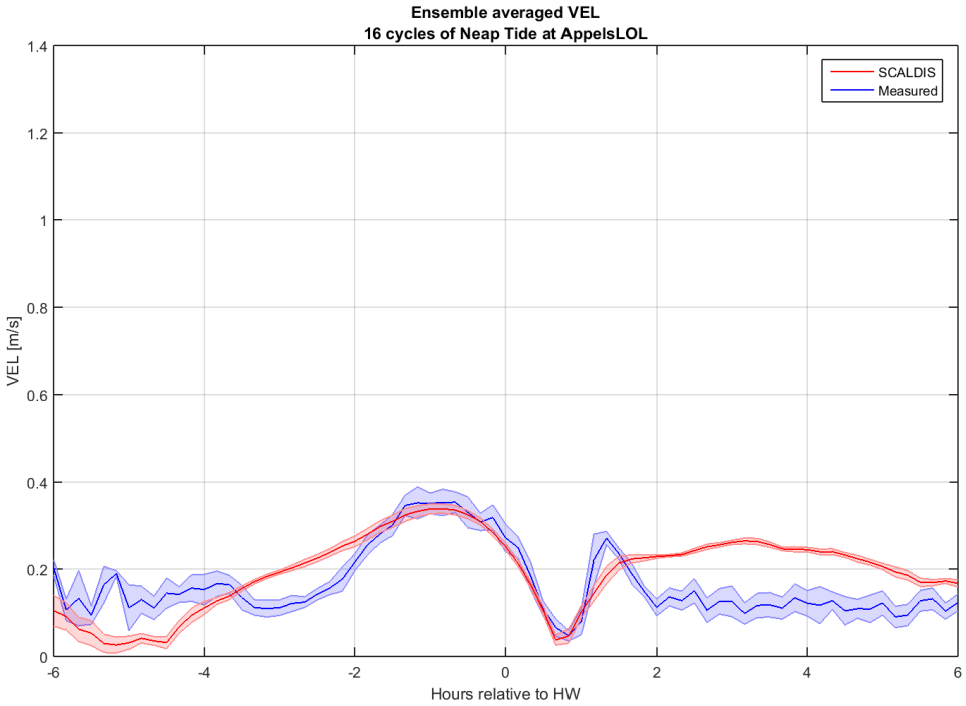

Appels – right bank

Figure 100 – Measured (blue) and computed (red) flow velocities at AppelsRO-High (averaged tide)

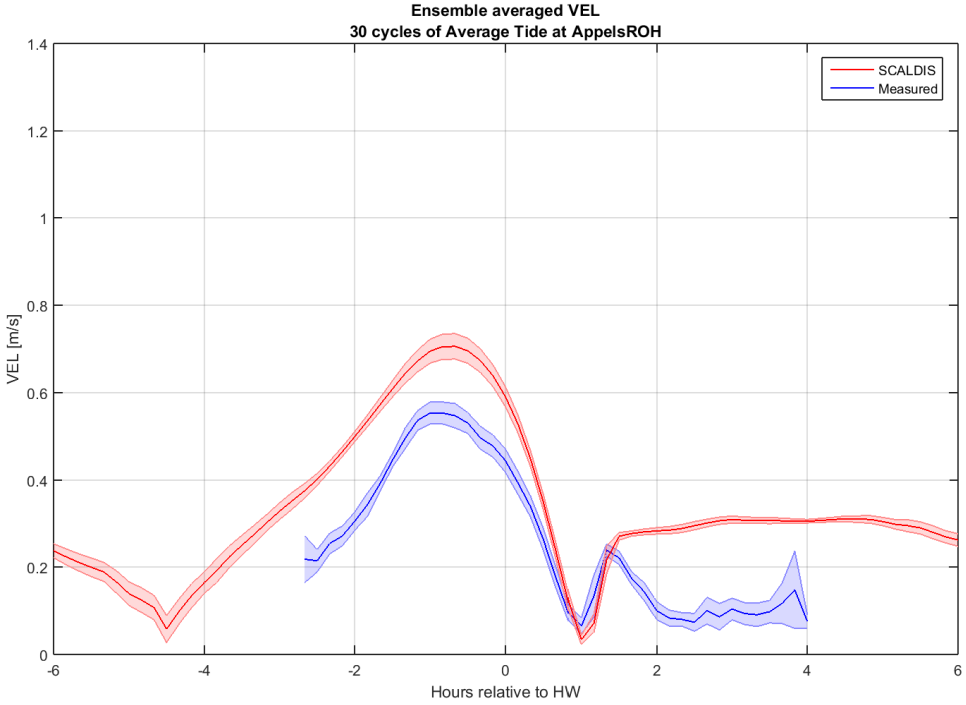

Figure 101 – Measured (blue) and computed (red) flow velocities at AppelsRO-High (neap tide)

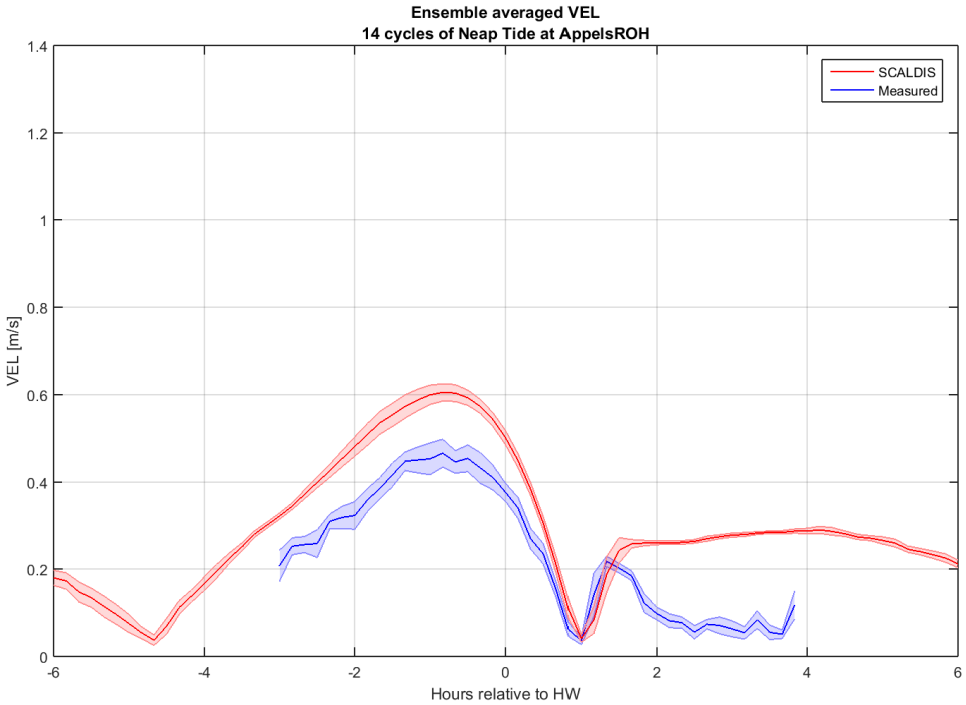

Figure 102 – Measured (blue) and computed (red) flow velocities at AppelsRO-Low (averaged tide)

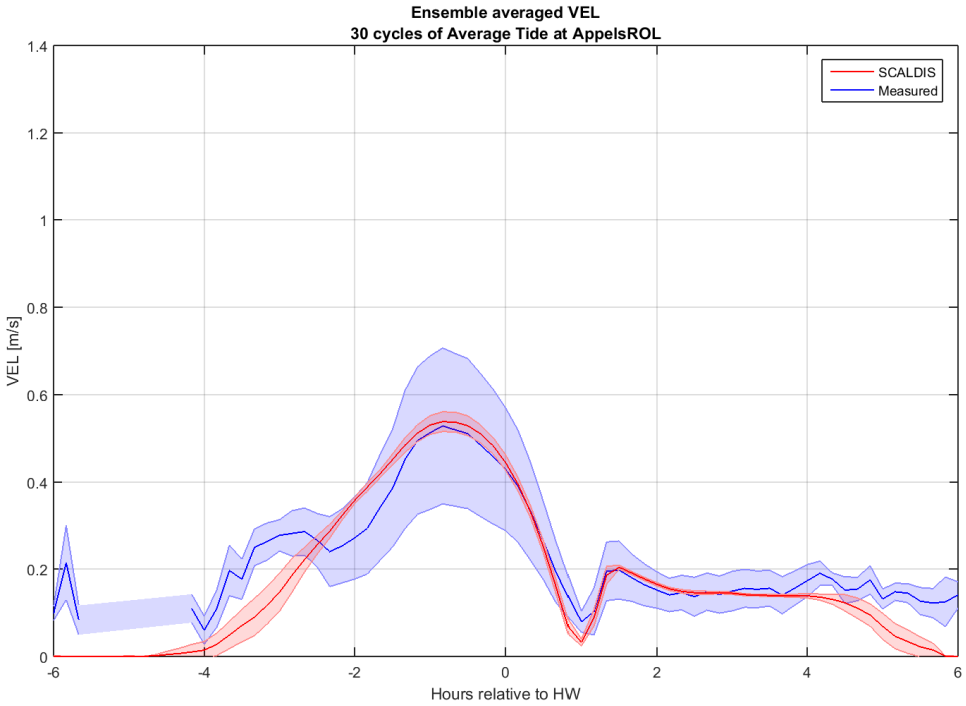

Figure 103 – Measured (blue) and computed (red) flow velocities at AppelsRO-Low (neap tide)

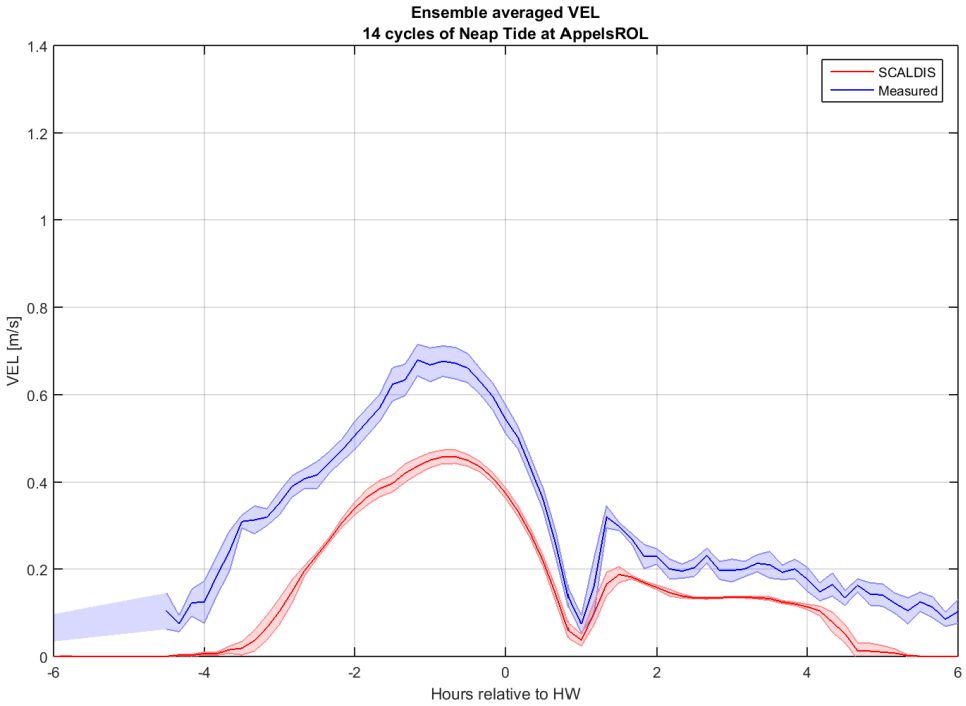

DEPARTMENT **MOBILITY & PUBLIC WORKS**
Flanders hydraulics Research

Berchemlei 115, 2140 Antwerp
T +32 (0)3 224 60 35
F +32 (0)3 224 60 36
waterbouwkundiglabo@vlaanderen.be
www.flandershydraulicsresearch.be